On high-mass binary black-hole templates for LIGO S2 data analysis

Alessandra Buonanno,[1,2] Yanbei Chen,[2] and Michele Vallisneri[3]

[1] *groupe de Cosmologie et Gravitation (GReCO), Institut d'Astrophysique de Paris (CNRS), 98$^{\rm bis}$ Boulevard Arago, 75014 Paris, France*

[2] *Theoretical Astrophysics, California Institute of Technology, Pasadena, CA 91125*

[3] *Jet Propulsion Laboratory, California Institute of Technology, Pasadena, CA 91109*

(Dated: January 20, 2004)

We study the range of binary black-hole masses for which upper limits could be set with the LIGO S2 runs using the detection template family we proposed.

I. INTRODUCTION AND NOTATIONS

In Ref. [1, henceforth BCV1] we created a template bank that models *directly* the Fourier transform of the GW signals of various PN models (expanded and resummed, adiabatic and nonadiabatic), by writing the amplitude and phasing as simple polynomials in the GW frequency $f_{\rm GW}$. We took the specific powers of $f_{\rm GW}$ that appear in these polynomials from the Fourier transforms of PN expanded adiabatic signals, as computed in the stationary-phase approximation (SPA); however, we did not constrain their coefficients to their functional dependence on the physical parameters. More specifically in BCV1, we defined our generic family of Fourier-domain effective templates as ($f \equiv f_{\rm GW}$)

$$h_{\rm eff}(f) = \mathcal{A}_{\rm eff}(f)\, e^{i\psi_{\rm eff}(f)}\,, \tag{1}$$

where

$$\mathcal{A}_{\rm eff}(f) \;=\; f^{-7/6}\left(1-\alpha\, f^{2/3}\right)\theta(f_{\rm cut}-f)\,, \tag{2}$$

$$\psi_{\rm eff}(f) \;=\; 2\pi f t_0 + \phi_0 + f^{-5/3}\left(\psi_0 + \psi_{1/2}\, f^{1/3} + \psi_1\, f^{2/3} + \psi_{3/2}\, f + \psi_2\, f^{4/3} + \cdots\right)\,, \tag{3}$$

where t_0 and ϕ_0 are the time of arrival and the frequency-domain phase offset, and where $\theta(\ldots)$ is the Heaviside step function. Because in BCV1 we considered BBHs with total masses 10–40$M_\odot$, the GW signal can end within the LIGO frequency band and the predictions of the ending frequency given by different PN models can be quite different [1]. Thus we also modified the Newtonian-order formula for the amplitude, by introducing the cutoff frequency $f_{\rm cut}$ and the parameter α to model the shape of the amplitude curve. [Note that the amplitude's correction we introduce is the PN amplitude's correction if the SPA is used and if we consider the *restricted waveform*: $h(t) = v^2 \cos\varphi_{\rm GW}(t)$, where the GW phase $\varphi_{\rm GW}$ is twice the orbital phase φ and $v = (M\dot\varphi)^{1/3} = (\pi M f_{\rm GW})^{1/3}$.]

In BCV1 we found that taking only the two parameters ψ_0 and $\psi_{3/2}$ in the phasing (and setting all other ψ coefficients to zero) and two amplitude parameters, $f_{\rm cut}$ and α, we can already match all the PN models with high fitting factor FF [for a definition of FF's, e.g., see Sec. IIC of BCV1]. This is possible largely because we restrict our focus to BBHs with relatively high masses, where the number of GW cycles in the LIGO range (and thus the total range of the phasing $\psi(f)$ that we need to consider) is small. In the following we shall denote by DTF the detection template family defined by the Eqs. (1)–(3) with only the two parameters ψ_0 and $\psi_{3/2}$.

model	shorthand	evolution equation
adiabatic model with Taylor-expanded energy $\mathcal{E}(v)$ and flux $\mathcal{F}(v)$ [2]	$\mathrm{T}(n\mathrm{PN}, m\mathrm{PN}; \hat\theta)$	energy-balance equation
adiabatic model with Padé-resummed energy $\mathcal{E}(v)$ and flux $\mathcal{F}(v)$ [3]	$\mathrm{P}(n\mathrm{PN}, m\mathrm{PN}; \hat\theta)$	energy-balance equation
nonadiabatic effective-one-body (EOB) model [4, 5] with Padé-resummed GW flux [3]	$\mathrm{EP}(n\mathrm{PN}, m\mathrm{PN}; \hat\theta)$	EOB Hamilton equations

TABLE I: Post–Newtonian models of two-body dynamics defined in BCV1. The notation $\mathrm{X}(n\mathrm{PN}, m\mathrm{PN}; \hat\theta)$ denotes the model X, with terms up to order nPN for the conservative dynamics, and with terms up to order mPN for radiation-reaction effects; for $m \geq 3$ we also need to specify the arbitrary flux parameter $\hat\theta$ (see Sec. IIIA in BCV1); for $n \geq 3$.

LIGO-T050235-00-Z

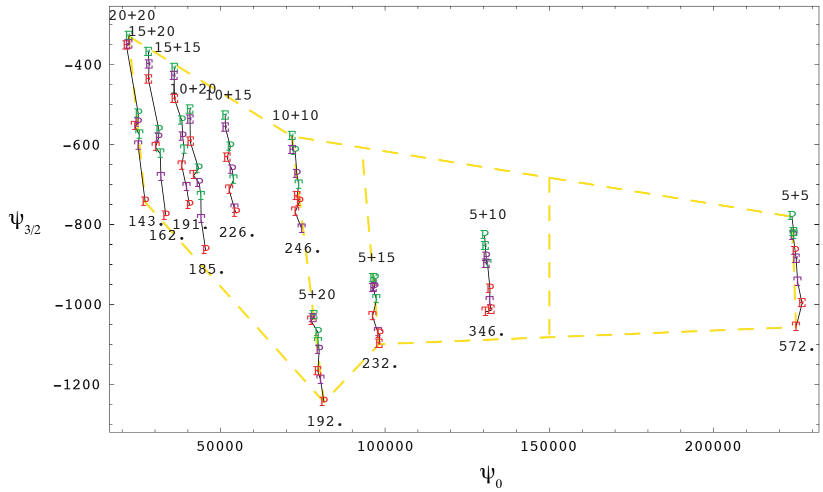

FIG. 1: Projection points with mass lines, restricted to the following models: T(2, 2), T(3, 7/2, 2), T(3, 7/2, −2); P(2, 5/2), P(3, 7/2, 2), P(3, 7/2, −2); EP(2, 5/2), EP(3, 7/2, 2), EP(3, 7/2, −2) when the $(\psi_0, \psi_{3/2})_{\alpha,\mathrm{cutoff}}$ template family is used. Mass configurations and minimal ending/cutoff frequencies are marked at the top and bottom of the corresponding mass lines. Models with different PN expansion techniques are marked by different letters, T, P and E (which stands for EP); while different PN orders are illustrated by color, red (for 2 or 2.5 PN), green (for 3 PN with with $\hat{\theta} = 2$) and blue (for 3 PN with $\hat{\theta} = +2$). The region spanned by these projections are scoped out roughly by the yellow dashed lines. This region is further divided into four subregions, which require different sets of cutoff frequencies.

For the two-body models listed in Table I (henceforth denoted by restricted models), we summarize in Figs. 1, 2 and Table III the main results obtained in BCV1 with LIGO-I noise curve. In Fig. 1 we show the projection of the template space spanned by the DTF on the $(\psi_0, \psi_{3/2})$ plane. In the plot we have linked the points that correspond to the same BBH parameters in different PN models. In BCV1 these lines were denoted *BH mass lines*. In Fig. 2 we compare it to the full region proposed in BCV1 which includes all the 17 two-body models investigated. The full region was obtained assuming that the projection of the true BBH waveform onto the $(\psi_0, \psi_{3/2})$ plane would lie near the BH mass line with the true BBH parameters, or perhaps near the extension of the BH mass line in either direction. For this reason we suggested to lay down the detection templates in the region traced out by extending the BH mass lines (of the 17 two-body models) in both directions by half of their length. [We note that this extension is rather arbitrary.] In BCV1 we estimated the number of templates associated to the full region: $\mathcal{N}_{\mathrm{templates}} \simeq 10^4$ with minimal-match (MM) MM $= 0.96$. If we consider only the models listed in Table I we obtain: $\mathcal{N}_{\mathrm{templates}} \simeq 2150$ with MM $= 0.96$.

II. PERFORMANCES OF DTF WITH S2 NOISE CURVES

The noise curves of Hanford (H1, H2) and Livingston (L1) interferometers during the S2 runs [see Fig. 3] are different from each other and from that of the LIGO-I goal (LIGO-I in short), in both the bandwidth, and the frequency of best sensitivity. Because of these differences, we expect the performances (FF's) of our DTF to differ from each other and from those evaluated in BCV1, depending on the binary masses. In the following studies, we use the noise curves shown on the right panel of Fig. 3, obtained by a fit to the S2 noise curves shown on the left panel.

In Figs. 4 we plot the signal-to-noise ratio (SNR) versus binary total mass, assuming equal masses ($\eta = 1/4$), for optimal matching using LIGO-I and S2 noise curves. As an example, the SNR is calculated using (i) the Fourier amplitude for the model T(2,2) (continuous curve) [7], (ii) the Newtonian Fourier amplitude ($\propto f^{-7/6}$) cut at the ending frequency (which in this case corresponds to the minimum of the 2PN orbital energy for quasi-circular orbits) (dashed curve), and (iii) the Newtonian Fourier amplitude cut at the Schwarzschild ISCO ($f_{\mathrm{ISCO}} \simeq 4400/M$) (dotted curve). The difference between (i) and (ii) is due to two reasons: the deviation of amplitude evolution from that of the Newtonian during the late stage, and the fact that we cut the signal abruptly in the time domain. The difference arises because the signal terminates in the detection band. [These effects will be analysed in more details in Sec. III.] From the continuous lines plotted in Figs. 4 we deduce that while for LIGO-I the SNR reaches a maximum around $M \sim 40M_\odot$, for the S2-noise curves it does around $M \sim 24M_\odot$. This suggests that the FF's evaluated with the S2-noise curves start decreasing for $M > 24M_\odot$ (see discussion below).

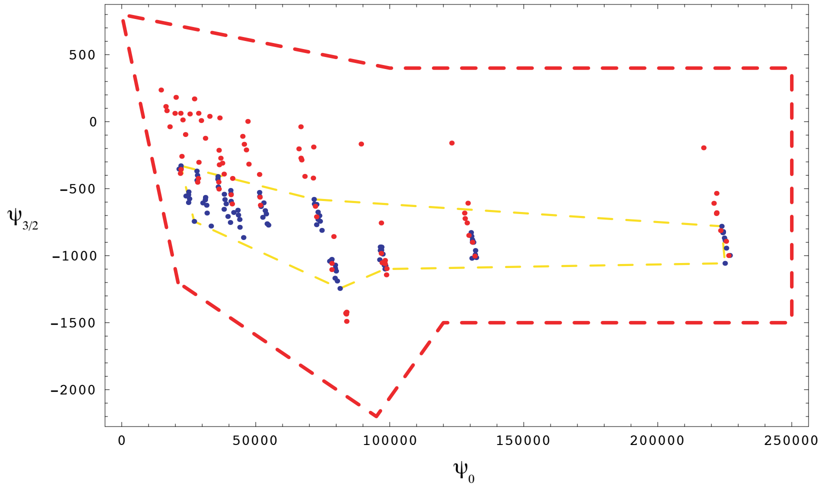

FIG. 2: Comparison between the restricted region of search (bounded by yellow dashed lines) and the full region proposed in BCV1 (bounded by red dashed lines). Projections of the restricted models are shown in blue dots, others are shown in red.

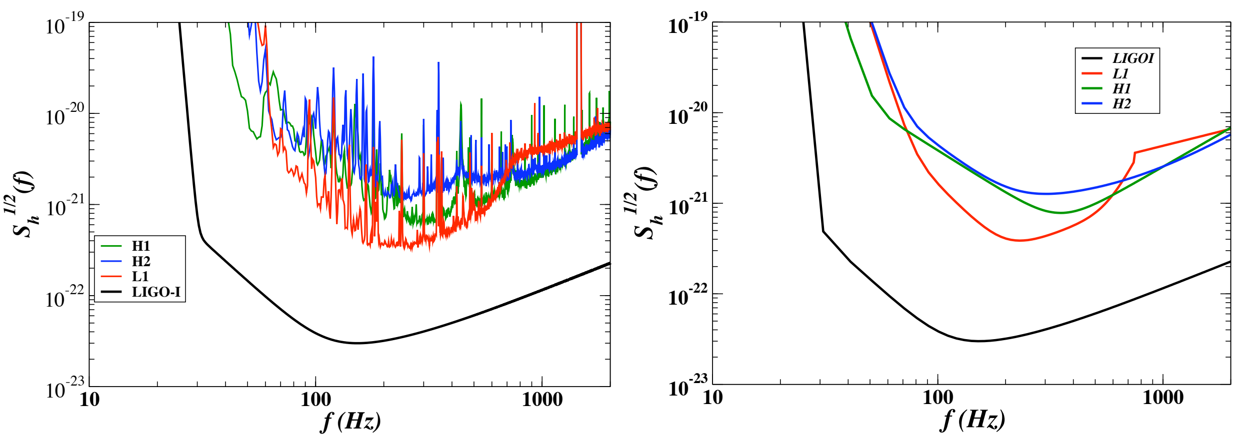

FIG. 3: In the left panel we show the sensitivity during S2 runs [from Peter S]. In the right panel we plot the noise curves we use in our calculations. They were obtained by fitting the noise curves in the left panel.

In Tables V–XIII we list the FF's for the same range of masses used in BCV1, i.e., $m_{1,2} = 5, 10, 15, 20 M_\odot$, and also for the new range of masses $m_{1,2} = 1, 3, 6, 9, 12 M_\odot$.

In Figs. 5, 6 and 7, we plot the $(\psi_0, \psi_{3/2})$ section (upper panels) and the $(\mathcal{M}, \psi_{3/2})$ section (lower panels) (being $\mathcal{M}$ the chirp mass) of the PN-model projections into the $(\psi_0, \psi_{3/2}, f_{\rm cutoff})$ space, using S2-H1, S2-H2 and S2-L1 noise curves, respectively. The solid circles, squares, diamonds show the BBHs with the same set of fifteen mass pairs as in Tables VI, IX and XII. Generally, each PN model is projected to a curved-triangular region, with boundaries given by the sequences of BBHs with masses $(m + m)$ (equal mass), $(12 + m)$ and $(m + 1)$. Since we have many points, we do not show the curved-triangular regions.

In Figs. 8, 9 and 10, we plot the $(\psi_0, \psi_{3/2})$ section of the PN-model projections for the LIGO-I, S2-H1, S2-H2 and S2-L1 noise curves for the BH masses $m_{1,2} = 1, 3, 6, 9, 12 M_\odot$ and the BH masses $m_{1,2} = 5, 10, 15, 20 M_\odot$.

From the figures and the tables we observe the following:

- With the S2 noise curves, except for the EOB two-body model, the FF's for total masses $M > 24 M_\odot$ decrease to values < 0.95. This lowering of the FF's can be explained in part by observing that the SNR reaches a maximum around $M = 24 M_\odot$, but also because of *tail effects*. Because the signal is abruptly cut in time domain the Fourier-domain signal has power also at frequencies larger than the ending frequency.

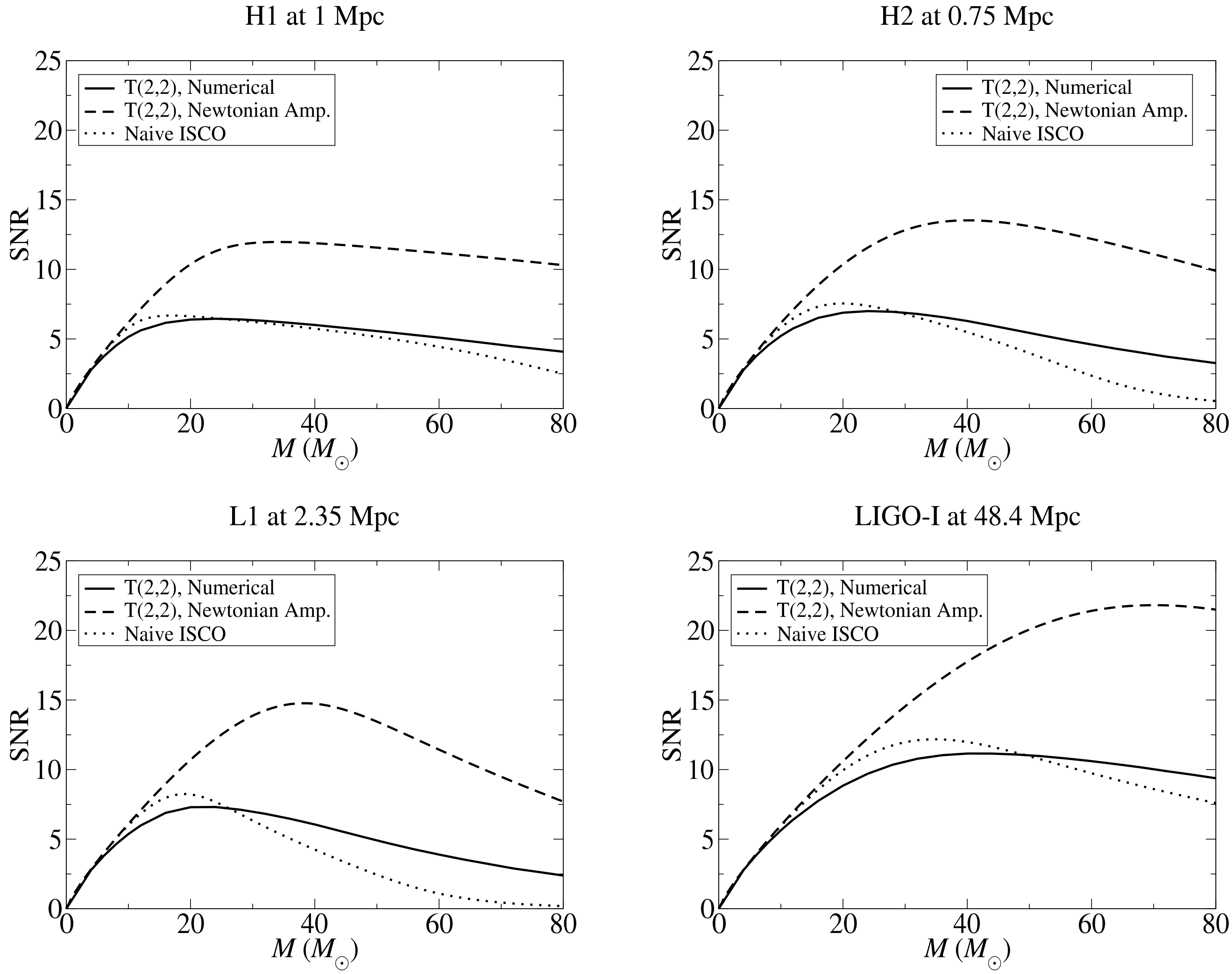

FIG. 4: SNR evaluated from T(2,2) model [with numerical (continuous curve) and Newtonian (dashed curve) amplitudes] and from Newtonian amplitude cut off at Naive ISCO (dotted curve), for H1, H2, L1 and LIGO-I noise curves.

- The FF's for binary masses with $m_{1,2} = 1M_\odot$ can be smaller than 0.95 when S2-H1 noise curve is used. For these binaries, the GW signal lasts for many cycles in the interferometer frequency band, and to obtain a high FF the target and template phasing should match extremely well. Since the phase of our DTF contains only two terms among the ones predicted by PN calculations, we think that the two parameters ψ_0 and $\psi_{3/2}$ cannot match extremely well the target phasing both at low and high frequency. With S2-H2 and S2-L1 noise curves the FF's can still be rather high and this can be explained noticing that the S2-H2 and S2-L1 frequency band are shorter than the frequency band of S2-H1.

- The mass lines evaluated with S2-H1, S2-H2 and S2-L1 noise curves are sometime displaced from the LIGO-I mass lines. However, for BH masses $m_{1,2} = 5, 10, 15, 20M_\odot$, the full region that was suggested in BCV1 can still be used, as the S2 mass lines are inside that region.

- As already noticed in BCV1 the T(2,5/2) model is always very distant from the other two-body models. The reason is that at 2.5PN order the GW flux goes to zero at frequencies inside the LIGO band, well before the ending frequency criterion (minimum of orbital energy) can be applied. We could have a reduction of the number of templates (by a factor ~ 5) if we exclude the T(2,5/2) model.

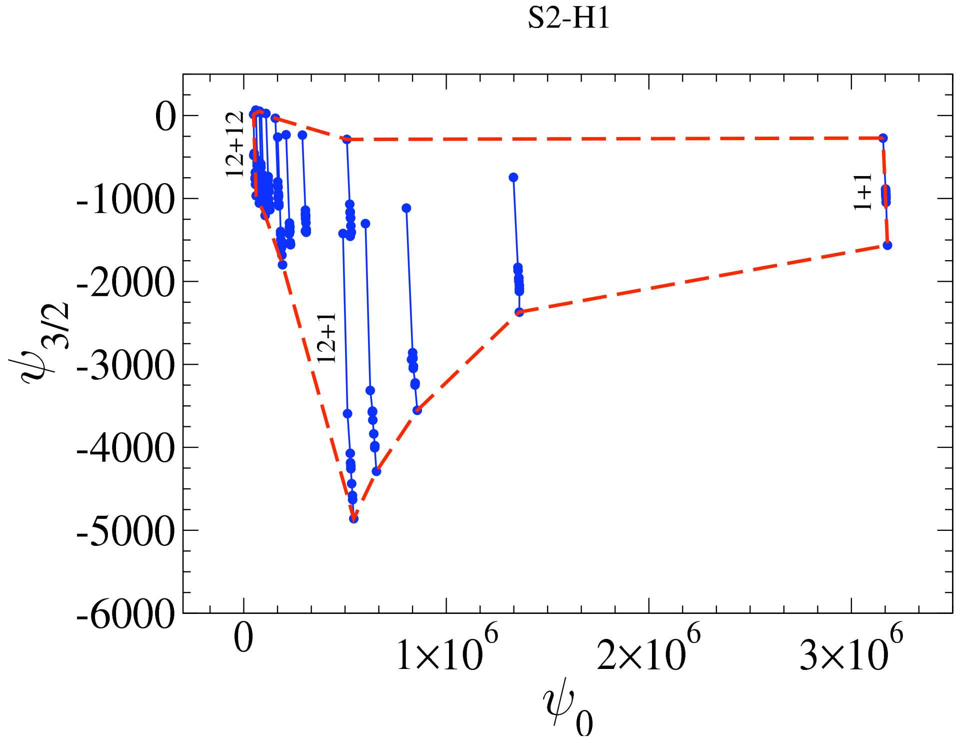

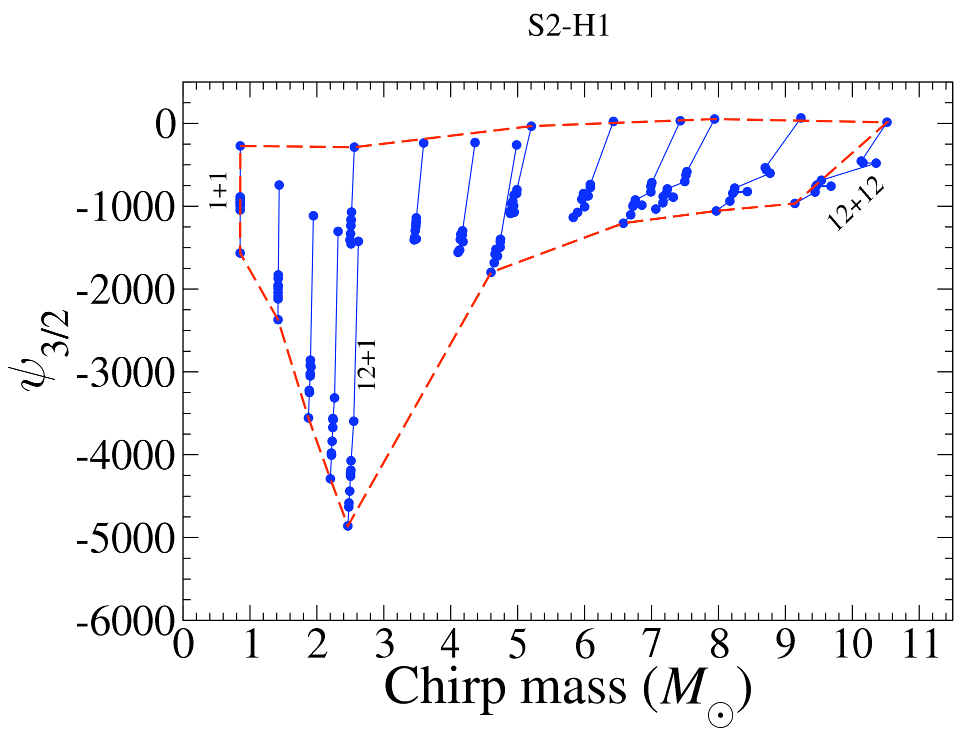

FIG. 5: Projection points with mass lines restricted to the following models: T(2, 5/2), T(2, 2), T(3, 7/2, 2), T(3, 7/2, −2); P(2, 5/2),P(3, 7/2, 2), P(3, 7/2, −2); EP(2, 5/2), EP(3, 7/2, 2), EP(3, 7/2, −2) when the $(\psi_0, \psi_{3/2})_{\alpha,\mathrm{cutoff}}$ template family is used with S2-H1 noise curve. The mass lines refer to the BH masses $m_{1,2} = 1, 3, 6, 9, 12 M_\odot$. The data are listed in Table VI. For each mass lines the T(2,5/2) model is always the first from the top.

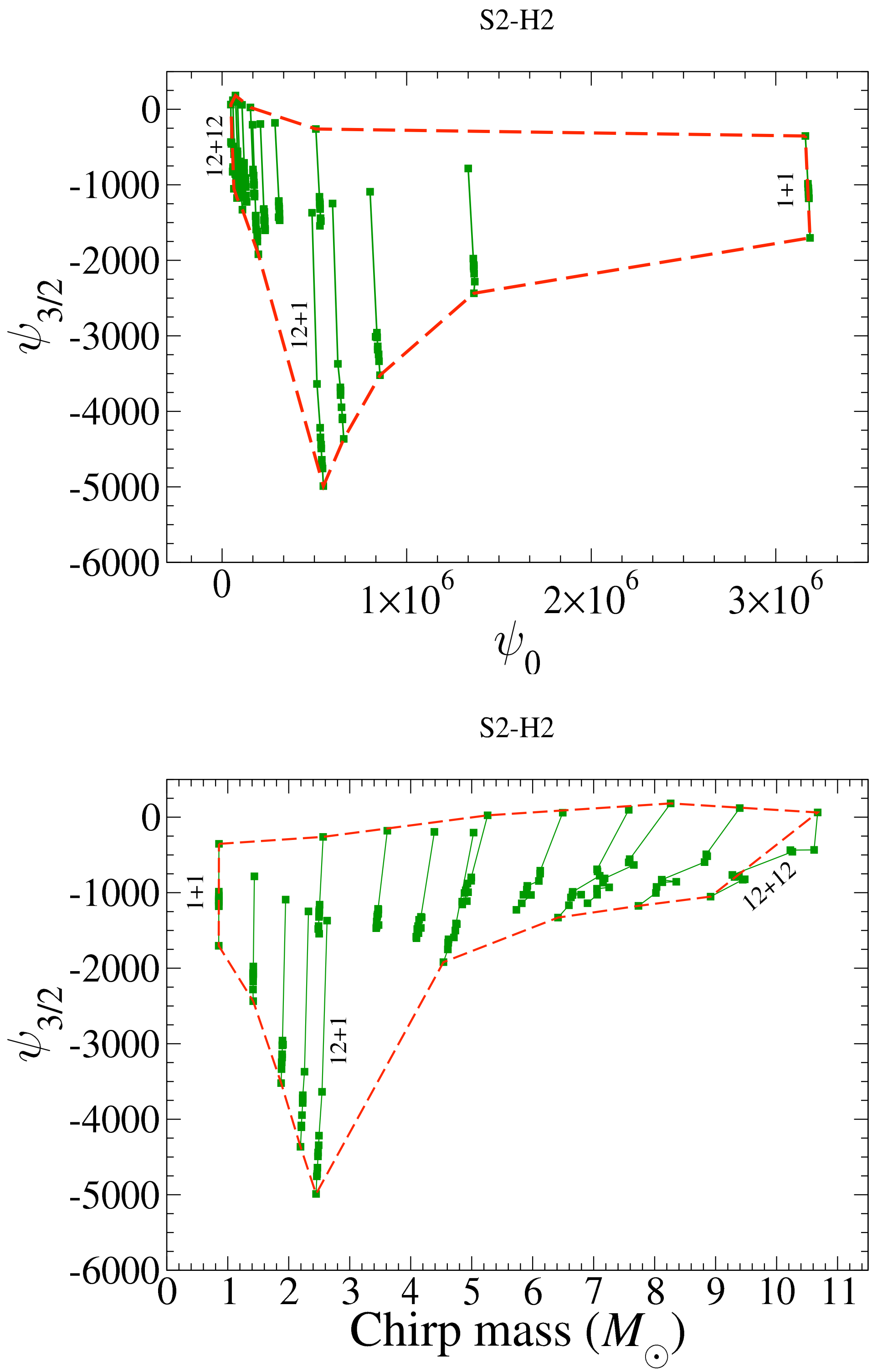

FIG. 6: Projection points with mass lines restricted to the following models: T(2, 5/2), T(2, 2), T(3, 7/2, 2), T(3, 7/2, −2); P(2, 5/2),P(3, 7/2, 2), P(3, 7/2, −2); EP(2, 5/2), EP(3, 7/2, 2), EP(3, 7/2, −2) when the $(\psi_0, \psi_{3/2})_{\alpha,\mathrm{cutoff}}$ template family is used with S2-H2 noise curve. The mass lines refer to the BH masses $m_{1,2} = 1, 3, 6, 9, 12 M_\odot$. The data are listed in Table IX. For each mass lines the T(2,5/2) model is always the first from the top.

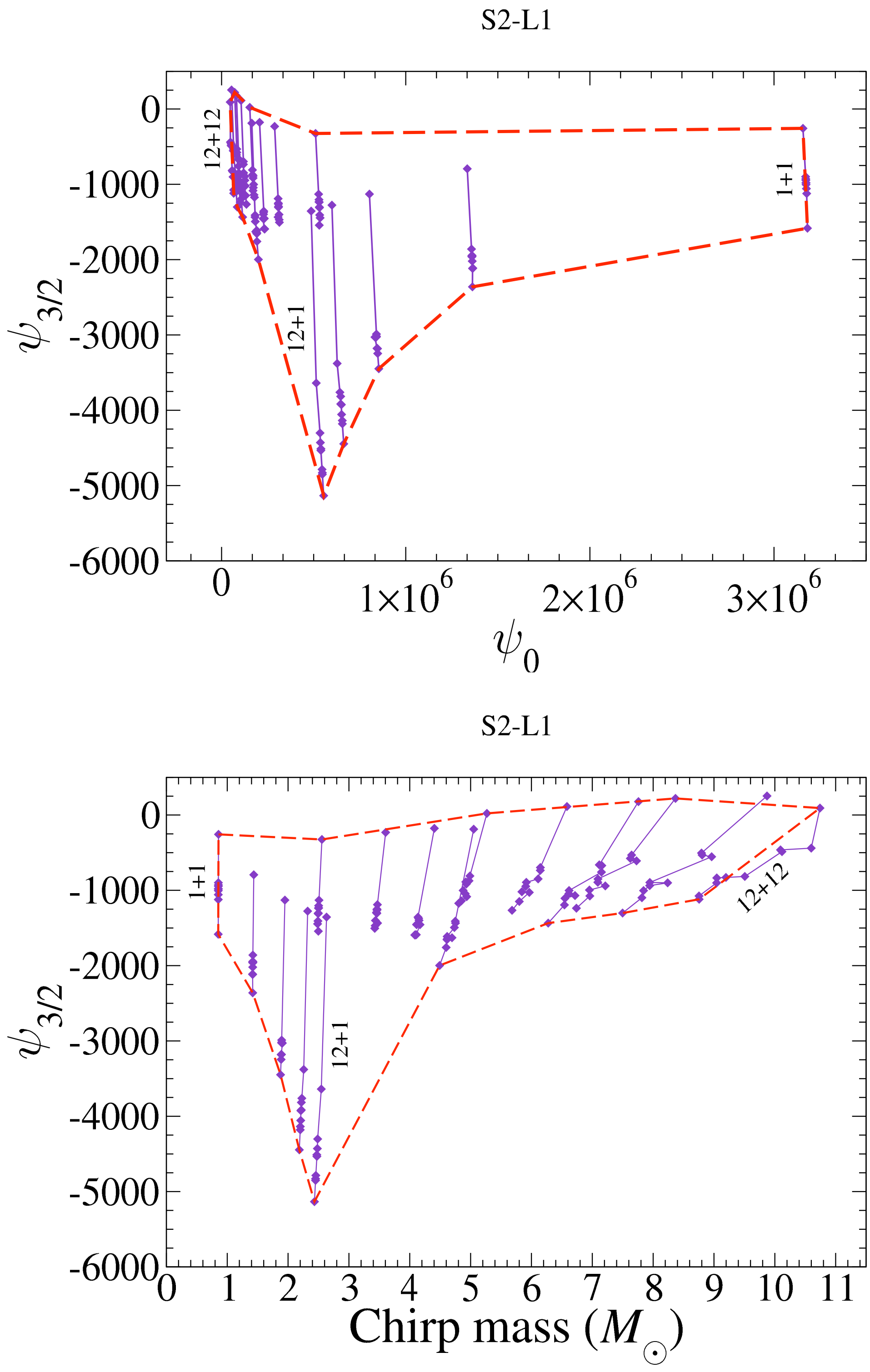

FIG. 7: Projection points with mass lines restricted to the following models: $T(2, 5/2)$, $T(2, 2)$, $T(3, 7/2, 2)$, $T(3, 7/2, -2)$; $P(2, 5/2)$,$P(3, 7/2, 2)$, $P(3, 7/2, -2)$; $EP(2, 5/2)$, $EP(3, 7/2, 2)$, $EP(3, 7/2, -2)$ when the $(\psi_0, \psi_{3/2})_{\alpha,\mathrm{cutoff}}$ template family is used with S2-H1 noise curve. The mass lines refer to the BH masses $m_{1,2} = 1, 3, 6, 9, 12 M_\odot$. The data are listed in Table XII. For each mass lines the T(2,5/2) model is always the first from the top.

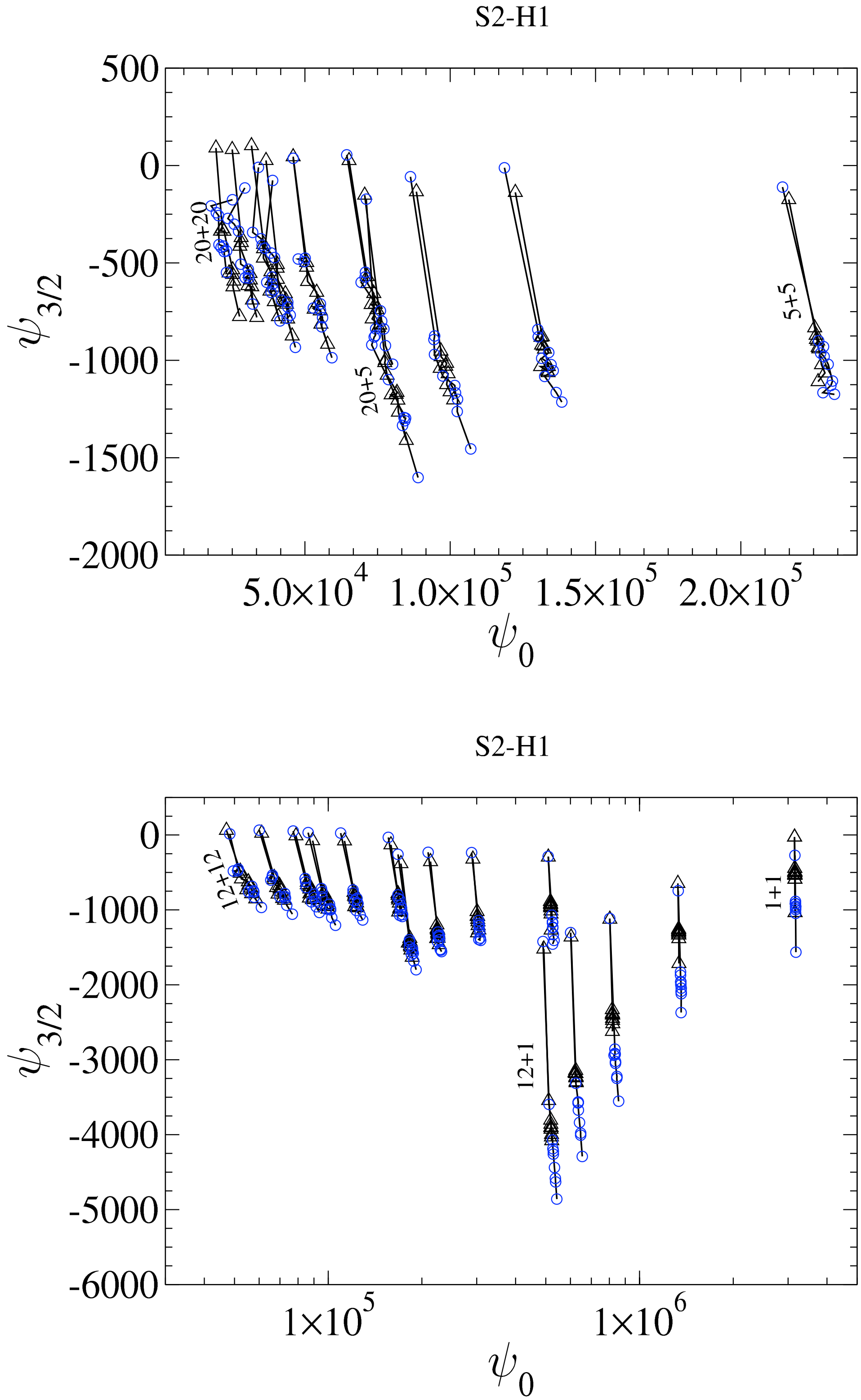

FIG. 8: Projection points with mass lines restricted to the following models: T$(2, 5/2)$, T$(2, 2)$, T$(3, 7/2, 2)$, T$(3, 7/2, -2)$; P$(2, 5/2)$,P$(3, 7/2, 2)$, P$(3, 7/2, -2)$; EP$(2, 5/2)$, EP$(3, 7/2, 2)$, EP$(3, 7/2, -2)$ when the $(\psi_0, \psi_{3/2})_{\alpha,\mathrm{cutoff}}$ template family is used with LIGO-I (black triangles) and S2-H1 (blue circles) noise curves. The mass lines refer to the BH masses $m_{1,2} = 5, 10, 15, 20 M_\odot$ (upper panel) or $m_{1,2} = 1, 3, 6, 9, 12 M_\odot$ (lower panel). For each mass lines the T(2,5/2) model is always the first from the top.
.

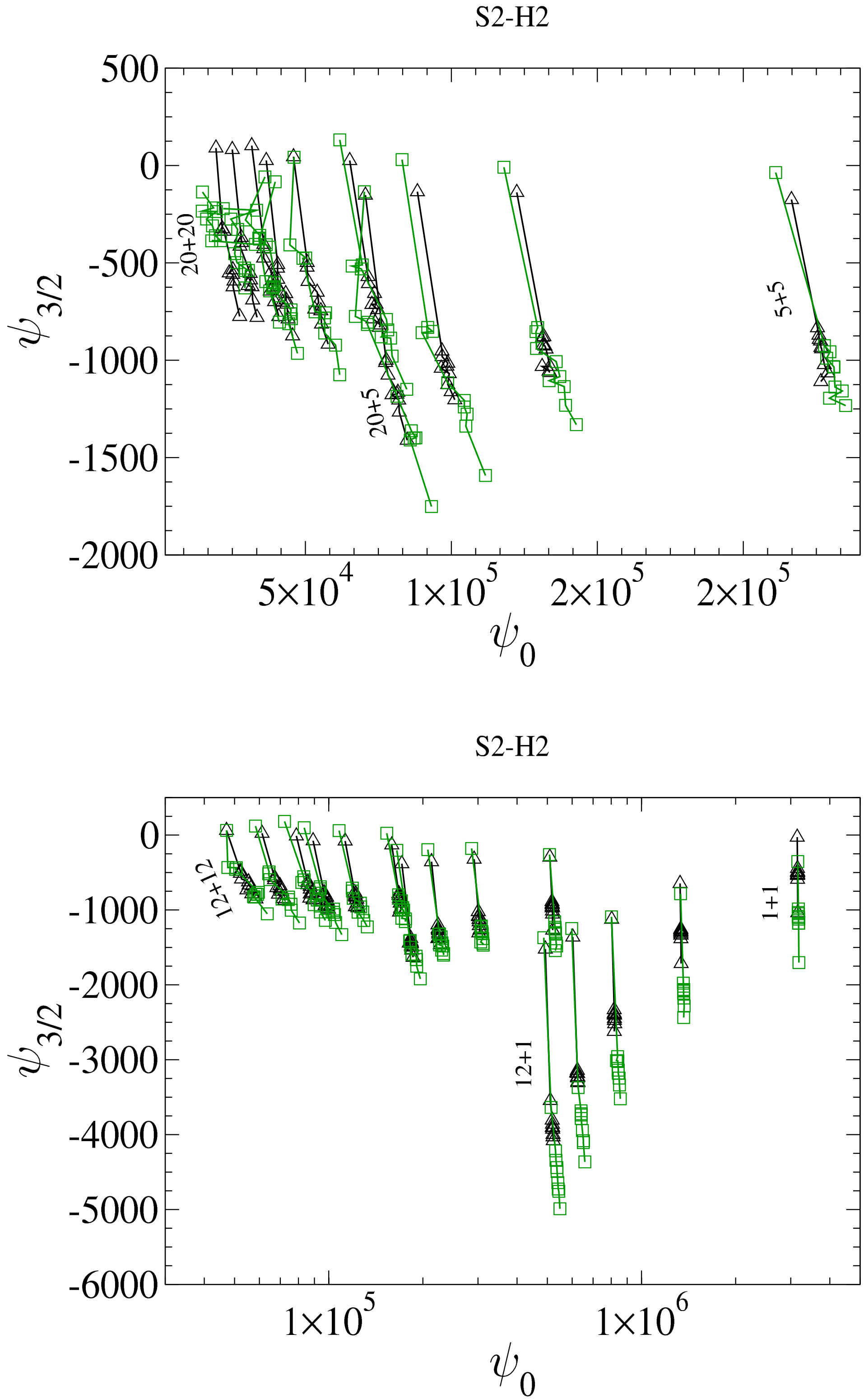

FIG. 9: Projection points with mass lines restricted to the following models: T$(2, 5/2)$, T$(2, 2)$, T$(3, 7/2, 2)$, T$(3, 7/2, -2)$; P$(2, 5/2)$,P$(3, 7/2, 2)$, P$(3, 7/2, -2)$; EP$(2, 5/2)$, EP$(3, 7/2, 2)$, EP$(3, 7/2, -2)$ when the $(\psi_0, \psi_{3/2})_{\alpha,\mathrm{cutoff}}$ template family is used with LIGO-I (black triangles) and S2-H2 (green squres) noise curves. The mass lines refer to the BH masses $m_{1,2} = 5, 10, 15, 20 M_\odot$ (upper panel) or $m_{1,2} = 1, 3, 6, 9, 12 M_\odot$ (lower panel). For each mass lines the T(2,5/2) model is always the first from the top. .

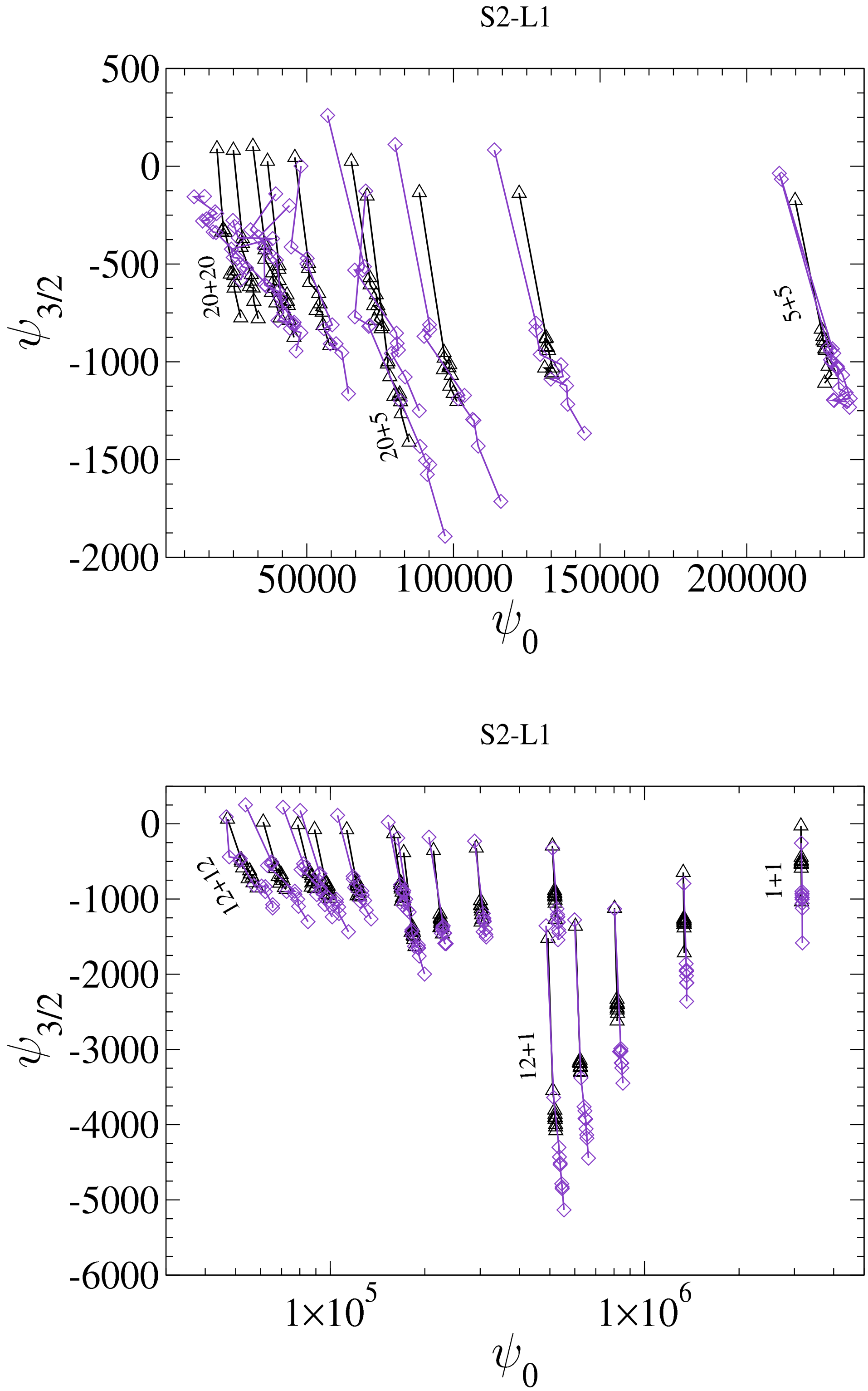

FIG. 10: Projection points with mass lines restricted to the following models: T(2, 5/2), T(2, 2), T(3, 7/2, 2), T(3, 7/2, −2); P(2, 5/2),P(3, 7/2, 2), P(3, 7/2, −2); EP(2, 5/2), EP(3, 7/2, 2), EP(3, 7/2, −2) when the $(\psi_0, \psi_{3/2})_{\alpha,\mathrm{cutoff}}$ template family is used with LIGO-I (black triangles) and S2-L1 (purple diamonds) noise curves. The mass lines refer to the BH masses $m_{1,2} = 5, 10, 15, 20 M_\odot$ (upper panel) or $m_{1,2} = 1, 3, 6, 9, 12 M_\odot$ (lower panel). For each mass lines the T(2,5/2) model is always the first from the top. .

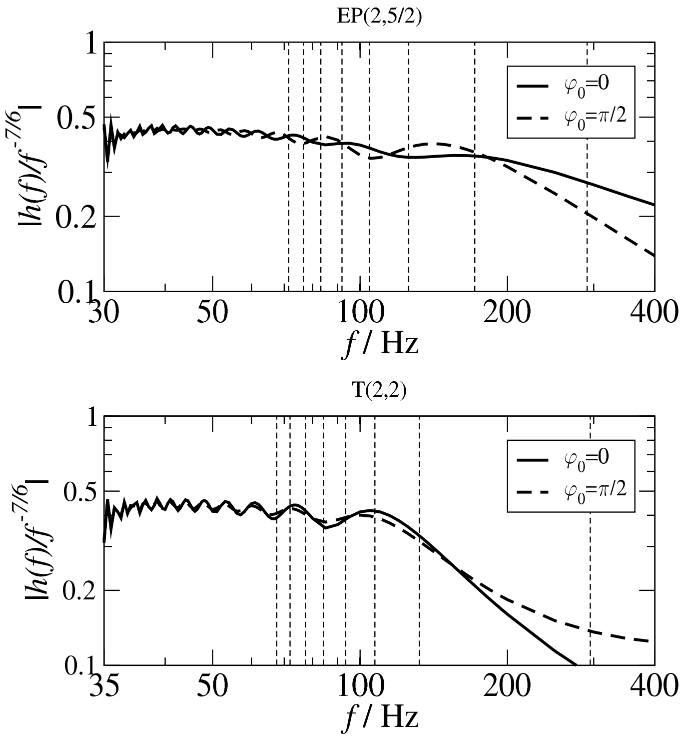

FIG. 11: Frequency-domain amplitude $|h(f)|$ normalized to the Newtonian prediction $f^{-7/6}$ for EP(2,5/2) (upper panel) and T(2,2) (lower panel) models, with initial GW phase $\varphi_0 = 0$ (thick continuous curve) and $\pi/2$ (thick dashed curve). Also shown are vertical lines at the ending frequency, and the instantanesou frequencies 1,2,3,. . . 7 GW cycles before the end.

III. THE SIGNIFICANCE OF THE LAST GW CYCLES

To better understand why the FF's decrease as we increase the binary total mass we investigated the significance of the last GW cycles in the adiabatic model T(2,2) and the non-adiabatic EOB model EP(2,5/2).

As pointed out in BCV1, for GW signals that end in the interferometer frequency band, is crucial to match extremely well not only the phase but also the amplitude. In Figs. 11 we show the Fourier-domain amplitude (normalized by the Newtonian amplitude $f^{-7/6}$) for the T(2,2) (lower) and the EP(2,5/2) (upper panel) models, for a $(15 + 15)M_\odot$ binary. The two curves in each panel refer to the initial orbital phases $\varphi_0 = 0$ (continuous) and $\varphi_0 = \pi/2$ (dashed). The vertical (thin dashed) lines correspond to the instantaneous GW frequency at times when $0, 1, \cdots, 7$ GW cycles are left. From the location of the vertical lines, we notice that whereas in the T(2,2) model the frequency when the last cycle starts is almost half the ending frequency, in the EP(2,5/2) model the increase in frequency during the last cycle is milder. Moreover, the EP(2,5/2) model has more cycles than the T(2,2) model in the high frequency band and this explains why $|h(f)|$ remains closer to the Newtonian prediction $f^{-7/6}$ in the EOB case. In this sense, the EOB waveforms (for equal-mass binaries) appear to be more "adiabatic" than the T waveforms in the final stage of inspiral. Note that the last cycle in the EOB model is the "plunge cycle", i.e. it describes the evolution beyond the EOB's ISCO [4].

Let us investigate more quantitatively how the above phenomenon affect the detection, and the significance of the last cycles and tail effects. For T(2,2) and EP(2,5/2) models, we have listed in Table II (using LIGO-I design sensitivity) the instantaneous frequencies when 0,1,2,. . . 7 GW cycles are left, and the corresponding fractional SNR squared (with respect to the full SNR achievable with the entire signal) if this portion of signal is detected with perfect match. [We evaluate the SNR squared since it accumulates additively, we shall call it the "signal power".] We note that there are two ways to characterize the fractional signal power: we can cut the signal either in the time domain, or in the frequency domain, at the corresponding instantaneous frequency. From Table II it is striking to note that the last few cycles contains most of the signal power. From both ways of evaluating the SNR, we see that the last 3 GW cycles carry more than 50% of the signal power, while the last cycle carries almost 20% of the signal power. However, for T(2,2) model, the last cycle suffer more from tail effects and non-adiabaticities, as we see in Fig. 11, this makes this model harder to detect with the BCV templates. Indeed, because of tail effects, when we increase the total

	T(2,2)			EP(2,5/2)		
Number of cycles left	frequency	time-domain fractional sig. power	frequency-domain fractional sig. power	frequency	time-domain fractional sig. power	frequency-domain fractional sig. power
0	295.17	1.000	0.997	290.81	1.000	0.975
1	132.18	0.747	0.821	171.45	0.766	0.819
2	107.24	0.562	0.577	125.66	0.572	0.600
3	93.45	0.434	0.411	104.52	0.434	0.448
4	84.17	0.344	0.327	91.87	0.338	0.336
5	77.32	0.280	0.266	83.15	0.271	0.264
6	71.95	0.231	0.211	76.62	0.222	0.213
7	67.59	0.194	0.174	71.50	0.185	0.173

TABLE II: Instantaneous frequencies and fractional signal power (SNR squared) when 0,1,2,. . . 7 GW cycles are left, for T(2,2) and EP(2,5/2) models.

mass binary (or shift the peak sensitivity at much higher frequencies, as happens in the S2 noise curves), the signal power coming from the inspiral motion decrease more and more, and the tail part become more and more important. In this case our DTF tries to match the tail part but it cannot do it very well because of the special choice of the DTF's amplitude (2) we made.

IV. PRELIMINARY CONCLUSIONS AND FUTURE DIRECTIONS

The research done so far would suggest that it is robust (FF > 0.97) to use the DTF for binaries with single BH mass 3–12$M_\odot$ [see Fig. 12, 13]. For binaries with single BH mass 12–20$M_\odot$ the DTF have high FF's only with the non-adiabatic EOB model. For binaries with single BH mass $1M_\odot$ the FF's with S2-H2 and S2-L1 noise curves are higher than 0.95, but with S2-H1 noise curves they can be lower than 0.95.

The following are items which could be tackled in the near future:

- Monte Carlo simulation to evaluate the efficiency of the DTF.
- How to extend the $(\psi_0, \psi_{3/2})$ template region for single BH mass 3–12$M_\odot$ using physical motivations.
- Lay down templates for the region of single BH mass 3–12$M_\odot$ including the cutoff frequency. The parameter α in Eq. (2) should be treated as extrinsic parameter.
- If we want to have high FF's with binaries with single BH mass $> 12M_\odot$ we could modify the DTF's amplitude (2) used in BCV1.
- For low masses ($m_{1,2} = 1$–$3M_\odot$), we could compare the results obtained with our DTF with a modified version of SPA templates at 2PN order which includes the modification of the amplitude (α parameter) and the cutoff frequency.

Acknowledgments

We wish to thank B.S. Sathyaprakash and Peter Shawhan for very useful discussions.

A. B. thanks the LIGO Caltech Laboratory under NSF cooperative agreement PHY92-10038 for support and the Theoretical Astrophysics group for hospitality during her visit at Caltech during the summer 2003. The research of Y. C. was supported by NSF grant PHY-0099568, NASA grant NAG5-12834, and by the David and Barbara Groce Fund at the San Diego Foundation. M. V. performed this research at the Jet Propulsion Laboratory, California Institute of Technology, under contract with the National Aeronautics and Space Administration.

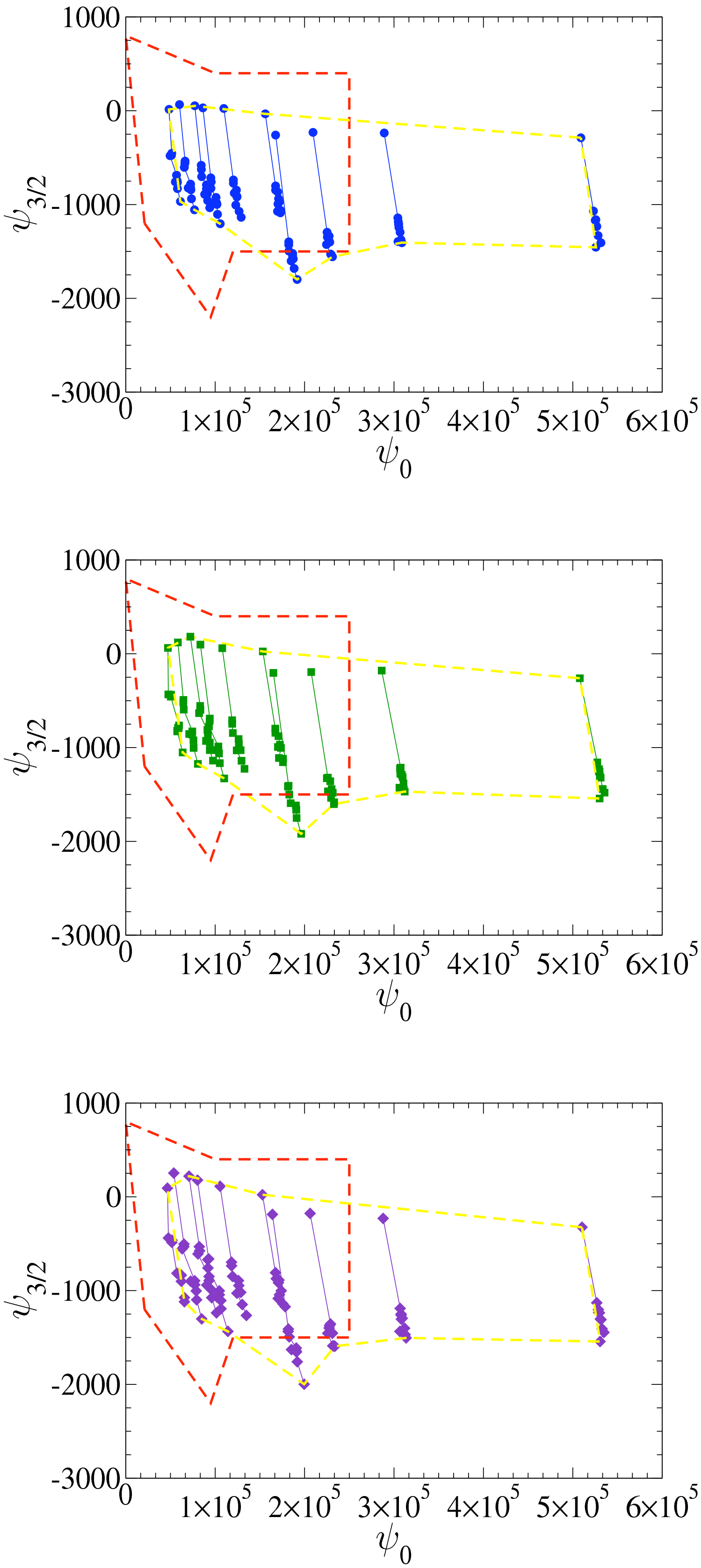

FIG. 12: Regions for (ψ_0,$\psi_{3/2}$) for the range of masses 3–12 $M_\odot$ (yellow dashed line), with S2-H1 (upper panel), S2-H2 (middle panel) and S2-L1 (lower panel) noise curves; compared with the full region proposed in BCV1 (red dashed line) for 5–20 $M_\odot$ binaries, for LIGO-I noise curve.

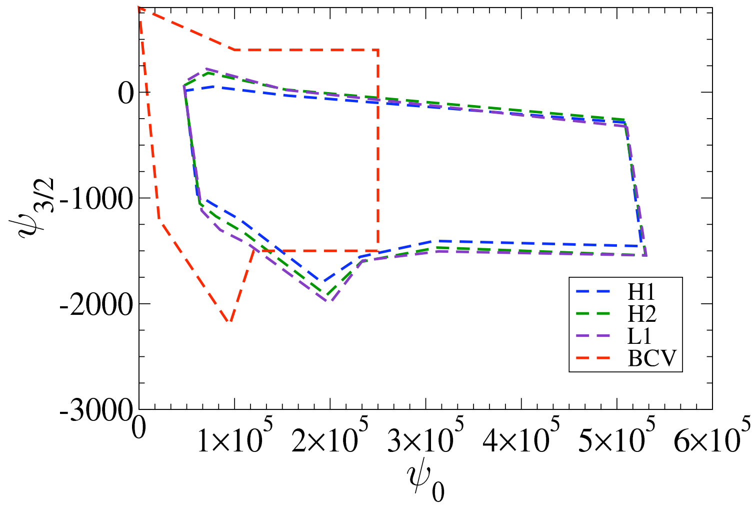

FIG. 13: Comparison between the regions (ψ_0,$\psi_{3/2}$) spanned by the DTF for binaries of total mass 3–12 $M_\odot$ when S2-H1, S2-H2 and S2-L1 noise curves are used [see Fig. 12] and the full region proposed in BCV1 (red dashed line) for 5–20 $M_\odot$ binaries, for LIGO-I noise curve.

PN model	FF (minmax) with $(\psi_0, \psi_{3/2})_{\alpha,\mathrm{cut}}$ template family when LIGO-I noise curve is used	f_{end}	mn	ψ_0	$\psi_{3/2}$	$\alpha f_{\mathrm{cut}}^{2/3}$	f_{cut}		f_{end}	mn	ψ_0	$\psi_{3/2}$	$\alpha f_{\mathrm{cut}}^{2/3}$	f_{cut}
	$(20{+}20)M_\odot$	221.4	0.982	23913.	−551.10	0.997	284.3	$(20{+}5)M_\odot$	341.1	0.991	78308.	−1076.30	0.998	417.6
	$(20{+}15)M_\odot$	252.5	0.985	30393.	−616.02	1.000	281.2	$(10{+}10)M_\odot$	442.7	0.992	73129.	−787.29	1.007	559.8
$T(2,2)$	$(15{+}15)M_\odot$	295.1	0.988	37966.	−644.53	1.001	328.7	$(15{+}5)M_\odot$	431.3	0.994	96536.	−1040.90	0.997	568.1
	$(20{+}10)M_\odot$	291.7	0.989	42194.	−701.85	0.998	333.1	$(10{+}5)M_\odot$	583.4	0.995	131100.	−1032.00	0.951	770.6
	$(15{+}10)M_\odot$	352.7	0.990	53194.	−737.35	1.000	417.2	$(5{+}5)M_\odot$	885.5	0.995	226560.	−1109.30	1.118	1700.5
	$(20{+}20)M_\odot$	160.8	0.970	19380.	90.11	0.539	203.3	$(20{+}5)M_\odot$	282.0	0.987	70577.	−151.97	0.235	312.7
	$(20{+}15)M_\odot$	185.3	0.975	24976.	82.49	0.387	218.6	$(10{+}10)M_\odot$	324.2	0.987	65181.	25.68	0.055	361.5
$T(2,2.5)$	$(15{+}15)M_\odot$	215.7	0.979	31624.	101.99	0.174	249.8	$(15{+}5)M_\odot$	345.9	0.988	88366.	−134.40	0.109	380.0
	$(20{+}10)M_\odot$	219.8	0.980	36607.	25.92	0.246	251.5	$(10{+}5)M_\odot$	444.5	0.991	122400.	−137.89	0.000	460.1
	$(15{+}10)M_\odot$	260.4	0.984	45946.	45.34	0.140	294.6	$(5{+}5)M_\odot$	644.5	0.994	216480.	−174.82	0.045	640.0
	$(20{+}20)M_\odot$	207.9	0.976	26509.	−678.73	1.228	333.9	$(20{+}5)M_\odot$	276.1	0.988	81961.	−1229.30	1.000	344.7
	$(20{+}15)M_\odot$	234.5	0.985	31779.	−653.27	1.000	260.2	$(10{+}10)M_\odot$	415.8	0.991	75057.	−785.95	1.011	524.6
$T(3,3.5,0)$	$(15{+}15)M_\odot$	277.2	0.988	39394.	−669.35	0.999	313.4	$(15{+}5)M_\odot$	362.3	0.990	99488.	−1109.90	0.783	339.1
	$(20{+}10)M_\odot$	259.2	0.986	43912.	−752.47	0.999	299.8	$(10{+}5)M_\odot$	518.5	0.992	132920.	−996.93	1.044	729.0
	$(15{+}10)M_\odot$	324.3	0.989	55773.	−798.52	1.000	385.0	$(5{+}5)M_\odot$	831.7	0.991	226940.	−955.89	1.208	1668.9
	$(20{+}20)M_\odot$	207.9	0.976	25224.	−622.47	1.000	257.4	$(20{+}5)M_\odot$	276.1	0.988	82147.	−1265.90	1.002	343.7
	$(20{+}15)M_\odot$	234.5	0.983	31948.	−690.24	0.999	253.3	$(10{+}10)M_\odot$	415.9	0.991	75353.	−830.80	1.025	501.8
$T(3,3.5,-2)$	$(15{+}15)M_\odot$	277.2	0.988	39467.	−698.74	1.000	308.5	$(15{+}5)M_\odot$	362.3	0.990	99935.	−1161.30	1.003	462.1
	$(20{+}10)M_\odot$	259.3	0.986	44068.	−787.47	1.001	292.1	$(10{+}5)M_\odot$	518.5	0.992	133680.	−1063.00	1.181	884.5
	$(15{+}10)M_\odot$	324.3	0.989	55515.	−814.09	0.998	377.9	$(5{+}5)M_\odot$	831.7	0.991	227740.	−1022.20	1.018	1263.3
	$(20{+}20)M_\odot$	207.9	0.980	25528.	−592.85	1.000	237.6	$(20{+}5)M_\odot$	276.1	0.988	81378.	−1174.10	1.004	344.2
	$(20{+}15)M_\odot$	234.5	0.986	31709.	−622.41	1.015	286.6	$(10{+}10)M_\odot$	415.8	0.991	74749.	−739.58	0.928	472.6
$T(3,3.5,+2)$	$(15{+}15)M_\odot$	277.2	0.988	39078.	−623.95	1.001	323.7	$(15{+}5)M_\odot$	362.3	0.990	99275.	−1068.70	0.715	320.6
	$(20{+}10)M_\odot$	259.2	0.986	43662.	−711.69	0.999	303.1	$(10{+}5)M_\odot$	518.5	0.992	132420.	−942.21	1.091	807.8
	$(15{+}10)M_\odot$	324.3	0.988	55299.	−745.79	0.997	395.8	$(5{+}5)M_\odot$	831.7	0.992	226430.	−900.91	0.896	1218.2
	$(20{+}20)M_\odot$	142.9	0.968	27497.	−775.12	1.002	196.8	$(20{+}5)M_\odot$	207.8	0.981	84875.	−1410.70	1.002	267.3
	$(20{+}15)M_\odot$	162.5	0.978	33431.	−779.63	0.996	216.1	$(10{+}10)M_\odot$	285.9	0.986	75702.	−818.58	0.697	257.8
$P(2,2.5)$	$(15{+}15)M_\odot$	190.6	0.981	40892.	−775.60	0.999	250.5	$(15{+}5)M_\odot$	267.5	0.984	101170.	−1203.00	1.113	415.6
	$(20{+}10)M_\odot$	185.0	0.980	45619.	−874.88	1.000	240.4	$(10{+}5)M_\odot$	370.0	0.990	133780.	−1031.50	0.508	298.0
	$(15{+}10)M_\odot$	226.3	0.982	57802.	−917.24	1.000	297.6	$(5{+}5)M_\odot$	571.7	0.989	226820.	−940.67	0.799	754.0
	$(20{+}20)M_\odot$	216.4	0.983	25183.	−539.20	0.996	253.9	$(20{+}5)M_\odot$	265.0	0.986	81419.	−1156.50	1.006	344.7
	$(20{+}15)M_\odot$	243.6	0.986	31101.	−557.76	1.004	300.7	$(10{+}10)M_\odot$	432.8	0.991	73375.	−648.05	0.676	369.9
$P(3,3.5,0)$	$(15{+}15)M_\odot$	288.5	0.988	38568.	−565.61	1.042	361.3	$(15{+}5)M_\odot$	359.2	0.990	98590.	−1013.20	0.989	488.3
	$(20{+}10)M_\odot$	265.7	0.987	43200.	−657.79	0.999	328.0	$(10{+}5)M_\odot$	531.3	0.994	131300.	−867.60	0.491	379.5
	$(15{+}10)M_\odot$	336.1	0.988	54273.	−665.86	1.003	426.8	$(5{+}5)M_\odot$	865.6	0.994	225280.	−835.45	0.857	1261.4
	$(20{+}20)M_\odot$	216.4	0.980	25103.	−558.59	1.000	261.8	$(20{+}5)M_\odot$	265.0	0.987	81976.	−1204.00	1.003	340.3
	$(20{+}15)M_\odot$	243.6	0.984	31221.	−587.34	1.000	273.6	$(10{+}10)M_\odot$	432.8	0.991	74194.	−711.74	0.997	565.6
$P(3,3.5,-2)$	$(15{+}15)M_\odot$	288.5	0.988	38633.	−590.74	1.000	334.3	$(15{+}5)M_\odot$	359.2	0.990	98461.	−1030.30	0.725	314.8
	$(20{+}10)M_\odot$	265.7	0.986	43387.	−689.99	1.002	319.1	$(10{+}5)M_\odot$	531.3	0.993	132030.	−926.59	1.097	867.3
	$(15{+}10)M_\odot$	336.1	0.989	54550.	−703.27	0.999	405.8	$(5{+}5)M_\odot$	865.6	0.993	226000.	−892.45	1.006	1511.5
	$(20{+}20)M_\odot$	216.4	0.981	25149.	−535.00	0.999	255.3	$(20{+}5)M_\odot$	265.0	0.986	81685.	−1164.40	0.996	337.5
	$(20{+}15)M_\odot$	243.6	0.985	31109.	−553.53	1.001	288.7	$(10{+}10)M_\odot$	432.8	0.991	73695.	−656.88	0.733	394.4
$P(3,3.5,+2)$	$(15{+}15)M_\odot$	288.5	0.988	38299.	−545.10	1.000	345.6	$(15{+}5)M_\odot$	359.2	0.989	98777.	−1015.10	0.706	322.4
	$(20{+}10)M_\odot$	265.7	0.986	43273.	−657.68	1.002	328.1	$(10{+}5)M_\odot$	531.3	0.994	131690.	−878.59	0.509	394.2
	$(15{+}10)M_\odot$	336.1	0.989	54057.	−650.42	0.998	422.5	$(5{+}5)M_\odot$	865.6	0.994	225400.	−833.02	0.907	1456.6
	$(20{+}20)M_\odot$	218.1	0.989	20951.	−336.59	0.917	442.1	$(20{+}5)M_\odot$	345.8	0.988	79652.	−1177.00	0.668	352.2
	$(20{+}15)M_\odot$	249.1	0.989	27605.	−413.95	0.807	420.1	$(10{+}10)M_\odot$	436.2	0.991	72784.	−713.15	0.579	511.6
$EP(2,2.5)$	$(15{+}15)M_\odot$	290.8	0.989	35703.	−475.06	0.649	431.4	$(15{+}5)M_\odot$	433.1	0.992	98772.	−1124.40	0.629	435.8
	$(20{+}10)M_\odot$	289.8	0.988	40544.	−584.08	0.669	399.9	$(10{+}5)M_\odot$	579.6	0.995	133450.	−1055.90	0.601	624.3
	$(15{+}10)M_\odot$	348.5	0.989	50915.	−594.97	0.627	475.9	$(5{+}5)M_\odot$	872.4	0.991	228930.	−1064.60	0.790	1614.9
	$(20{+}20)M_\odot$	218.4	0.989	22099.	−336.11	1.001	406.6	$(20{+}5)M_\odot$	351.7	0.992	77846.	−1012.10	0.712	403.1
	$(20{+}15)M_\odot$	250.2	0.990	28066.	−373.39	1.002	498.2	$(10{+}10)M_\odot$	434.6	0.993	71305.	−569.35	0.657	617.0
$EP(3,3.5,0)$	$(15{+}15)M_\odot$	289.2	0.992	35672.	−403.06	1.002	629.9	$(15{+}5)M_\odot$	445.3	0.993	96708.	−953.27	0.715	550.4
	$(20{+}10)M_\odot$	294.3	0.991	40351.	−502.78	0.901	522.2	$(10{+}5)M_\odot$	581.6	0.996	131240.	−888.07	0.578	642.8
	$(15{+}10)M_\odot$	350.3	0.992	50456.	−494.22	0.809	600.8	$(5{+}5)M_\odot$	869.0	0.995	226080.	−885.82	0.679	1602.9
	$(20{+}20)M_\odot$	215.6	0.991	21559.	−324.79	1.048	480.3	$(20{+}5)M_\odot$	353.7	0.989	77463.	−1011.10	1.022	624.2
	$(20{+}15)M_\odot$	248.3	0.991	28115.	−395.18	1.002	472.9	$(10{+}10)M_\odot$	432.6	0.992	71595.	−606.33	0.667	579.8
$EP(3,3.5,-2)$	$(15{+}15)M_\odot$	284.9	0.991	35750.	−427.04	1.005	601.7	$(15{+}5)M_\odot$	439.0	0.994	96847.	−981.32	0.630	470.0
	$(20{+}10)M_\odot$	289.1	0.991	40460.	−526.95	1.038	607.4	$(10{+}5)M_\odot$	580.9	0.996	131430.	−921.47	0.588	641.1
	$(15{+}10)M_\odot$	347.1	0.990	50584.	−521.81	0.821	581.3	$(5{+}5)M_\odot$	864.2	0.995	226580.	−933.76	0.719	1668.8
	$(20{+}20)M_\odot$	220.2	0.990	22160.	−337.41	0.999	413.6	$(20{+}5)M_\odot$	351.8	0.991	77682.	−999.58	0.729	421.8
	$(20{+}15)M_\odot$	250.6	0.990	28043.	−369.49	1.002	490.6	$(10{+}10)M_\odot$	437.4	0.993	71448.	−570.24	0.661	604.6
$EP(3,3.5,+2)$	$(15{+}15)M_\odot$	292.7	0.991	35777.	−404.58	0.983	631.8	$(15{+}5)M_\odot$	443.1	0.994	96805.	−952.13	0.659	489.9
	$(20{+}10)M_\odot$	294.8	0.991	40526.	−508.08	0.907	515.3	$(10{+}5)M_\odot$	583.9	0.996	131240.	−881.57	0.552	633.6
	$(15{+}10)M_\odot$	353.5	0.991	50633.	−497.52	0.749	559.6	$(5{+}5)M_\odot$	872.0	0.995	225890.	−871.09	0.752	1757.4

TABLE III: Fitting factors for the projection of the target models (in the rows) onto the $(\psi_0, \psi_{3/2}, \alpha, f_{\mathrm{cut}})$ Fourier-domain detection template family when LIGO-I noise curve is used. For BBH masses $m_{1,2} = 5, 10, 15, 20 M_\odot$, this table shows the minmax matches between the target models and the Fourier-domain search model, *maximized over the intrinsic parameters* ψ_0, $\psi_{3/2}$, and f_{cut}, and over the extrinsic parameter α. For each intersection, the six numbers shown report the *ending frequency* f_{end} (defined in BCV1) of the PN model for the BBH masses quoted, the minmax FF mn, and the search parameters at which the maximum is attained.

	FF (minmax) with $(\psi_0, \psi_{3/2})_{\alpha,\mathrm{cut}}$ template family when LIGO-I noise curve is used													
PN model		f_{end}	mn	ψ_0	$\psi_{3/2}$	$\alpha f_{\mathrm{cut}}^{2/3}$	f_{cut}		f_{end}	mn	ψ_0	$\psi_{3/2}$	$\alpha f_{\mathrm{cut}}^{2/3}$	f_{cut}
	$(12{+}12)M_\odot$	369.0	0.991	54745.	−730.60	1.004	432.6	$(12{+}1)M_\odot$	633.5	0.994	510763.	−3543.30	0.884	897.5
	$(12{+}9)M_\odot$	420.8	0.992	69024.	−787.91	0.996	515.7	$(9{+}1)M_\odot$	829.6	0.987	620420.	−3174.00	1.007	1372.3
	$(12{+}6)M_\odot$	486.2	0.994	97370.	−939.14	1.004	648.5	$(6{+}3)M_\odot$	972.3	0.993	301845.	−1305.80	0.973	1533.5
$\mathrm{T}(2,2)$	$(12{+}3)M_\odot$	568.6	0.996	180867.	−1440.70	0.941	775.7	$(6{+}1)M_\odot$	1200.2	0.973	818200.	−2621.10	1.143	1524.8
	$(9{+}9)M_\odot$	491.9	0.994	87003.	−841.46	1.004	649.8	$(3{+}3)M_\odot$	1475.8	0.983	520076.	−1268.70	1.289	2815.7
	$(9{+}6)M_\odot$	587.8	0.995	121657.	−955.91	0.973	787.6	$(3{+}1)M_\odot$	2156.4	0.957	1338608.	−1714.60	1.342	1972.0
	$(9{+}3)M_\odot$	718.8	0.996	223158.	−1381.50	0.980	1103.6	$(1{+}1)M_\odot$	4427.3	0.971	3159884.	−1035.90	1.669	3492.2
	$(6{+}6)M_\odot$	737.9	0.995	168375.	−1027.20	0.974	1065.6							
	$(12{+}12)M_\odot$	268.0	0.984	47115.	62.42	0.114	302.1	$(12{+}1)M_\odot$	593.3	0.995	492696.	−1521.50	0.364	558.1
	$(12{+}9)M_\odot$	310.2	0.986	61172.	24.12	0.064	352.4	$(9{+}1)M_\odot$	748.9	0.997	602742.	−1361.20	0.573	1744.0
	$(12{+}6)M_\odot$	372.4	0.988	89131.	−75.52	0.048	405.2	$(6{+}3)M_\odot$	736.7	0.996	291600.	−321.31	0.069	641.9
$\mathrm{T}(2,2.5)$	$(12{+}3)M_\odot$	470.1	0.993	171240.	−382.17	0.127	464.3	$(6{+}1)M_\odot$	1043.9	0.998	802967.	−1123.60	0.468	2687.9
	$(9{+}9)M_\odot$	360.2	0.988	78761.	−10.93	0.169	405.5	$(3{+}3)M_\odot$	1079.3	0.998	509279.	−293.97	0.051	991.6
	$(9{+}6)M_\odot$	435.9	0.990	112807.	−79.02	0.036	468.9	$(3{+}1)M_\odot$	1725.5	0.986	1328133.	−645.72	0.593	3160.6
	$(9{+}3)M_\odot$	574.6	0.994	213109.	−355.18	0.089	530.9	$(1{+}1)M_\odot$	3235.0	0.984	3147292.	−27.59	1.122	4332.4
	$(6{+}6)M_\odot$	537.0	0.993	159049.	−131.12	0.026	543.9							
	$(12{+}12)M_\odot$	346.5	0.989	56603.	−747.11	1.001	413.9	$(12{+}1)M_\odot$	467.3	0.979	518730.	−3856.30	0.639	344.1
	$(12{+}9)M_\odot$	390.8	0.989	70978.	−795.46	0.991	461.8	$(9{+}1)M_\odot$	622.5	0.968	625199.	−3246.00	1.047	911.0
	$(12{+}6)M_\odot$	432.1	0.991	99659.	−947.96	0.683	353.9	$(6{+}3)M_\odot$	864.1	0.988	302370.	−1148.90	1.040	1489.3
$\mathrm{T}(3,3.5,0)$	$(12{+}3)M_\odot$	460.2	0.994	183490.	−1463.40	0.523	341.1	$(6{+}1)M_\odot$	930.1	0.962	818424.	−2410.90	1.371	1437.2
	$(9{+}9)M_\odot$	462.0	0.992	88394.	−802.20	0.663	344.9	$(3{+}3)M_\odot$	1386.2	0.979	518915.	−995.19	1.019	1794.2
	$(9{+}6)M_\odot$	540.5	0.992	123467.	−915.69	1.091	809.4	$(3{+}1)M_\odot$	1811.5	0.957	1335997.	−1328.30	0.770	806.4
	$(9{+}3)M_\odot$	603.9	0.993	224863.	−1319.50	0.469	410.0	$(1{+}1)M_\odot$	4158.6	0.973	3154883.	−533.50	2.026	5153.7
	$(6{+}6)M_\odot$	693.1	0.993	169289.	−917.85	0.963	963.8							
	$(12{+}12)M_\odot$	346.5	0.988	56752.	−783.94	1.003	399.6	$(12{+}1)M_\odot$	467.3	0.976	519056.	−3899.30	1.039	698.0
	$(12{+}9)M_\odot$	390.8	0.989	71419.	−846.90	0.997	452.2	$(9{+}1)M_\odot$	622.5	0.967	625607.	−3293.80	1.092	939.6
	$(12{+}6)M_\odot$	432.1	0.991	99843.	−988.88	1.119	643.1	$(6{+}3)M_\odot$	864.1	0.988	303033.	−1208.90	0.925	1166.0
$\mathrm{T}(3,3.5,-2)$	$(12{+}3)M_\odot$	460.2	0.991	184383.	−1535.20	1.074	691.9	$(6{+}1)M_\odot$	930.1	0.960	819229.	−2474.30	1.431	1538.7
	$(9{+}9)M_\odot$	462.0	0.992	89013.	−862.76	1.020	583.8	$(3{+}3)M_\odot$	1386.1	0.978	519598.	−1053.90	1.017	1679.6
	$(9{+}6)M_\odot$	540.5	0.992	123973.	−970.90	0.980	687.7	$(3{+}1)M_\odot$	1811.5	0.955	1336713.	−1383.70	1.091	1297.7
	$(9{+}3)M_\odot$	603.9	0.991	225447.	−1377.20	0.971	827.9	$(1{+}1)M_\odot$	4158.3	0.972	3155823.	−589.66	1.614	3570.4
	$(6{+}6)M_\odot$	693.1	0.992	169885.	−977.12	0.995	914.1							
	$(12{+}12)M_\odot$	346.5	0.989	56437.	−708.81	1.002	419.2	$(12{+}1)M_\odot$	467.3	0.976	518281.	−3805.40	0.987	665.3
	$(12{+}9)M_\odot$	390.8	0.989	70683.	−749.70	1.078	544.5	$(9{+}1)M_\odot$	622.4	0.969	624423.	−3182.10	1.055	922.0
	$(12{+}6)M_\odot$	432.1	0.991	98882.	−880.02	0.665	337.4	$(6{+}3)M_\odot$	864.2	0.989	301549.	−1081.70	0.962	1438.8
$\mathrm{T}(3,3.5,+2)$	$(12{+}3)M_\odot$	460.2	0.993	183537.	−1433.30	0.502	343.2	$(6{+}1)M_\odot$	930.0	0.963	818756.	−2397.00	1.177	1278.2
	$(9{+}9)M_\odot$	462.0	0.991	88335.	−766.86	1.017	620.7	$(3{+}3)M_\odot$	1386.1	0.981	518008.	−927.52	1.328	2926.8
	$(9{+}6)M_\odot$	540.6	0.992	122850.	−855.39	0.998	741.0	$(3{+}1)M_\odot$	1811.6	0.959	1335509.	−1282.30	1.642	2592.9
	$(9{+}3)M_\odot$	603.9	0.991	224252.	−1261.20	0.966	877.7	$(1{+}1)M_\odot$	4158.5	0.974	3154708.	−502.39	1.861	5053.9
	$(6{+}6)M_\odot$	693.1	0.992	168354.	−843.81	1.001	1039.8							
	$(12{+}12)M_\odot$	238.2	0.984	58496.	−852.61	1.000	313.3	$(12{+}1)M_\odot$	364.0	0.974	521485.	−3996.30	0.387	272.9
	$(12{+}9)M_\odot$	270.8	0.984	72382.	−869.88	1.137	437.8	$(9{+}1)M_\odot$	482.7	0.969	625241.	−3230.50	0.314	299.1
	$(12{+}6)M_\odot$	308.3	0.988	99336.	−932.65	0.588	252.3	$(6{+}3)M_\odot$	616.7	0.987	302136.	−1126.30	0.937	1054.6
$\mathrm{P}(2,2.5)$	$(12{+}3)M_\odot$	346.4	0.991	184168.	−1494.50	0.476	270.5	$(6{+}1)M_\odot$	713.5	0.958	818912.	−2402.90	1.039	861.6
	$(9{+}9)M_\odot$	317.6	0.987	89607.	−860.18	0.997	441.0	$(3{+}3)M_\odot$	952.9	0.980	518671.	−969.85	0.570	822.8
	$(9{+}6)M_\odot$	377.1	0.991	123348.	−905.88	0.550	301.0	$(3{+}1)M_\odot$	1337.3	0.956	1335867.	−1293.70	1.236	1570.7
	$(9{+}3)M_\odot$	445.8	0.992	224711.	−1304.10	0.385	328.7	$(1{+}1)M_\odot$	2858.7	0.973	3154393.	−489.49	1.474	3128.2
	$(6{+}6)M_\odot$	476.4	0.989	169246.	−908.27	0.854	627.9							
	$(12{+}12)M_\odot$	360.6	0.989	55496.	−633.24	0.998	466.5	$(12{+}1)M_\odot$	399.5	0.978	519504.	−3883.20	0.394	294.8
	$(12{+}9)M_\odot$	406.0	0.990	69695.	−675.49	0.989	537.0	$(9{+}1)M_\odot$	545.4	0.967	624532.	−3187.90	0.751	527.3
	$(12{+}6)M_\odot$	442.8	0.991	98278.	−827.87	0.995	628.2	$(6{+}3)M_\odot$	885.5	0.991	300673.	−1028.90	0.869	1400.0
$\mathrm{P}(3,3.5,0)$	$(12{+}3)M_\odot$	441.6	0.993	182733.	−1378.80	0.490	333.7	$(6{+}1)M_\odot$	850.4	0.963	817861.	−2348.50	1.321	1417.7
	$(9{+}9)M_\odot$	480.9	0.992	87440.	−699.28	0.638	394.1	$(3{+}3)M_\odot$	1442.6	0.984	517533.	−899.36	0.561	1061.5
	$(9{+}6)M_\odot$	560.2	0.995	121810.	−784.50	0.502	411.7	$(3{+}1)M_\odot$	1795.8	0.960	1335559.	−1276.30	1.065	1442.0
	$(9{+}3)M_\odot$	598.6	0.992	223521.	−1209.90	1.006	998.3	$(1{+}1)M_\odot$	4327.8	0.974	3154075.	−475.48	1.501	3531.4
	$(6{+}6)M_\odot$	721.3	0.994	167742.	−797.77	0.887	1026.6							
	$(12{+}12)M_\odot$	360.6	0.988	55640.	−665.69	0.999	441.4	$(12{+}1)M_\odot$	399.5	0.978	519616.	−3904.00	0.399	294.3
	$(12{+}9)M_\odot$	406.0	0.990	70047.	−717.86	1.007	524.4	$(9{+}1)M_\odot$	545.4	0.966	625009.	−3227.00	0.908	676.5
	$(12{+}6)M_\odot$	442.8	0.991	98658.	−869.29	0.648	357.0	$(6{+}3)M_\odot$	885.5	0.991	301270.	−1079.60	0.954	1519.2
$\mathrm{P}(3,3.5,-2)$	$(12{+}3)M_\odot$	441.6	0.994	183065.	−1416.00	0.512	337.7	$(6{+}1)M_\odot$	850.4	0.962	818109.	−2379.30	1.077	1017.2
	$(9{+}9)M_\odot$	480.9	0.992	87324.	−720.64	0.612	366.6	$(3{+}3)M_\odot$	1442.6	0.982	518203.	−951.67	0.982	2071.5
	$(9{+}6)M_\odot$	560.2	0.993	122208.	−829.41	1.128	972.6	$(3{+}1)M_\odot$	1795.8	0.958	1336435.	−1333.60	1.708	3063.0
	$(9{+}3)M_\odot$	598.6	0.992	223889.	−1249.80	1.060	1040.9	$(1{+}1)M_\odot$	4327.8	0.973	3155313.	−538.15	1.136	2322.4
	$(6{+}6)M_\odot$	721.3	0.994	168197.	−844.11	0.962	1085.4							
	$(12{+}12)M_\odot$	360.6	0.989	55400.	−623.67	1.007	480.9	$(12{+}1)M_\odot$	399.5	0.978	519174.	−3860.30	0.396	293.2
	$(12{+}9)M_\odot$	406.0	0.990	69801.	−675.20	0.984	532.0	$(9{+}1)M_\odot$	545.4	0.973	623723.	−3140.70	0.325	326.6
	$(12{+}6)M_\odot$	442.8	0.991	98435.	−828.41	0.637	368.4	$(6{+}3)M_\odot$	885.5	0.991	300676.	−1021.70	0.740	1094.7
$\mathrm{P}(3,3.5,+2)$	$(12{+}3)M_\odot$	441.6	0.993	182916.	−1380.00	0.495	334.8	$(6{+}1)M_\odot$	850.4	0.963	817652.	−2330.70	1.205	1223.2
	$(9{+}9)M_\odot$	480.9	0.992	87240.	−684.94	0.967	661.2	$(3{+}3)M_\odot$	1442.6	0.984	517427.	−887.15	0.563	1065.7
	$(9{+}6)M_\odot$	560.2	0.994	121974.	−785.20	0.505	415.1	$(3{+}1)M_\odot$	1795.8	0.960	1335220.	−1253.20	1.151	1578.7
	$(9{+}3)M_\odot$	598.6	0.994	223450.	−1198.40	0.390	423.1	$(1{+}1)M_\odot$	4327.8	0.974	3153427.	−445.05	1.648	3916.1
	$(6{+}6)M_\odot$	721.3	0.994	167544.	−782.68	1.001	1198.0							
	$(12{+}12)M_\odot$	363.5	0.989	52612.	−585.85	0.626	488.6	$(12{+}1)M_\odot$	665.0	0.963	522280.	−4080.40	0.397	262.6
	$(12{+}9)M_\odot$	415.2	0.991	68263.	−701.24	0.631	506.1	$(9{+}1)M_\odot$	863.6	0.964	626004.	−3305.60	0.309	287.9
	$(12{+}6)M_\odot$	483.0	0.993	98999.	−955.57	0.586	490.3	$(6{+}3)M_\odot$	965.9	0.983	304597.	−1266.30	1.006	1535.5
$\mathrm{EP}(2,2.5)$	$(12{+}3)M_\odot$	576.3	0.994	186108.	−1631.30	0.710	641.2	$(6{+}1)M_\odot$	1233.3	0.958	820782.	−2518.80	0.410	411.1
	$(9{+}9)M_\odot$	484.7	0.994	87317.	−785.70	0.571	542.0	$(3{+}3)M_\odot$	1454.1	0.976	519062.	−1013.30	1.073	1541.4
	$(9{+}6)M_\odot$	580.8	0.996	123537.	−951.18	0.584	619.2	$(3{+}1)M_\odot$	2165.6	0.954	1336199.	−1331.60	1.276	1523.9
	$(9{+}3)M_\odot$	721.9	0.991	227351.	−1463.40	0.921	1296.8	$(1{+}1)M_\odot$	4362.2	0.972	3154771.	−522.97	2.190	5400.0
	$(6{+}6)M_\odot$	727.0	0.995	170279.	−989.35	0.656	999.3							
	$(12{+}12)M_\odot$	361.5	0.991	52197.	−487.54	0.736	571.1	$(12{+}1)M_\odot$	680.0	0.955	521271.	−4007.30	1.131	598.2

PN model		$f_{\rm end}$	mn	ψ_0	$\psi_{3/2}$	$\alpha f_{\rm cut}^{2/3}$	$f_{\rm cut}$		$f_{\rm end}$	mn	ψ_0	$\psi_{3/2}$	$\alpha f_{\rm cut}^{2/3}$	$f_{\rm cut}$
	FF (minmax) with $(\psi_0, \psi_{3/2})_{\alpha,{\rm cut}}$ template family when LIGO-I noise curve is used													
EP$(3, 3.5, 0)$	$(12{+}9)M_\odot$	419.3	0.993	67163.	-573.66	0.674	569.7	$(9{+}1)M_\odot$	882.5	0.968	624838.	-3228.20	0.314	309.7
	$(12{+}6)M_\odot$	488.8	0.995	96756.	-780.51	0.600	557.9	$(6{+}3)M_\odot$	971.8	0.990	302004.	-1104.10	0.755	1645.0
	$(12{+}3)M_\odot$	598.1	0.996	183664.	-1454.90	0.640	626.9	$(6{+}1)M_\odot$	1264.7	0.964	819483.	-2438.70	0.341	421.6
	$(9{+}9)M_\odot$	488.6	0.994	85466.	-628.01	0.578	603.5	$(3{+}3)M_\odot$	1468.7	0.981	517890.	-925.72	1.015	1843.8
	$(9{+}6)M_\odot$	584.2	0.996	120851.	-763.59	0.578	732.3	$(3{+}1)M_\odot$	2205.5	0.957	1335535.	-1283.30	1.786	2832.2
	$(9{+}3)M_\odot$	730.5	0.995	224519.	-1279.80	0.802	1245.8	$(1{+}1)M_\odot$	4422.6	0.974	3154631.	-498.68	1.879	4998.1
	$(6{+}6)M_\odot$	724.6	0.997	167802.	-818.28	0.508	814.7							
EP$(3, 3.5, -2)$	$(12{+}12)M_\odot$	361.2	0.991	52169.	-509.45	0.834	615.9	$(12{+}1)M_\odot$	677.4	0.955	521392.	-4028.70	1.139	602.2
	$(12{+}9)M_\odot$	407.9	0.993	67098.	-594.80	0.713	593.5	$(9{+}1)M_\odot$	883.5	0.967	624674.	-3240.50	0.365	313.8
	$(12{+}6)M_\odot$	482.3	0.995	96644.	-800.20	0.619	578.7	$(6{+}3)M_\odot$	961.7	0.990	302677.	-1157.30	0.726	1528.4
	$(12{+}3)M_\odot$	586.4	0.995	183711.	-1478.90	0.669	652.6	$(6{+}1)M_\odot$	1265.9	0.959	819217.	-2447.20	1.344	1428.4
	$(9{+}9)M_\odot$	475.9	0.994	85693.	-663.13	0.615	597.5	$(3{+}3)M_\odot$	1438.6	0.979	518313.	-967.96	1.242	2277.8
	$(9{+}6)M_\odot$	580.6	0.996	121491.	-816.36	0.552	639.7	$(3{+}1)M_\odot$	2219.2	0.956	1335728.	-1311.10	0.765	774.5
	$(9{+}3)M_\odot$	739.2	0.994	224960.	-1322.40	0.677	968.4	$(1{+}1)M_\odot$	4278.8	0.973	3154883.	-528.51	1.821	4563.9
	$(6{+}6)M_\odot$	718.5	0.997	168309.	-866.35	0.532	848.3							
EP$(3, 3.5, +2)$	$(12{+}12)M_\odot$	364.7	0.991	52189.	-482.82	0.793	603.2	$(12{+}1)M_\odot$	677.8	0.967	519792.	-3927.00	0.455	270.4
	$(12{+}9)M_\odot$	418.5	0.993	67083.	-565.07	0.757	671.3	$(9{+}1)M_\odot$	883.8	0.968	624018.	-3181.70	0.303	294.6
	$(12{+}6)M_\odot$	492.3	0.995	96631.	-769.61	0.594	571.1	$(6{+}3)M_\odot$	984.4	0.990	301806.	-1088.30	0.837	1673.8
	$(12{+}3)M_\odot$	594.3	0.996	183654.	-1447.60	0.640	631.4	$(6{+}1)M_\odot$	1258.8	0.959	818680.	-2395.20	0.975	876.3
	$(9{+}9)M_\odot$	489.3	0.994	85658.	-630.60	0.554	566.9	$(3{+}3)M_\odot$	1463.3	0.981	517822.	-915.23	1.022	1917.0
	$(9{+}6)M_\odot$	589.5	0.996	121033.	-764.98	0.562	684.7	$(3{+}1)M_\odot$	2231.3	0.957	1335322.	-1265.50	0.796	817.7
	$(9{+}3)M_\odot$	732.3	0.995	224573.	-1274.50	0.730	1106.0	$(1{+}1)M_\odot$	4393.5	0.973	3154601.	-486.86	1.940	5340.1
	$(6{+}6)M_\odot$	729.3	0.997	167669.	-806.04	0.655	1150.3							

TABLE IV: Fitting factors for the projection of the target models (in the rows) onto the $(\psi_0, \psi_{3/2}, \alpha, f_{\rm cut})$ Fourier-domain detection template family when LIGO-I noise curve is used. For BBH masses $m_{1,2} = 1, 3, 6, 9, 12 M_\odot$, this table shows the minmax matches between the target models and the Fourier-domain search model, *maximized over the intrinsic parameters* ψ_0, $\psi_{3/2}$, and $f_{\rm cut}$, and over the extrinsic parameter α. For each intersection, the six numbers shown report the *ending frequency* $f_{\rm end}$ (defined in BCV1) of the PN model for the BBH masses quoted, the minmax FF mn, and the search parameters at which the maximum is attained.

PN model		$f_{\rm end}$	mn	ψ_0	$\psi_{3/2}$	$\alpha f_{\rm cut}^{2/3}$	$f_{\rm cut}$		$f_{\rm end}$	mn	ψ_0	$\psi_{3/2}$	$\alpha f_{\rm cut}^{2/3}$	$f_{\rm cut}$
	FF (minmax) with $(\psi_0, \psi_{3/2})_{\alpha,{\rm cut}}$ template family when S2-H1 noise curve is used													
T$(2, 2)$	$(20{+}20)M_\odot$	221.4	0.920	21174.	-419.89	0.997	454.5	$(20{+}5)M_\odot$	341.1	0.973	78731.	-1098.90	0.987	454.0
	$(20{+}15)M_\odot$	252.5	0.930	27932.	-505.95	0.999	429.9	$(10{+}10)M_\odot$	442.7	0.983	74344.	-838.06	1.001	511.5
	$(15{+}15)M_\odot$	295.1	0.950	36888.	-599.56	0.998	453.4	$(15{+}5)M_\odot$	431.3	0.985	97429.	-1080.20	1.002	535.8
	$(20{+}10)M_\odot$	291.7	0.957	41889.	-691.34	0.989	434.0	$(10{+}5)M_\odot$	583.4	0.988	132482.	-1082.10	1.014	663.7
	$(15{+}10)M_\odot$	352.7	0.971	52870.	-731.76	0.997	499.5	$(5{+}5)M_\odot$	885.5	0.990	228227.	-1166.10	0.928	1022.3
T$(2, 2.5)$	$(20{+}20)M_\odot$	160.8	0.943	25076.	-175.45	1.002	388.4	$(20{+}5)M_\odot$	282.0	0.967	71100.	-173.28	0.843	415.5
	$(20{+}15)M_\odot$	185.3	0.954	29326.	-114.99	1.007	407.3	$(10{+}10)M_\odot$	324.2	0.967	64410.	54.78	0.656	441.2
	$(15{+}15)M_\odot$	215.7	0.960	34004.	-9.82	0.994	439.9	$(15{+}5)M_\odot$	345.9	0.970	86328.	-57.88	0.544	434.0
	$(20{+}10)M_\odot$	219.8	0.962	38883.	-76.49	0.995	425.6	$(10{+}5)M_\odot$	444.5	0.976	118653.	-11.27	0.214	514.5
	$(15{+}10)M_\odot$	260.4	0.963	45991.	36.35	0.898	426.7	$(5{+}5)M_\odot$	644.5	0.984	214325.	-110.73	0.012	661.0
T$(3, 3.5, 0)$	$(20{+}20)M_\odot$	207.9	0.897	21056.	-419.12	0.961	389.0	$(20{+}5)M_\odot$	276.1	0.966	83717.	-1307.90	0.984	394.7
	$(20{+}15)M_\odot$	234.5	0.929	30113.	-576.27	0.982	394.2	$(10{+}10)M_\odot$	415.8	0.981	77187.	-872.81	0.998	516.7
	$(15{+}15)M_\odot$	277.2	0.949	38671.	-639.62	1.006	468.4	$(15{+}5)M_\odot$	362.3	0.977	102453.	-1230.70	1.009	472.7
	$(20{+}10)M_\odot$	259.2	0.950	44096.	-765.84	1.001	414.7	$(10{+}5)M_\odot$	518.5	0.982	136328.	-1121.70	1.012	582.4
	$(15{+}10)M_\odot$	324.3	0.966	55980.	-809.87	1.002	479.3	$(5{+}5)M_\odot$	831.7	0.984	231040.	-1095.10	1.119	1187.1
T$(3, 3.5, -2)$	$(20{+}20)M_\odot$	207.9	0.901	20441.	-405.79	0.977	439.6	$(20{+}5)M_\odot$	276.1	0.965	83625.	-1334.20	0.996	385.1
	$(20{+}15)M_\odot$	234.5	0.920	29423.	-575.85	0.994	394.1	$(10{+}10)M_\odot$	415.9	0.980	77703.	-925.00	0.986	492.1
	$(15{+}15)M_\odot$	277.2	0.947	38335.	-650.94	1.013	462.6	$(15{+}5)M_\odot$	362.3	0.977	102405.	-1263.40	0.996	457.2
	$(20{+}10)M_\odot$	259.3	0.946	43872.	-784.60	1.010	411.7	$(10{+}5)M_\odot$	518.5	0.983	136459.	-1165.10	1.019	592.4
	$(15{+}10)M_\odot$	324.3	0.966	55739.	-827.95	0.986	460.1	$(5{+}5)M_\odot$	831.7	0.984	232191.	-1174.60	0.735	633.3
T$(3, 3.5, +2)$	$(20{+}20)M_\odot$	207.9	0.909	22186.	-442.11	0.986	381.2	$(20{+}5)M_\odot$	276.1	0.965	84088.	-1294.00	0.996	417.8
	$(20{+}15)M_\odot$	234.5	0.934	30747.	-577.88	0.991	425.6	$(10{+}10)M_\odot$	415.8	0.981	77154.	-838.88	1.026	545.2
	$(15{+}15)M_\odot$	277.2	0.951	39267.	-637.78	1.088	535.6	$(15{+}5)M_\odot$	362.3	0.977	102527.	-1200.20	1.004	458.2
	$(20{+}10)M_\odot$	259.2	0.952	44921.	-767.79	0.966	401.0	$(10{+}5)M_\odot$	518.5	0.981	135434.	-1053.30	0.997	586.6
	$(15{+}10)M_\odot$	324.3	0.967	56051.	-781.54	0.990	470.3	$(5{+}5)M_\odot$	831.7	0.985	230071.	-1020.80	1.132	1281.8
P$(2, 2.5)$	$(20{+}20)M_\odot$	142.9	0.858	22981.	-549.30	1.003	340.6	$(20{+}5)M_\odot$	207.8	0.950	88920.	-1601.90	0.998	331.4
	$(20{+}15)M_\odot$	162.5	0.900	32041.	-711.03	0.999	350.0	$(10{+}10)M_\odot$	285.9	0.969	80174.	-1019.80	0.967	411.2
	$(15{+}15)M_\odot$	190.6	0.924	41398.	-797.78	0.958	367.4	$(15{+}5)M_\odot$	267.5	0.965	107075.	-1454.80	0.995	388.1
	$(20{+}10)M_\odot$	185.0	0.925	46732.	-933.50	0.993	368.4	$(10{+}5)M_\odot$	370.0	0.970	138389.	-1214.50	1.126	567.8
	$(15{+}10)M_\odot$	226.3	0.947	59282.	-986.94	0.988	381.7	$(5{+}5)M_\odot$	571.7	0.979	231517.	-1106.60	0.657	473.3
P$(3, 3.5, 0)$	$(20{+}20)M_\odot$	216.4	0.923	23283.	-447.20	1.003	409.2	$(20{+}5)M_\odot$	265.0	0.965	84310.	-1285.90	0.996	381.6
	$(20{+}15)M_\odot$	243.6	0.939	29065.	-478.26	0.916	386.9	$(10{+}10)M_\odot$	432.8	0.984	76120.	-754.71	1.013	559.7
	$(15{+}15)M_\odot$	288.5	0.958	38187.	-555.93	1.003	471.1	$(15{+}5)M_\odot$	359.2	0.978	101518.	-1130.70	1.026	471.0
	$(20{+}10)M_\odot$	265.7	0.958	43838.	-693.87	0.986	428.3	$(10{+}5)M_\odot$	531.3	0.983	133868.	-965.51	1.148	794.0
	$(15{+}10)M_\odot$	336.1	0.970	55715.	-730.19	0.995	480.7	$(5{+}5)M_\odot$	865.6	0.989	228134.	-928.84	0.516	582.0
P$(3, 3.5, -2)$	$(20{+}20)M_\odot$	216.4	0.910	21887.	-414.06	1.002	433.2	$(20{+}5)M_\odot$	265.0	0.962	84371.	-1309.90	1.003	402.4
	$(20{+}15)M_\odot$	243.6	0.936	30589.	-562.11	0.964	389.3	$(10{+}10)M_\odot$	432.8	0.982	76402.	-799.24	0.996	518.7
	$(15{+}15)M_\odot$	288.5	0.958	38948.	-608.61	0.987	457.8	$(15{+}5)M_\odot$	359.2	0.977	101790.	-1167.40	0.996	463.9
	$(20{+}10)M_\odot$	265.7	0.954	44076.	-726.78	0.993	412.8	$(10{+}5)M_\odot$	531.3	0.983	134677.	-1022.50	1.002	616.2
	$(15{+}10)M_\odot$	336.1	0.971	55337.	-743.03	1.015	497.7	$(5{+}5)M_\odot$	865.6	0.987	228671.	-980.91	1.115	1313.4
	$(20{+}20)M_\odot$	216.4	0.918	23039.	-438.16	0.986	396.4	$(20{+}5)M_\odot$	265.0	0.963	84636.	-1296.60	1.003	382.7
	$(20{+}15)M_\odot$	243.6	0.941	30572.	-532.37	0.942	386.3	$(10{+}10)M_\odot$	432.8	0.982	75966.	-745.85	1.031	558.7

PN model		$f_{\rm end}$	mn	ψ_0	$\psi_{3/2}$	$\alpha f_{\rm cut}^{2/3}$	$f_{\rm cut}$		$f_{\rm end}$	mn	ψ_0	$\psi_{3/2}$	$\alpha f_{\rm cut}^{2/3}$	$f_{\rm cut}$
	FF (minmax) with $(\psi_0, \psi_{3/2})_{\alpha,{\rm cut}}$ template family when S2-H1 noise curve is used													
$\mathrm{P}(3, 3.5, +2)$	$(15{+}15)M_\odot$	288.5	0.961	38711.	−572.45	0.985	458.4	$(15{+}5)M_\odot$	359.2	0.977	101567.	−1129.30	1.018	464.8
	$(20{+}10)M_\odot$	265.7	0.958	44079.	−701.65	0.981	407.9	$(10{+}5)M_\odot$	531.3	0.984	133925.	−960.49	1.007	644.3
	$(15{+}10)M_\odot$	336.1	0.973	55340.	−709.86	1.030	520.4	$(5{+}5)M_\odot$	865.6	0.989	228400.	−929.57	0.522	615.5
$\mathrm{EP}(2, 2.5)$	$(20{+}20)M_\odot$	218.1	0.970	17734.	−207.66	0.936	557.3	$(20{+}5)M_\odot$	345.8	0.971	72987.	−921.14	0.842	527.4
	$(20{+}15)M_\odot$	249.1	0.977	23506.	−272.06	0.894	519.1	$(10{+}10)M_\odot$	436.2	0.988	69348.	−599.40	0.727	685.3
	$(15{+}15)M_\odot$	290.8	0.985	32047.	−343.27	0.896	647.0	$(15{+}5)M_\odot$	433.1	0.984	94579.	−969.78	0.763	605.8
	$(20{+}10)M_\odot$	289.8	0.983	36219.	−424.49	1.023	705.9	$(10{+}5)M_\odot$	579.6	0.990	131471.	−989.48	0.629	725.8
	$(15{+}10)M_\odot$	348.5	0.986	47699.	−480.20	0.841	690.4	$(5{+}5)M_\odot$	872.4	0.993	230979.	−1129.40	0.564	1030.2
$\mathrm{EP}(3, 3.5, 0)$	$(20{+}20)M_\odot$	218.4	0.965	20306.	−264.33	1.004	527.5	$(20{+}5)M_\odot$	351.7	0.982	73780.	−863.18	0.941	602.9
	$(20{+}15)M_\odot$	250.2	0.975	26165.	−304.30	0.925	474.6	$(10{+}10)M_\odot$	434.6	0.991	70147.	−529.37	0.942	756.1
	$(15{+}15)M_\odot$	289.2	0.981	36296.	−423.76	0.936	597.7	$(15{+}5)M_\odot$	445.3	0.990	94704.	−879.84	0.911	666.5
	$(20{+}10)M_\odot$	294.3	0.984	38859.	−449.82	0.992	581.2	$(10{+}5)M_\odot$	581.6	0.992	130118.	−847.39	0.837	870.8
	$(15{+}10)M_\odot$	350.3	0.989	49649.	−469.41	0.973	688.3	$(5{+}5)M_\odot$	869.0	0.994	226994.	−916.78	0.759	1727.9
$\mathrm{EP}(3, 3.5, -2)$	$(20{+}20)M_\odot$	215.6	0.965	19530.	−242.38	0.914	489.8	$(20{+}5)M_\odot$	353.7	0.983	73837.	−880.11	0.892	545.8
	$(20{+}15)M_\odot$	248.3	0.974	25647.	−301.11	0.995	558.8	$(10{+}10)M_\odot$	432.6	0.990	70712.	−572.04	0.915	686.2
	$(15{+}15)M_\odot$	284.9	0.983	35272.	−409.03	0.973	566.9	$(15{+}5)M_\odot$	439.0	0.989	94401.	−893.75	0.855	650.2
	$(20{+}10)M_\odot$	289.1	0.982	38308.	−449.06	1.007	609.1	$(10{+}5)M_\odot$	580.9	0.993	130268.	−879.57	0.861	895.4
	$(15{+}10)M_\odot$	347.1	0.987	49756.	−492.74	0.890	551.4	$(5{+}5)M_\odot$	864.2	0.994	227457.	−963.04	0.717	1391.9
$\mathrm{EP}(3, 3.5, +2)$	$(20{+}20)M_\odot$	220.2	0.966	20280.	−256.62	0.999	551.7	$(20{+}5)M_\odot$	351.8	0.982	74233.	−872.52	0.978	620.6
	$(20{+}15)M_\odot$	250.6	0.975	27154.	−336.77	0.962	508.3	$(10{+}10)M_\odot$	437.4	0.990	70814.	−547.63	0.958	765.7
	$(15{+}15)M_\odot$	292.7	0.985	34920.	−375.70	0.968	588.3	$(15{+}5)M_\odot$	443.1	0.991	94619.	−875.10	0.894	663.4
	$(20{+}10)M_\odot$	294.8	0.983	39562.	−472.45	0.985	578.3	$(10{+}5)M_\odot$	583.9	0.993	130130.	−842.14	0.777	843.2
	$(15{+}10)M_\odot$	353.5	0.989	50073.	−475.40	0.946	661.4	$(5{+}5)M_\odot$	872.0	0.994	226744.	−899.28	0.675	1311.6

TABLE V: Fitting factors for the projection of the target models (in the rows) onto the $(\psi_0, \psi_{3/2}, \alpha, f_{\rm cut})$ Fourier-domain detection template family when S2-H1 noise curve is used. For BBH masses $m_{1,2} = 5, 10, 15, 20 M_\odot$, this table shows the minmax matches between the target models and the Fourier-domain search model, *maximized over the intrinsic parameters* ψ_0, $\psi_{3/2}$, and $f_{\rm cut}$, and over the extrinsic parameter α. For each intersection, the six numbers shown report the *ending frequency* $f_{\rm end}$ (defined in BCV1) of the PN model for the BBH masses quoted, the minmax FF mn, and the search parameters at which the maximum is attained.

PN model		$f_{\rm end}$	mn	ψ_0	$\psi_{3/2}$	$\alpha f_{\rm cut}^{2/3}$	$f_{\rm cut}$		$f_{\rm end}$	mn	ψ_0	$\psi_{3/2}$	$\alpha f_{\rm cut}^{2/3}$	$f_{\rm cut}$
	FF (minmax) with $(\psi_0, \psi_{3/2})_{\alpha,{\rm cut}}$ template family when LIGO-S2-H1-fit noise curve is used													
$\mathrm{T}(2, 2)$	$(12{+}12)M_\odot$	369.0	0.972	55463.	−758.16	0.980	502.9	$(12{+}1)M_\odot$	633.5	0.992	512229.	−3595.30	1.004	877.9
	$(12{+}9)M_\odot$	420.8	0.982	69814.	−823.33	0.992	520.5	$(9{+}1)M_\odot$	829.6	0.991	624594.	−3314.10	0.986	1255.8
	$(12{+}6)M_\odot$	486.2	0.987	98587.	−987.48	1.009	579.0	$(6{+}3)M_\odot$	972.3	0.990	304475.	−1394.10	1.003	1310.2
	$(12{+}3)M_\odot$	568.6	0.990	182481.	−1495.90	1.008	670.7	$(6{+}1)M_\odot$	1200.2	0.982	828120.	−2941.70	1.152	2748.5
	$(9{+}9)M_\odot$	491.9	0.987	88302.	−891.76	1.001	578.4	$(3{+}3)M_\odot$	1475.8	0.986	525848.	−1455.70	0.937	2064.5
	$(9{+}6)M_\odot$	587.8	0.988	123072.	−1005.80	0.990	630.4	$(3{+}1)M_\odot$	2156.4	0.958	1360387.	−2369.10	0.425	2366.4
	$(9{+}3)M_\odot$	718.8	0.990	224552.	−1427.00	1.069	939.3	$(1{+}1)M_\odot$	4427.3	0.942	3178240.	−1563.80	1.119	4587.4
	$(6{+}6)M_\odot$	737.9	0.989	169715.	−1072.40	1.041	877.2							
$\mathrm{T}(2, 2.5)$	$(12{+}12)M_\odot$	268.0	0.964	48300.	13.78	0.949	473.2	$(12{+}1)M_\odot$	593.3	0.988	489604.	−1423.10	0.402	619.2
	$(12{+}9)M_\odot$	310.2	0.965	60034.	65.81	0.707	440.0	$(9{+}1)M_\odot$	748.9	0.990	600893.	−1303.10	0.599	1644.7
	$(12{+}6)M_\odot$	372.4	0.971	86191.	31.17	0.352	444.5	$(6{+}3)M_\odot$	736.7	0.985	288942.	−236.10	0.383	1681.6
	$(12{+}3)M_\odot$	470.1	0.980	167641.	−259.31	0.272	522.7	$(6{+}1)M_\odot$	1043.9	0.996	802599.	−1115.00	0.226	900.8
	$(9{+}9)M_\odot$	360.2	0.970	77157.	52.13	0.486	455.7	$(3{+}3)M_\odot$	1079.3	0.995	509035.	−287.42	0.058	971.6
	$(9{+}6)M_\odot$	435.9	0.976	109685.	24.77	0.243	499.0	$(3{+}1)M_\odot$	1725.5	0.995	1331338.	−743.87	0.110	2532.7
	$(9{+}3)M_\odot$	574.6	0.983	209315.	−230.37	0.081	630.4	$(1{+}1)M_\odot$	3235.0	0.979	3156073.	−271.39	0.386	3776.2
	$(6{+}6)M_\odot$	537.0	0.980	156009.	−32.94	0.000	590.2							
$\mathrm{T}(3, 3.5, 0)$	$(12{+}12)M_\odot$	346.5	0.972	57496.	−789.92	0.992	477.8	$(12{+}1)M_\odot$	467.3	0.972	526632.	−4145.60	0.661	392.4
	$(12{+}9)M_\odot$	390.8	0.976	73507.	−898.66	1.002	472.9	$(9{+}1)M_\odot$	622.5	0.972	634620.	−3572.10	0.589	470.4
	$(12{+}6)M_\odot$	432.1	0.981	102331.	−1053.00	0.987	491.2	$(6{+}3)M_\odot$	864.1	0.985	307292.	−1311.00	0.627	589.2
	$(12{+}3)M_\odot$	460.2	0.981	187539.	−1620.70	0.999	539.8	$(6{+}1)M_\odot$	930.1	0.960	835930.	−2988.60	0.871	1410.8
	$(9{+}9)M_\odot$	462.0	0.982	91498.	−923.81	1.011	542.4	$(3{+}3)M_\odot$	1386.2	0.979	526735.	−1246.10	0.971	2289.3
	$(9{+}6)M_\odot$	540.5	0.983	126203.	−1017.70	1.007	595.9	$(3{+}1)M_\odot$	1811.5	0.948	1359484.	−2038.40	0.793	3134.4
	$(9{+}3)M_\odot$	603.9	0.982	228758.	−1460.80	0.971	684.7	$(1{+}1)M_\odot$	4158.6	0.947	3170349.	−981.76	1.156	4266.2
	$(6{+}6)M_\odot$	693.1	0.984	172160.	−1019.20	1.060	841.8							
$\mathrm{T}(3, 3.5, -2)$	$(12{+}12)M_\odot$	346.5	0.971	57818.	−830.00	0.997	459.5	$(12{+}1)M_\odot$	467.3	0.972	526854.	−4186.20	0.695	396.2
	$(12{+}9)M_\odot$	390.8	0.975	73591.	−937.24	1.007	468.3	$(9{+}1)M_\odot$	622.5	0.973	636536.	−3671.10	0.535	467.5
	$(12{+}6)M_\odot$	432.1	0.981	102714.	−1103.00	1.013	503.2	$(6{+}3)M_\odot$	864.1	0.982	307930.	−1375.20	1.101	1191.5
	$(12{+}3)M_\odot$	460.2	0.981	188254.	−1682.30	1.028	572.3	$(6{+}1)M_\odot$	930.1	0.959	836587.	−3048.10	0.900	1318.1
	$(9{+}9)M_\odot$	462.0	0.983	91502.	−958.99	0.991	534.5	$(3{+}3)M_\odot$	1386.1	0.977	528229.	−1330.60	0.901	2016.6
	$(9{+}6)M_\odot$	540.5	0.984	126791.	−1073.90	1.018	624.4	$(3{+}1)M_\odot$	1811.5	0.946	1361025.	−2119.80	0.757	2726.9
	$(9{+}3)M_\odot$	603.9	0.981	229899.	−1536.00	1.206	929.4	$(1{+}1)M_\odot$	4158.3	0.944	3171483.	−1045.10	1.242	4322.3
	$(6{+}6)M_\odot$	693.1	0.984	173036.	−1089.10	1.144	911.1							
$\mathrm{T}(3, 3.5, +2)$	$(12{+}12)M_\odot$	346.5	0.972	57706.	−763.52	1.014	499.4	$(12{+}1)M_\odot$	467.3	0.972	525524.	−4072.00	0.649	389.9
	$(12{+}9)M_\odot$	390.8	0.977	72921.	−843.00	0.999	476.5	$(9{+}1)M_\odot$	622.4	0.974	635449.	−3563.60	0.505	472.8
	$(12{+}6)M_\odot$	432.1	0.980	101849.	−998.77	1.002	518.8	$(6{+}3)M_\odot$	864.2	0.987	305082.	−1205.70	0.610	591.9
	$(12{+}3)M_\odot$	460.2	0.979	186566.	−1550.60	1.127	649.9	$(6{+}1)M_\odot$	930.0	0.966	835136.	−2928.70	0.486	631.5
	$(9{+}9)M_\odot$	462.0	0.983	91381.	−882.60	1.008	553.6	$(3{+}3)M_\odot$	1386.1	0.981	525497.	−1166.90	0.864	2245.9
	$(9{+}6)M_\odot$	540.6	0.982	124482.	−918.73	1.009	613.3	$(3{+}1)M_\odot$	1811.6	0.951	1357786.	−1955.40	0.626	2487.8
	$(9{+}3)M_\odot$	603.9	0.982	228211.	−1399.60	0.803	514.3	$(1{+}1)M_\odot$	4158.5	0.950	3169214.	−918.26	1.065	4259.6
	$(6{+}6)M_\odot$	693.1	0.983	171977.	−970.83	1.043	829.2							
	$(12{+}12)M_\odot$	238.2	0.956	61023.	−967.35	0.987	397.7	$(12{+}1)M_\odot$	364.0	0.952	532918.	−4438.00	0.607	309.2
	$(12{+}9)M_\odot$	270.8	0.964	76727.	−1056.20	1.003	399.7	$(9{+}1)M_\odot$	482.7	0.938	641871.	−3837.30	1.085	704.2

PN model		$f_{\rm end}$	mn	ψ_0	$\psi_{3/2}$	$\alpha f_{\rm cut}^{2/3}$	$f_{\rm cut}$		$f_{\rm end}$	mn	ψ_0	$\psi_{3/2}$	$\alpha f_{\rm cut}^{2/3}$	$f_{\rm cut}$
	FF (minmax) with $(\psi_0, \psi_{3/2})_{\alpha,{\rm cut}}$ template family when LIGO-S2-H1-fit noise curve is used													
P$(2, 2.5)$	$(12{+}6)M_\odot$	308.3	0.969	105619.	-1204.70	1.000	409.3	$(6{+}3)M_\odot$	616.7	0.981	306975.	-1294.40	0.501	474.7
	$(12{+}3)M_\odot$	346.4	0.964	191589.	-1798.60	1.024	449.6	$(6{+}1)M_\odot$	713.5	0.947	837372.	-3022.40	0.921	1045.5
	$(9{+}9)M_\odot$	317.6	0.972	93768.	-1034.00	1.003	451.6	$(3{+}3)M_\odot$	952.9	0.976	526754.	-1230.80	0.810	1401.6
	$(9{+}6)M_\odot$	377.1	0.971	129105.	-1134.80	1.006	491.9	$(3{+}1)M_\odot$	1337.3	0.947	1360894.	-2043.70	0.546	2021.7
	$(9{+}3)M_\odot$	445.8	0.967	231317.	-1556.80	1.016	567.9	$(1{+}1)M_\odot$	2858.7	0.947	3170331.	-950.23	1.045	3819.3
	$(6{+}6)M_\odot$	476.4	0.975	173399.	-1062.80	0.792	451.3							
P$(3, 3.5, 0)$	$(12{+}12)M_\odot$	360.6	0.977	56983.	-695.17	1.004	515.0	$(12{+}1)M_\odot$	399.5	0.959	529970.	-4281.90	0.629	341.5
	$(12{+}9)M_\odot$	406.0	0.980	72199.	-772.52	0.995	505.8	$(9{+}1)M_\odot$	545.4	0.967	634980.	-3562.30	0.543	416.0
	$(12{+}6)M_\odot$	442.8	0.981	101289.	-938.79	1.016	555.6	$(6{+}3)M_\odot$	885.5	0.989	304214.	-1147.40	0.441	590.6
	$(12{+}3)M_\odot$	441.6	0.978	186197.	-1514.60	1.074	597.6	$(6{+}1)M_\odot$	850.4	0.960	833104.	-2857.40	0.876	1227.3
	$(9{+}9)M_\odot$	480.9	0.984	89455.	-774.60	0.986	553.8	$(3{+}3)M_\odot$	1442.6	0.985	523122.	-1078.80	0.750	2058.0
	$(9{+}6)M_\odot$	560.2	0.984	123322.	-840.86	1.257	926.9	$(3{+}1)M_\odot$	1795.8	0.955	1356142.	-1898.20	0.541	2410.9
	$(9{+}3)M_\odot$	598.6	0.983	226911.	-1327.40	0.722	505.7	$(1{+}1)M_\odot$	4327.8	0.951	3169285.	-912.01	0.983	4278.6
	$(6{+}6)M_\odot$	721.3	0.985	170320.	-885.46	0.791	633.3							
P$(3, 3.5, -2)$	$(12{+}12)M_\odot$	360.6	0.975	57547.	-745.61	1.003	485.4	$(12{+}1)M_\odot$	399.5	0.960	528884.	-4258.80	0.631	336.9
	$(12{+}9)M_\odot$	406.0	0.979	72628.	-819.94	0.992	504.9	$(9{+}1)M_\odot$	545.4	0.963	634866.	-3577.00	0.677	436.7
	$(12{+}6)M_\odot$	442.8	0.981	101681.	-982.77	1.010	537.6	$(6{+}3)M_\odot$	885.5	0.985	305247.	-1212.30	0.968	1183.3
	$(12{+}3)M_\odot$	441.6	0.979	187361.	-1579.30	1.025	569.7	$(6{+}1)M_\odot$	850.4	0.960	834159.	-2914.90	0.830	1182.3
	$(9{+}9)M_\odot$	480.9	0.984	90292.	-834.29	1.007	567.4	$(3{+}3)M_\odot$	1442.6	0.983	525119.	-1167.30	0.924	2473.3
	$(9{+}6)M_\odot$	560.2	0.985	124479.	-912.50	1.024	666.6	$(3{+}1)M_\odot$	1795.8	0.953	1357695.	-1967.50	0.604	2528.6
	$(9{+}3)M_\odot$	598.6	0.983	226919.	-1359.60	0.716	500.3	$(1{+}1)M_\odot$	4327.8	0.949	3169727.	-952.24	1.190	4783.5
	$(6{+}6)M_\odot$	721.3	0.985	170933.	-938.96	1.175	1130.6							
P$(3, 3.5, +2)$	$(12{+}12)M_\odot$	360.6	0.977	56849.	-685.74	1.021	511.6	$(12{+}1)M_\odot$	399.5	0.959	528659.	-4223.00	0.647	334.1
	$(12{+}9)M_\odot$	406.0	0.979	72521.	-781.52	1.001	518.0	$(9{+}1)M_\odot$	545.4	0.967	635544.	-3570.80	0.535	425.2
	$(12{+}6)M_\odot$	442.8	0.981	100975.	-924.19	1.007	538.4	$(6{+}3)M_\odot$	885.5	0.987	304301.	-1141.20	0.976	1292.9
	$(12{+}3)M_\odot$	441.6	0.977	186557.	-1520.30	1.005	533.8	$(6{+}1)M_\odot$	850.4	0.960	833535.	-2858.20	0.835	1212.1
	$(9{+}9)M_\odot$	480.9	0.983	90114.	-790.55	0.989	568.5	$(3{+}3)M_\odot$	1442.6	0.985	523177.	-1070.10	0.714	2008.1
	$(9{+}6)M_\odot$	560.2	0.984	123691.	-847.13	0.994	647.5	$(3{+}1)M_\odot$	1795.8	0.955	1353538.	-1828.50	0.619	2334.6
	$(9{+}3)M_\odot$	598.6	0.982	227417.	-1338.20	0.738	528.4	$(1{+}1)M_\odot$	4327.8	0.952	3168731.	-886.73	1.010	4303.4
	$(6{+}6)M_\odot$	721.3	0.985	169855.	-863.85	1.065	961.9							
EP$(2, 2.5)$	$(12{+}12)M_\odot$	363.5	0.988	49577.	-480.20	0.868	691.8	$(12{+}1)M_\odot$	665.0	0.963	542729.	-4859.80	0.808	617.6
	$(12{+}9)M_\odot$	415.2	0.989	65390.	-602.28	0.926	773.6	$(9{+}1)M_\odot$	863.6	0.952	654948.	-4289.80	0.902	1243.9
	$(12{+}6)M_\odot$	483.0	0.988	95424.	-827.49	0.789	755.4	$(6{+}3)M_\odot$	965.9	0.990	308867.	-1406.00	0.698	1460.9
	$(12{+}3)M_\odot$	576.3	0.988	185120.	-1600.80	0.688	634.1	$(6{+}1)M_\odot$	1233.3	0.938	856629.	-3553.70	0.243	812.2
	$(9{+}9)M_\odot$	484.7	0.989	84948.	-702.39	0.717	721.6	$(3{+}3)M_\odot$	1454.1	0.973	531527.	-1407.70	0.728	2642.2
	$(9{+}6)M_\odot$	580.8	0.991	121357.	-876.51	0.728	835.6	$(3{+}1)M_\odot$	2165.6	0.940	1360713.	-2087.30	0.925	2847.2
	$(9{+}3)M_\odot$	721.9	0.992	229188.	-1527.70	0.652	759.9	$(1{+}1)M_\odot$	4362.2	0.943	3170943.	-995.33	1.244	4272.3
	$(6{+}6)M_\odot$	727.0	0.993	170365.	-994.43	0.553	872.1							
EP$(3, 3.5, 0)$	$(12{+}12)M_\odot$	361.5	0.988	52298.	-484.74	0.868	594.4	$(12{+}1)M_\odot$	680.0	0.971	537529.	-4611.90	0.763	636.5
	$(12{+}9)M_\odot$	419.3	0.990	66504.	-549.02	0.869	638.1	$(9{+}1)M_\odot$	882.5	0.962	647261.	-3995.70	0.955	1504.2
	$(12{+}6)M_\odot$	488.8	0.992	94850.	-713.33	1.011	912.2	$(6{+}3)M_\odot$	971.8	0.993	304505.	-1186.10	0.736	1743.4
	$(12{+}3)M_\odot$	598.1	0.992	182212.	-1406.20	0.785	741.1	$(6{+}1)M_\odot$	1264.7	0.950	845578.	-3223.90	0.681	2056.6
	$(9{+}9)M_\odot$	488.6	0.991	84356.	-588.58	0.802	699.6	$(3{+}3)M_\odot$	1468.7	0.985	525394.	-1165.50	0.627	2736.7
	$(9{+}6)M_\odot$	584.2	0.992	119783.	-728.86	0.779	874.2	$(3{+}1)M_\odot$	2205.5	0.950	1355784.	-1913.40	0.954	3576.3
	$(9{+}3)M_\odot$	730.5	0.994	225599.	-1317.20	0.684	884.3	$(1{+}1)M_\odot$	4422.6	0.949	3168885.	-909.79	1.172	4435.8
	$(6{+}6)M_\odot$	724.6	0.993	167749.	-815.81	0.670	1029.0							
EP$(3, 3.5, -2)$	$(12{+}12)M_\odot$	361.2	0.988	51189.	-477.20	0.992	634.4	$(12{+}1)M_\odot$	677.4	0.971	537454.	-4630.50	0.761	636.8
	$(12{+}9)M_\odot$	407.9	0.991	66061.	-560.85	0.970	758.3	$(9{+}1)M_\odot$	883.5	0.963	646639.	-4005.20	0.744	998.9
	$(12{+}6)M_\odot$	482.3	0.992	95444.	-758.41	0.814	718.4	$(6{+}3)M_\odot$	961.7	0.993	305474.	-1245.00	0.731	1702.1
	$(12{+}3)M_\odot$	586.4	0.990	182279.	-1429.50	0.983	1038.0	$(6{+}1)M_\odot$	1265.9	0.952	845361.	-3247.50	0.286	794.4
	$(9{+}9)M_\odot$	475.9	0.991	84637.	-625.21	0.917	778.0	$(3{+}3)M_\odot$	1438.6	0.984	526774.	-1236.00	0.660	2665.3
	$(9{+}6)M_\odot$	580.6	0.992	120240.	-772.93	0.897	972.5	$(3{+}1)M_\odot$	2219.2	0.948	1357892.	-1997.70	0.812	2624.4
	$(9{+}3)M_\odot$	739.2	0.993	225609.	-1345.20	0.645	862.2	$(1{+}1)M_\odot$	4278.8	0.946	3170248.	-971.57	1.148	4293.5
	$(6{+}6)M_\odot$	718.5	0.993	167707.	-846.85	0.618	882.4							
EP$(3, 3.5, +2)$	$(12{+}12)M_\odot$	364.7	0.988	51392.	-454.63	0.925	590.8	$(12{+}1)M_\odot$	677.8	0.970	536824.	-4581.20	1.143	1104.0
	$(12{+}9)M_\odot$	418.5	0.991	66283.	-535.83	0.900	686.7	$(9{+}1)M_\odot$	883.8	0.962	646930.	-3980.00	0.739	1007.5
	$(12{+}6)M_\odot$	492.3	0.992	95107.	-715.45	0.909	815.2	$(6{+}3)M_\odot$	984.4	0.993	304768.	-1185.10	0.708	1434.1
	$(12{+}3)M_\odot$	594.3	0.990	182223.	-1398.40	0.952	1032.9	$(6{+}1)M_\odot$	1258.8	0.950	846072.	-3223.20	0.748	2076.7
	$(9{+}9)M_\odot$	489.3	0.991	84331.	-581.99	0.931	884.2	$(3{+}3)M_\odot$	1463.3	0.985	525640.	-1161.50	0.550	2366.2
	$(9{+}6)M_\odot$	589.5	0.992	120251.	-736.39	0.790	881.4	$(3{+}1)M_\odot$	2231.3	0.949	1354464.	-1870.70	1.011	2780.0
	$(9{+}3)M_\odot$	732.3	0.993	225156.	-1296.10	0.693	936.2	$(1{+}1)M_\odot$	4393.5	0.949	3169592.	-915.61	1.083	4498.8
	$(6{+}6)M_\odot$	729.3	0.993	167480.	-799.91	0.605	938.8							

TABLE VI: Fitting factors for the projection of the target models (in the rows) onto the $(\psi_0, \psi_{3/2}, \alpha, f_{\rm cut})$ Fourier-domain detection template family when S2-H1 noise curve is used. For BBH masses $m_{1,2} = 1, 3, 6, 9, 12M_\odot$, this table shows the minmax matches between the target models and the Fourier-domain search model, *maximized over the intrinsic parameters* ψ_0, $\psi_{3/2}$, and $f_{\rm cut}$, and over the extrinsic parameter α. For each intersection, the six numbers shown report the *ending frequency* $f_{\rm end}$ (defined in BCV1) of the PN model for the BBH masses quoted, the minmax FF mn, and the search parameters at which the maximum is attained.

PN model		$f_{\rm end}$	mn	ψ_0	$\psi_{3/2}$	$\alpha f_{\rm cut}^{2/3}$	$f_{\rm cut}$		$f_{\rm end}$	mn	ψ_0	$\psi_{3/2}$	$\alpha f_{\rm cut}^{2/3}$	$f_{\rm cut}$
	FF (minmax) with $(\psi_0, \psi_{3/2})_{\alpha,{\rm cut}}$ template family when LIGO-S2-H1-fit noise curve is used													
	$(21{+}21)M_\odot$	210.8	0.900	17392.	-329.43	1.000	451.7	$(15{+}6)M_\odot$	413.5	0.983	83620.	-992.99	1.000	502.8
	$(21{+}18)M_\odot$	226.9	0.905	21028.	-389.05	1.000	462.5	$(15{+}3)M_\odot$	469.8	0.988	155341.	-1543.90	1.002	554.1
	$(21{+}15)M_\odot$	245.2	0.925	27542.	-531.08	0.997	400.9	$(15{+}1)M_\odot$	512.2	0.992	439530.	-3825.20	0.999	643.0

PN model		FF (minmax) with $(\psi_0,\psi_{3/2})_{\alpha,\text{cut}}$ template family when LIGO-S2-H1-fit noise curve is used												
		f_{end}	mn	ψ_0	$\psi_{3/2}$	$\alpha f_{\text{cut}}^{2/3}$	f_{cut}		f_{end}	mn	ψ_0	$\psi_{3/2}$	$\alpha f_{\text{cut}}^{2/3}$	f_{cut}
	$(21{+}12)M_\odot$	266.2	0.933	33028.	-573.45	1.000	445.6	$(12{+}12)M_\odot$	369.0	0.972	55463.	-758.16	0.980	502.9
	$(21{+}9)M_\odot$	290.2	0.955	44372.	-737.88	0.974	409.2	$(12{+}9)M_\odot$	420.8	0.982	69814.	-823.33	0.992	520.5
	$(21{+}6)M_\odot$	317.5	0.968	64199.	-961.96	0.998	470.9	$(12{+}6)M_\odot$	486.2	0.987	98587.	-987.48	1.009	579.0
	$(21{+}3)M_\odot$	348.3	0.980	121747.	-1615.90	1.001	454.6	$(12{+}3)M_\odot$	568.6	0.990	182481.	-1495.90	1.008	670.7
	$(21{+}1)M_\odot$	370.4	0.989	348767.	-4192.30	1.001	455.4	$(12{+}1)M_\odot$	633.5	0.992	512229.	-3595.30	1.004	877.9
$T(2,2)$	$(18{+}18)M_\odot$	246.0	0.916	25445.	-460.62	0.963	398.0	$(9{+}9)M_\odot$	491.9	0.987	88302.	-891.76	1.001	578.4
	$(18{+}15)M_\odot$	268.1	0.942	31141.	-543.22	0.944	414.0	$(9{+}6)M_\odot$	587.8	0.988	123072.	-1005.80	0.990	630.4
	$(18{+}12)M_\odot$	293.9	0.949	37910.	-606.48	0.999	477.9	$(9{+}3)M_\odot$	718.8	0.990	224552.	-1427.00	1.069	939.3
	$(18{+}9)M_\odot$	324.1	0.961	50716.	-772.92	1.000	467.3	$(9{+}1)M_\odot$	829.6	0.991	624594.	-3314.10	0.986	1255.8
	$(18{+}6)M_\odot$	359.4	0.974	71687.	-948.02	1.001	480.4	$(6{+}6)M_\odot$	737.9	0.989	169715.	-1072.40	1.041	877.2
	$(18{+}3)M_\odot$	400.1	0.986	136189.	-1584.70	1.000	495.3	$(6{+}3)M_\odot$	972.3	0.990	304475.	-1394.10	1.003	1310.2
	$(18{+}1)M_\odot$	429.9	0.991	387940.	-4026.20	1.001	528.9	$(6{+}1)M_\odot$	1200.2	0.982	828120.	-2941.70	1.152	2748.5
	$(15{+}15)M_\odot$	295.1	0.950	36888.	-599.56	0.998	453.4	$(3{+}3)M_\odot$	1475.8	0.986	525848.	-1455.70	0.937	2064.5
	$(15{+}12)M_\odot$	327.5	0.959	45855.	-701.12	1.000	467.3	$(3{+}1)M_\odot$	2156.4	0.958	1360387.	-2369.10	0.425	2366.4
	$(15{+}9)M_\odot$	366.5	0.972	59729.	-839.38	1.000	468.5	$(1{+}1)M_\odot$	4427.3	0.942	3178240.	-1563.80	1.119	4587.4
	$(21{+}21)M_\odot$	153.4	0.806	14483.	259.91	0.289	155.9	$(15{+}6)M_\odot$	322.4	0.967	71616.	26.18	0.582	405.8
	$(21{+}18)M_\odot$	166.3	0.945	26210.	-177.90	0.990	390.6	$(15{+}3)M_\odot$	397.2	0.976	142400.	-318.92	0.475	461.3
	$(21{+}15)M_\odot$	181.0	0.950	28113.	-103.45	0.967	373.5	$(15{+}1)M_\odot$	485.6	0.984	419685.	-1573.40	0.421	499.8
	$(21{+}12)M_\odot$	200.1	0.956	31910.	-55.71	0.999	398.1	$(12{+}12)M_\odot$	268.0	0.964	48300.	13.78	0.949	473.2
	$(21{+}9)M_\odot$	222.5	0.961	41538.	-112.45	1.000	424.7	$(12{+}9)M_\odot$	310.2	0.965	60034.	65.81	0.707	440.0
	$(21{+}6)M_\odot$	256.4	0.964	57553.	-118.36	0.968	447.1	$(12{+}6)M_\odot$	372.4	0.971	86191.	31.17	0.352	444.5
	$(21{+}3)M_\odot$	307.0	0.969	111329.	-401.62	0.781	401.1	$(12{+}3)M_\odot$	470.1	0.980	167641.	-259.31	0.272	522.7
	$(21{+}1)M_\odot$	358.3	0.977	331128.	-1738.50	0.591	373.6	$(12{+}1)M_\odot$	593.3	0.988	489604.	-1423.10	0.402	619.2
$T(2,2.5)$	$(18{+}18)M_\odot$	179.0	0.950	28079.	-124.99	1.001	407.3	$(9{+}9)M_\odot$	360.2	0.970	77157.	52.13	0.486	455.7
	$(18{+}15)M_\odot$	196.5	0.954	30824.	-75.26	0.936	357.4	$(9{+}6)M_\odot$	435.9	0.976	109685.	24.77	0.243	499.0
	$(18{+}12)M_\odot$	217.1	0.959	35422.	-21.30	0.998	428.8	$(9{+}3)M_\odot$	574.6	0.983	209315.	-230.37	0.081	630.4
	$(18{+}9)M_\odot$	244.5	0.962	45121.	-39.37	0.998	460.5	$(9{+}1)M_\odot$	748.9	0.990	600893.	-1303.10	0.599	1644.7
	$(18{+}6)M_\odot$	286.0	0.960	60843.	41.27	0.719	373.6	$(6{+}6)M_\odot$	537.0	0.980	156009.	-32.94	0.000	590.2
	$(18{+}3)M_\odot$	345.2	0.972	123445.	-323.27	0.615	406.4	$(6{+}3)M_\odot$	736.7	0.985	288942.	-236.10	0.383	1681.6
	$(18{+}1)M_\odot$	413.0	0.981	368678.	-1646.30	0.506	427.8	$(6{+}1)M_\odot$	1043.9	0.996	802599.	-1115.00	0.226	900.8
	$(15{+}15)M_\odot$	215.7	0.960	34004.	-9.82	0.994	439.9	$(3{+}3)M_\odot$	1079.3	0.995	509035.	-287.42	0.058	971.6
	$(15{+}12)M_\odot$	240.1	0.962	40043.	16.44	1.001	462.0	$(3{+}1)M_\odot$	1725.5	0.995	1331338.	-743.87	0.110	2532.7
	$(15{+}9)M_\odot$	274.1	0.956	46796.	164.51	0.724	381.3	$(1{+}1)M_\odot$	3235.0	0.979	3156073.	-271.39	0.386	3776.2
	$(21{+}21)M_\odot$	198.0	0.905	17901.	-340.65	1.001	428.1	$(15{+}6)M_\odot$	356.4	0.978	87737.	-1106.90	1.014	481.4
	$(21{+}18)M_\odot$	212.4	0.894	23085.	-461.61	0.999	414.2	$(15{+}3)M_\odot$	370.7	0.979	161943.	-1782.00	1.001	458.4
	$(21{+}15)M_\odot$	226.9	0.919	28502.	-558.62	1.002	382.7	$(15{+}1)M_\odot$	373.9	0.969	456655.	-4620.50	0.818	356.7
	$(21{+}12)M_\odot$	240.7	0.926	34747.	-628.28	1.000	433.7	$(12{+}12)M_\odot$	346.5	0.972	57496.	-789.92	0.992	477.8
	$(21{+}9)M_\odot$	252.5	0.948	46505.	-813.69	1.030	417.0	$(12{+}9)M_\odot$	390.8	0.976	73507.	-898.66	1.002	472.9
	$(21{+}6)M_\odot$	261.3	0.956	68487.	-1148.70	0.999	382.9	$(12{+}6)M_\odot$	432.1	0.981	102331.	-1053.00	0.987	491.2
	$(21{+}3)M_\odot$	266.2	0.970	129813.	-2019.80	0.985	363.7	$(12{+}3)M_\odot$	460.2	0.981	187539.	-1620.70	0.999	539.8
	$(21{+}1)M_\odot$	267.1	0.970	370577.	-5452.70	1.000	340.3	$(12{+}1)M_\odot$	467.3	0.972	526632.	-4145.60	0.661	392.4
$T(3,3.5,0)$	$(18{+}18)M_\odot$	231.0	0.910	27751.	-539.42	1.002	411.7	$(9{+}9)M_\odot$	462.0	0.982	91498.	-923.81	1.011	542.4
	$(18{+}15)M_\odot$	250.7	0.932	32932.	-598.18	1.001	399.7	$(9{+}6)M_\odot$	540.5	0.983	126203.	-1017.70	1.007	595.9
	$(18{+}12)M_\odot$	270.2	0.950	41140.	-704.86	1.002	419.5	$(9{+}3)M_\odot$	603.9	0.982	228758.	-1460.80	0.971	684.7
	$(18{+}9)M_\odot$	288.0	0.961	53162.	-842.22	1.001	441.0	$(9{+}1)M_\odot$	622.5	0.972	634620.	-3572.10	0.589	470.4
	$(18{+}6)M_\odot$	301.9	0.967	75565.	-1084.30	1.000	437.4	$(6{+}6)M_\odot$	693.1	0.984	172160.	-1019.20	1.060	841.8
	$(18{+}3)M_\odot$	310.0	0.975	143899.	-1921.00	1.000	401.6	$(6{+}3)M_\odot$	864.1	0.985	307292.	-1311.00	0.627	589.2
	$(18{+}1)M_\odot$	311.6	0.969	408659.	-5103.60	1.000	388.2	$(6{+}1)M_\odot$	930.1	0.960	835930.	-2988.60	0.871	1410.8
	$(15{+}15)M_\odot$	277.2	0.949	38671.	-639.62	1.006	468.4	$(3{+}3)M_\odot$	1386.2	0.979	526735.	-1246.10	0.971	2289.3
	$(15{+}12)M_\odot$	305.6	0.959	48357.	-762.38	0.999	423.6	$(3{+}1)M_\odot$	1811.5	0.948	1359484.	-2038.40	0.793	3134.4
	$(15{+}9)M_\odot$	333.2	0.969	61611.	-870.11	1.000	432.8	$(1{+}1)M_\odot$	4158.6	0.947	3170349.	-981.76	1.156	4266.2
	$(21{+}21)M_\odot$	198.0	0.893	19345.	-416.81	0.994	382.2	$(15{+}6)M_\odot$	356.4	0.978	87654.	-1133.80	1.007	464.8
	$(21{+}18)M_\odot$	212.4	0.905	21196.	-397.92	0.937	411.1	$(15{+}3)M_\odot$	370.7	0.979	162019.	-1817.80	1.000	455.0
	$(21{+}15)M_\odot$	226.9	0.906	27172.	-523.89	1.000	429.6	$(15{+}1)M_\odot$	373.9	0.968	458047.	-4705.20	1.077	500.5
	$(21{+}12)M_\odot$	240.7	0.929	34800.	-649.72	0.953	412.1	$(12{+}12)M_\odot$	346.5	0.971	57818.	-830.00	0.997	459.5
	$(21{+}9)M_\odot$	252.5	0.938	46588.	-843.15	1.001	399.2	$(12{+}9)M_\odot$	390.8	0.975	73591.	-937.24	1.007	468.3
	$(21{+}6)M_\odot$	261.3	0.952	67611.	-1138.70	1.000	401.8	$(12{+}6)M_\odot$	432.1	0.981	102714.	-1103.00	1.013	503.2
	$(21{+}3)M_\odot$	266.2	0.968	129860.	-2049.50	1.000	368.2	$(12{+}3)M_\odot$	460.2	0.981	188254.	-1682.30	1.028	572.3
	$(21{+}1)M_\odot$	267.1	0.971	370512.	-5476.80	1.000	338.6	$(12{+}1)M_\odot$	467.3	0.972	526854.	-4186.20	0.695	396.2
$T(3,3.5,-2)$	$(18{+}18)M_\odot$	231.0	0.918	25970.	-480.83	0.968	439.9	$(9{+}9)M_\odot$	462.0	0.983	91502.	-958.99	0.991	534.5
	$(18{+}15)M_\odot$	250.7	0.922	32455.	-599.08	0.988	424.3	$(9{+}6)M_\odot$	540.5	0.984	126791.	-1073.90	1.018	624.4
	$(18{+}12)M_\odot$	270.3	0.939	40754.	-719.52	1.000	413.8	$(9{+}3)M_\odot$	603.9	0.981	229899.	-1536.00	1.206	929.4
	$(18{+}9)M_\odot$	288.0	0.958	52787.	-859.97	1.001	408.6	$(9{+}1)M_\odot$	622.5	0.973	636536.	-3671.10	0.535	467.5
	$(18{+}6)M_\odot$	301.9	0.969	76458.	-1145.20	0.999	444.0	$(6{+}6)M_\odot$	693.1	0.984	173036.	-1089.10	1.144	911.1
	$(18{+}3)M_\odot$	310.0	0.975	143424.	-1932.60	1.000	408.0	$(6{+}3)M_\odot$	864.1	0.982	307930.	-1375.20	1.101	1191.5
	$(18{+}1)M_\odot$	311.6	0.970	408309.	-5119.70	1.001	387.9	$(6{+}1)M_\odot$	930.1	0.959	836587.	-3048.10	0.900	1318.1
	$(15{+}15)M_\odot$	277.2	0.947	38335.	-650.94	1.013	462.6	$(3{+}3)M_\odot$	1386.1	0.977	528229.	-1330.60	0.901	2016.6
	$(15{+}12)M_\odot$	305.6	0.953	47624.	-760.46	1.007	448.7	$(3{+}1)M_\odot$	1811.5	0.946	1361025.	-2119.80	0.757	2726.9
	$(15{+}9)M_\odot$	333.2	0.966	61378.	-891.13	0.996	441.0	$(1{+}1)M_\odot$	4158.3	0.944	3171483.	-1045.10	1.242	4322.3
	$(21{+}21)M_\odot$	198.0	0.901	19138.	-373.41	0.918	404.3	$(15{+}6)M_\odot$	356.4	0.978	87274.	-1058.40	0.989	471.2
	$(21{+}18)M_\odot$	212.4	0.913	24308.	-486.03	0.965	372.4	$(15{+}3)M_\odot$	370.7	0.978	161324.	-1726.10	0.999	455.7
	$(21{+}15)M_\odot$	226.9	0.919	28198.	-509.42	0.891	377.0	$(15{+}1)M_\odot$	373.9	0.967	457729.	-4628.60	1.102	520.9
	$(21{+}12)M_\odot$	240.7	0.932	36383.	-669.66	0.997	395.6	$(12{+}12)M_\odot$	346.5	0.972	57706.	-763.52	1.014	499.4
	$(21{+}9)M_\odot$	252.5	0.948	46344.	-780.56	1.000	436.7	$(12{+}9)M_\odot$	390.8	0.977	72921.	-843.00	0.999	476.5
	$(21{+}6)M_\odot$	261.3	0.961	68560.	-1121.70	1.012	400.2	$(12{+}6)M_\odot$	432.1	0.980	101849.	-998.77	1.002	518.8
	$(21{+}3)M_\odot$	266.2	0.969	129609.	-1983.60	1.000	386.3	$(12{+}3)M_\odot$	460.2	0.979	186566.	-1550.60	1.127	649.9
	$(21{+}1)M_\odot$	267.1	0.968	370734.	-5431.70	1.002	341.5	$(12{+}1)M_\odot$	467.3	0.972	525524.	-4072.00	0.649	389.9
$T(3,3.5,+2)$	$(18{+}18)M_\odot$	231.0	0.926	28784.	-554.63	1.000	398.8	$(9{+}9)M_\odot$	462.0	0.983	91381.	-882.60	1.008	553.6
	$(18{+}15)M_\odot$	250.7	0.940	33377.	-585.00	0.974	419.0	$(9{+}6)M_\odot$	540.6	0.982	124482.	-918.73	1.009	613.3
	$(18{+}12)M_\odot$	270.2	0.950	41171.	-679.83	0.996	456.1	$(9{+}3)M_\odot$	603.9	0.982	228211.	-1399.60	0.803	514.3
	$(18{+}9)M_\odot$	288.0	0.960	53549.	-828.58	0.979	443.4	$(9{+}1)M_\odot$	622.4	0.974	635449.	-3563.60	0.505	472.8

PN model		FF (minmax) with $(\psi_0, \psi_{3/2})_{\alpha,\mathrm{cut}}$ template family when LIGO-S2-H1-fit noise curve is used												
		$f_{\rm end}$	mn	ψ_0	$\psi_{3/2}$	$\alpha f_{\rm cut}^{2/3}$	$f_{\rm cut}$		$f_{\rm end}$	mn	ψ_0	$\psi_{3/2}$	$\alpha f_{\rm cut}^{2/3}$	$f_{\rm cut}$
	$(18+6)M_\odot$	301.9	0.968	76863.	−1103.50	1.001	432.3	$(6+6)M_\odot$	693.1	0.983	171977.	−970.83	1.043	829.2
	$(18+3)M_\odot$	310.0	0.976	143426.	−1872.40	1.000	405.6	$(6+3)M_\odot$	864.2	0.987	305082.	−1205.70	0.610	591.9
	$(18+1)M_\odot$	311.6	0.967	408061.	−5050.30	1.000	382.1	$(6+1)M_\odot$	930.0	0.966	835136.	−2928.70	0.486	631.5
	$(15+15)M_\odot$	277.2	0.951	39267.	−637.78	1.088	535.6	$(3+3)M_\odot$	1386.1	0.981	525497.	−1166.90	0.864	2245.9
	$(15+12)M_\odot$	305.6	0.964	48998.	−754.77	1.009	449.2	$(3+1)M_\odot$	1811.6	0.951	1357786.	−1955.40	0.626	2487.8
	$(15+9)M_\odot$	333.2	0.972	61983.	−849.59	1.000	442.6	$(1+1)M_\odot$	4158.5	0.950	3169214.	−918.26	1.065	4259.6
P(2, 2.5)	$(21+21)M_\odot$	136.1	0.860	20245.	−484.20	0.940	355.1	$(15+6)M_\odot$	259.2	0.962	91401.	−1298.20	1.001	397.4
	$(21+18)M_\odot$	146.4	0.855	24886.	−597.00	1.000	318.0	$(15+3)M_\odot$	282.3	0.962	167745.	−2067.30	1.000	379.6
	$(21+15)M_\odot$	157.6	0.887	30413.	−682.80	0.965	318.8	$(15+1)M_\odot$	292.0	0.931	467360.	−5169.60	1.064	359.2
	$(21+12)M_\odot$	169.8	0.897	38512.	−847.05	1.000	326.0	$(12+12)M_\odot$	238.2	0.956	61023.	−967.35	0.987	397.7
	$(21+9)M_\odot$	182.6	0.916	49998.	−1020.20	1.000	359.8	$(12+9)M_\odot$	270.8	0.964	76727.	−1056.20	1.003	399.7
	$(21+6)M_\odot$	195.1	0.933	72927.	−1409.50	1.000	330.2	$(12+6)M_\odot$	308.3	0.969	105619.	−1204.70	1.000	409.3
	$(21+3)M_\odot$	205.3	0.950	137649.	−2469.80	1.000	312.3	$(12+3)M_\odot$	346.4	0.964	191589.	−1798.60	1.024	449.6
	$(21+1)M_\odot$	209.0	0.944	378884.	−6061.10	0.748	191.7	$(12+1)M_\odot$	364.0	0.952	532918.	−4438.00	0.607	309.2
	$(18+18)M_\odot$	158.8	0.877	29770.	−679.88	1.000	330.8	$(9+9)M_\odot$	317.6	0.972	93768.	−1034.00	1.003	451.6
	$(18+15)M_\odot$	172.9	0.909	35611.	−760.00	0.990	332.2	$(9+6)M_\odot$	377.1	0.971	129105.	−1134.80	1.006	491.9
	$(18+12)M_\odot$	188.6	0.925	43311.	−847.24	0.990	367.4	$(9+3)M_\odot$	445.8	0.967	231317.	−1556.80	1.016	567.9
	$(18+9)M_\odot$	205.6	0.936	56534.	−1033.30	0.995	376.0	$(9+1)M_\odot$	482.7	0.938	641871.	−3837.30	1.085	704.2
	$(18+6)M_\odot$	222.9	0.954	81306.	−1375.30	1.004	352.0	$(6+6)M_\odot$	476.4	0.975	173399.	−1062.80	0.792	451.3
	$(18+3)M_\odot$	237.8	0.955	150336.	−2271.50	1.000	340.1	$(6+3)M_\odot$	616.7	0.981	306975.	−1294.40	0.501	474.7
	$(18+1)M_\odot$	243.6	0.935	419906.	−5770.30	1.082	310.3	$(6+1)M_\odot$	713.5	0.947	837372.	−3022.40	0.921	1045.5
	$(15+15)M_\odot$	190.6	0.924	41398.	−797.78	0.958	367.4	$(3+3)M_\odot$	952.9	0.976	526754.	−1230.80	0.810	1401.6
	$(15+12)M_\odot$	211.1	0.943	50968.	−914.68	1.000	357.3	$(3+1)M_\odot$	1337.3	0.947	1360894.	−2043.70	0.546	2021.7
	$(15+9)M_\odot$	234.3	0.956	64449.	−1025.50	0.988	362.8	$(1+1)M_\odot$	2858.7	0.947	3170331.	−950.23	1.045	3819.3
P(3, 3.5, 0)	$(21+21)M_\odot$	206.1	0.911	19751.	−366.32	0.999	455.8	$(15+6)M_\odot$	359.4	0.979	86211.	−984.38	1.000	488.9
	$(21+18)M_\odot$	221.0	0.926	23987.	−438.86	0.998	438.5	$(15+3)M_\odot$	346.3	0.974	162515.	−1760.40	1.000	435.8
	$(21+15)M_\odot$	235.6	0.933	28199.	−484.52	1.023	489.2	$(15+1)M_\odot$	314.7	0.943	464041.	−4977.00	1.091	411.2
	$(21+12)M_\odot$	248.2	0.945	36173.	−625.07	0.999	401.9	$(12+12)M_\odot$	360.6	0.977	56983.	−695.17	1.004	515.0
	$(21+9)M_\odot$	256.1	0.948	46709.	−762.58	1.001	435.0	$(12+9)M_\odot$	406.0	0.980	72199.	−772.52	0.995	505.8
	$(21+6)M_\odot$	254.7	0.957	68208.	−1085.60	1.000	408.8	$(12+6)M_\odot$	442.8	0.981	101289.	−938.79	1.016	555.6
	$(21+3)M_\odot$	239.3	0.963	132153.	−2117.00	1.000	351.1	$(12+3)M_\odot$	441.6	0.978	186197.	−1514.60	1.074	597.6
	$(21+1)M_\odot$	220.6	0.946	379562.	−6039.50	1.111	301.1	$(12+1)M_\odot$	399.5	0.959	529970.	−4281.90	0.629	341.5
	$(18+18)M_\odot$	240.4	0.938	28193.	−494.17	0.990	421.6	$(9+9)M_\odot$	480.9	0.984	89455.	−774.60	0.986	553.8
	$(18+15)M_\odot$	260.7	0.950	33108.	−536.38	0.999	465.8	$(9+6)M_\odot$	560.2	0.984	123322.	−840.86	1.257	926.9
	$(18+12)M_\odot$	280.1	0.956	40389.	−612.69	1.000	473.9	$(9+3)M_\odot$	598.6	0.983	226911.	−1327.40	0.722	505.7
	$(18+9)M_\odot$	295.2	0.964	52632.	−756.86	1.002	473.6	$(9+1)M_\odot$	545.4	0.967	634980.	−3562.30	0.543	416.0
	$(18+6)M_\odot$	299.3	0.970	76337.	−1053.10	1.001	417.8	$(6+6)M_\odot$	721.3	0.985	170320.	−885.46	0.791	633.3
	$(18+3)M_\odot$	283.5	0.969	145621.	−1966.90	1.000	394.7	$(6+3)M_\odot$	885.5	0.989	304214.	−1147.40	0.441	590.6
	$(18+1)M_\odot$	259.4	0.945	416683.	−5566.80	1.110	353.7	$(6+1)M_\odot$	850.4	0.960	833104.	−2857.40	0.876	1227.3
	$(15+15)M_\odot$	288.5	0.958	38187.	−555.93	1.003	471.1	$(3+3)M_\odot$	1442.6	0.985	523122.	−1078.80	0.750	2058.0
	$(15+12)M_\odot$	317.7	0.969	48109.	−675.83	1.011	467.6	$(3+1)M_\odot$	1795.8	0.955	1356142.	−1898.20	0.541	2410.9
	$(15+9)M_\odot$	344.3	0.975	60419.	−751.77	1.001	455.2	$(1+1)M_\odot$	4327.8	0.951	3169285.	−912.01	0.983	4278.6
P(3, 3.5, −2)	$(21+21)M_\odot$	206.1	0.916	20080.	−393.32	1.002	439.8	$(15+6)M_\odot$	359.4	0.979	87124.	−1042.00	1.001	475.2
	$(21+18)M_\odot$	221.0	0.907	23827.	−457.65	1.001	410.8	$(15+3)M_\odot$	346.3	0.975	162443.	−1780.40	1.000	448.9
	$(21+15)M_\odot$	235.6	0.930	29142.	−543.72	1.007	400.9	$(15+1)M_\odot$	314.7	0.944	463837.	−4984.70	1.091	410.8
	$(21+12)M_\odot$	248.2	0.933	35488.	−620.60	0.996	425.3	$(12+12)M_\odot$	360.6	0.975	57547.	−745.61	1.003	485.4
	$(21+9)M_\odot$	256.1	0.953	47163.	−799.46	0.981	400.6	$(12+9)M_\odot$	406.0	0.979	72628.	−819.94	0.992	504.9
	$(21+6)M_\odot$	254.7	0.960	69144.	−1140.80	0.977	377.0	$(12+6)M_\odot$	442.8	0.981	101681.	−982.77	1.010	537.6
	$(21+3)M_\odot$	239.3	0.960	132576.	−2149.40	1.000	353.4	$(12+3)M_\odot$	441.6	0.979	187361.	−1579.30	1.025	569.7
	$(21+1)M_\odot$	220.6	0.947	376473.	−5900.00	0.778	206.1	$(12+1)M_\odot$	399.5	0.960	528884.	−4258.80	0.631	336.9
	$(18+18)M_\odot$	240.4	0.921	28296.	−523.98	1.000	416.9	$(9+9)M_\odot$	480.9	0.984	90292.	−834.29	1.007	567.4
	$(18+15)M_\odot$	260.7	0.942	34126.	−605.08	0.993	404.4	$(9+6)M_\odot$	560.2	0.985	124479.	−912.50	1.024	666.6
	$(18+12)M_\odot$	280.1	0.956	41573.	−681.30	1.000	428.5	$(9+3)M_\odot$	598.6	0.983	226919.	−1359.60	0.716	500.3
	$(18+9)M_\odot$	295.2	0.965	52265.	−767.38	0.999	437.6	$(9+1)M_\odot$	545.4	0.963	634866.	−3577.00	0.677	436.7
	$(18+6)M_\odot$	299.3	0.968	76412.	−1080.00	1.000	431.9	$(6+6)M_\odot$	721.3	0.985	170933.	−938.96	1.175	1130.6
	$(18+3)M_\odot$	283.5	0.970	145294.	−1972.00	1.000	378.5	$(6+3)M_\odot$	885.5	0.985	305247.	−1212.30	0.968	1183.3
	$(18+1)M_\odot$	259.4	0.945	416177.	−5558.30	1.110	352.2	$(6+1)M_\odot$	850.4	0.960	834159.	−2914.90	0.830	1182.3
	$(15+15)M_\odot$	288.5	0.958	38948.	−608.61	0.987	457.8	$(3+3)M_\odot$	1442.6	0.983	525119.	−1167.30	0.924	2473.3
	$(15+12)M_\odot$	317.7	0.961	46470.	−646.57	1.001	438.7	$(3+1)M_\odot$	1795.8	0.953	1357695.	−1967.50	0.604	2528.6
	$(15+9)M_\odot$	344.3	0.971	61460.	−818.84	1.000	456.8	$(1+1)M_\odot$	4327.8	0.949	3169727.	−952.24	1.190	4783.5
P(3, 3.5, +2)	$(21+21)M_\odot$	206.1	0.917	19224.	−342.82	1.000	459.2	$(15+6)M_\odot$	359.4	0.980	86247.	−978.19	1.000	483.7
	$(21+18)M_\odot$	221.0	0.925	23964.	−435.79	0.979	398.1	$(15+3)M_\odot$	346.3	0.973	162656.	−1759.70	1.001	438.1
	$(21+15)M_\odot$	235.6	0.935	28378.	−485.05	0.987	445.8	$(15+1)M_\odot$	314.7	0.943	463711.	−4957.20	1.087	407.9
	$(21+12)M_\odot$	248.2	0.941	36659.	−640.58	1.000	407.7	$(12+12)M_\odot$	360.6	0.977	56849.	−685.74	1.021	511.6
	$(21+9)M_\odot$	256.1	0.953	46754.	−757.23	0.999	450.9	$(12+9)M_\odot$	406.0	0.979	72521.	−781.52	1.001	518.0
	$(21+6)M_\odot$	254.7	0.959	68445.	−1089.60	0.999	417.5	$(12+6)M_\odot$	442.8	0.981	100975.	−924.19	1.007	538.4
	$(21+3)M_\odot$	239.3	0.962	132287.	−2117.30	1.000	340.3	$(12+3)M_\odot$	441.6	0.977	186557.	−1520.30	1.005	533.8
	$(21+1)M_\odot$	220.6	0.946	379686.	−6037.90	1.111	301.4	$(12+1)M_\odot$	399.5	0.959	528659.	−4223.00	0.647	334.1
	$(18+18)M_\odot$	240.4	0.936	28252.	−496.05	0.983	397.6	$(9+9)M_\odot$	480.9	0.983	90114.	−790.55	0.989	568.5
	$(18+15)M_\odot$	260.7	0.949	32795.	−524.84	0.970	420.4	$(9+6)M_\odot$	560.2	0.984	123691.	−847.13	0.994	647.5
	$(18+12)M_\odot$	280.1	0.959	41090.	−633.45	1.000	461.9	$(9+3)M_\odot$	598.6	0.982	227417.	−1338.20	0.738	528.4
	$(18+9)M_\odot$	295.2	0.965	52956.	−764.65	0.980	452.7	$(9+1)M_\odot$	545.4	0.967	635544.	−3570.80	0.535	425.2
	$(18+6)M_\odot$	299.3	0.969	76774.	−1065.70	0.999	419.8	$(6+6)M_\odot$	721.3	0.985	169855.	−863.85	1.065	961.9
	$(18+3)M_\odot$	283.5	0.970	145470.	−1954.80	1.000	396.0	$(6+3)M_\odot$	885.5	0.987	304301.	−1141.20	0.976	1292.9
	$(18+1)M_\odot$	259.4	0.944	416099.	−5536.40	1.107	349.6	$(6+1)M_\odot$	850.4	0.960	833535.	−2858.20	0.835	1212.1
	$(15+15)M_\odot$	288.5	0.961	38711.	−572.45	0.985	458.4	$(3+3)M_\odot$	1442.6	0.985	523177.	−1070.10	0.714	2008.1
	$(15+12)M_\odot$	317.7	0.968	47865.	−667.71	1.020	454.6	$(3+1)M_\odot$	1795.8	0.955	1353538.	−1828.50	0.619	2334.6
	$(15+9)M_\odot$	344.3	0.974	61165.	−775.48	1.006	472.1	$(1+1)M_\odot$	4327.8	0.952	3168731.	−886.73	1.010	4303.4
	$(21+21)M_\odot$	207.7	0.970	15889.	−194.71	0.930	509.3	$(15+6)M_\odot$	413.1	0.984	78619.	−791.41	0.812	661.0
	$(21+18)M_\odot$	223.7	0.972	18252.	−204.47	0.981	653.9	$(15+3)M_\odot$	479.8	0.981	157162.	−1681.00	0.751	546.0
	$(21+15)M_\odot$	242.1	0.972	22887.	−276.66	1.000	616.5	$(15+1)M_\odot$	540.9	0.965	469994.	−5345.70	0.811	483.0

PN model		$f_{\rm end}$	mn	ψ_0	$\psi_{3/2}$	$\alpha f_{\rm cut}^{2/3}$	$f_{\rm cut}$		$f_{\rm end}$	mn	ψ_0	$\psi_{3/2}$	$\alpha f_{\rm cut}^{2/3}$	$f_{\rm cut}$
	FF (minmax) with $(\psi_0, \psi_{3/2})_{\alpha,\rm cut}$ template family when LIGO-S2-H1-fit noise curve is used													
EP(2, 2.5)	$(21{+}12)M_\odot$	263.7	0.977	28343.	−332.07	0.989	694.7	$(12{+}12)M_\odot$	363.5	0.988	49577.	−480.20	0.868	691.8
	$(21{+}9)M_\odot$	289.4	0.981	38522.	−472.56	0.973	630.0	$(12{+}9)M_\odot$	415.2	0.989	65390.	−602.28	0.926	773.6
	$(21{+}6)M_\odot$	320.5	0.977	57325.	−718.40	0.859	570.7	$(12{+}6)M_\odot$	483.0	0.988	95424.	−827.49	0.789	755.4
	$(21{+}3)M_\odot$	359.7	0.952	119822.	−1717.00	0.794	436.5	$(12{+}3)M_\odot$	576.3	0.988	185120.	−1600.80	0.688	634.1
	$(21{+}1)M_\odot$	394.2	0.934	379481.	−6182.40	0.847	332.7	$(12{+}1)M_\odot$	665.0	0.963	542729.	−4859.80	0.808	617.6
	$(18{+}18)M_\odot$	242.3	0.976	22267.	−257.07	0.984	711.3	$(9{+}9)M_\odot$	484.7	0.989	84948.	−702.39	0.717	721.6
	$(18{+}15)M_\odot$	264.3	0.976	26798.	−309.89	0.998	621.1	$(9{+}6)M_\odot$	580.8	0.991	121357.	−876.51	0.728	835.6
	$(18{+}12)M_\odot$	290.4	0.983	33655.	−382.27	1.036	674.1	$(9{+}3)M_\odot$	721.9	0.992	229188.	−1527.70	0.652	759.9
	$(18{+}9)M_\odot$	322.0	0.984	44581.	−495.88	0.815	577.8	$(9{+}1)M_\odot$	863.6	0.952	654948.	−4289.80	0.902	1243.9
	$(18{+}6)M_\odot$	360.9	0.980	67275.	−781.78	0.849	574.4	$(6{+}6)M_\odot$	727.0	0.993	170365.	−994.43	0.553	872.1
	$(18{+}3)M_\odot$	411.1	0.969	136284.	−1713.10	0.786	485.9	$(6{+}3)M_\odot$	965.9	0.990	308867.	−1406.00	0.698	1460.9
	$(18{+}1)M_\odot$	456.0	0.954	419485.	−5823.40	0.824	387.4	$(6{+}1)M_\odot$	1233.3	0.938	856629.	−3553.70	0.243	812.2
	$(15{+}15)M_\odot$	290.8	0.985	32047.	−343.27	0.896	647.0	$(3{+}3)M_\odot$	1454.1	0.973	531527.	−1407.70	0.728	2642.2
	$(15{+}12)M_\odot$	323.0	0.985	40578.	−437.65	0.989	694.4	$(3{+}1)M_\odot$	2165.6	0.940	1360713.	−2087.30	0.925	2847.2
	$(15{+}9)M_\odot$	362.8	0.986	53629.	−558.54	0.838	627.5	$(1{+}1)M_\odot$	4362.2	0.943	3170943.	−995.33	1.244	4272.3
EP(3, 3.5, 0)	$(21{+}21)M_\odot$	206.6	0.966	17934.	−222.01	0.998	547.7	$(15{+}6)M_\odot$	417.4	0.990	79813.	−736.50	0.898	692.3
	$(21{+}18)M_\odot$	223.5	0.963	22147.	−297.31	0.954	457.1	$(15{+}3)M_\odot$	488.5	0.985	154764.	−1500.10	1.064	881.0
	$(21{+}15)M_\odot$	241.7	0.973	26068.	−333.73	1.000	544.5	$(15{+}1)M_\odot$	549.4	0.971	466062.	−5127.20	0.803	489.8
	$(21{+}12)M_\odot$	264.9	0.975	30939.	−364.50	1.000	574.3	$(12{+}12)M_\odot$	361.5	0.988	52298.	−484.74	0.868	594.4
	$(21{+}9)M_\odot$	291.5	0.983	40535.	−472.58	0.970	579.2	$(12{+}9)M_\odot$	419.3	0.990	66504.	−549.02	0.869	638.1
	$(21{+}6)M_\odot$	325.4	0.984	59012.	−697.45	0.956	571.2	$(12{+}6)M_\odot$	488.8	0.992	94850.	−713.33	1.011	912.2
	$(21{+}3)M_\odot$	367.7	0.967	119325.	−1605.00	0.845	467.4	$(12{+}3)M_\odot$	598.1	0.992	182212.	−1406.20	0.785	741.1
	$(21{+}1)M_\odot$	400.7	0.941	376505.	−5984.40	0.838	336.9	$(12{+}1)M_\odot$	680.0	0.971	537529.	−4611.90	0.763	636.5
	$(18{+}18)M_\odot$	241.9	0.970	25160.	−315.23	0.975	499.5	$(9{+}9)M_\odot$	488.6	0.991	84356.	−588.58	0.802	699.6
	$(18{+}15)M_\odot$	264.4	0.978	29361.	−336.77	1.017	557.1	$(9{+}6)M_\odot$	584.2	0.992	119783.	−728.86	0.779	874.2
	$(18{+}12)M_\odot$	291.7	0.983	35918.	−390.67	0.974	574.3	$(9{+}3)M_\odot$	730.5	0.994	225599.	−1317.20	0.684	884.3
	$(18{+}9)M_\odot$	323.4	0.986	46776.	−495.66	0.962	624.2	$(9{+}1)M_\odot$	882.5	0.962	647261.	−3995.70	0.955	1504.2
	$(18{+}6)M_\odot$	365.9	0.987	67747.	−709.34	1.225	961.4	$(6{+}6)M_\odot$	724.6	0.993	167749.	−815.81	0.670	1029.0
	$(18{+}3)M_\odot$	421.6	0.978	135478.	−1587.50	0.805	508.1	$(6{+}3)M_\odot$	971.8	0.993	304505.	−1186.10	0.736	1743.4
	$(18{+}1)M_\odot$	462.6	0.958	414284.	−5548.20	1.040	501.3	$(6{+}1)M_\odot$	1264.7	0.950	845578.	−3223.90	0.681	2056.6
	$(15{+}15)M_\odot$	289.2	0.981	36296.	−423.76	0.936	597.7	$(3{+}3)M_\odot$	1468.7	0.985	525394.	−1165.50	0.627	2736.7
	$(15{+}12)M_\odot$	322.7	0.986	42326.	−422.72	0.987	580.4	$(3{+}1)M_\odot$	2205.5	0.950	1355784.	−1913.40	0.954	3576.3
	$(15{+}9)M_\odot$	364.9	0.989	54779.	−512.39	0.980	634.4	$(1{+}1)M_\odot$	4422.6	0.949	3168885.	−909.79	1.172	4435.8
EP(3, 3.5, −2)	$(21{+}21)M_\odot$	203.0	0.959	18171.	−249.45	0.975	459.0	$(15{+}6)M_\odot$	414.7	0.990	79723.	−757.20	0.954	670.1
	$(21{+}18)M_\odot$	218.7	0.963	19965.	−234.35	1.005	568.7	$(15{+}3)M_\odot$	487.2	0.985	154871.	−1522.60	1.062	859.1
	$(21{+}15)M_\odot$	238.8	0.966	24756.	−307.42	1.001	545.9	$(15{+}1)M_\odot$	549.2	0.971	465882.	−5135.60	0.800	487.6
	$(21{+}12)M_\odot$	260.9	0.978	30769.	−370.66	1.079	669.7	$(12{+}12)M_\odot$	361.2	0.988	51189.	−477.20	0.992	634.4
	$(21{+}9)M_\odot$	290.1	0.978	39826.	−469.04	0.998	565.7	$(12{+}9)M_\odot$	407.9	0.991	66061.	−560.85	0.970	758.3
	$(21{+}6)M_\odot$	323.2	0.980	59170.	−721.07	0.996	604.7	$(12{+}6)M_\odot$	482.3	0.992	95444.	−758.41	0.814	718.4
	$(21{+}3)M_\odot$	366.7	0.967	119204.	−1614.70	0.861	469.9	$(12{+}3)M_\odot$	586.4	0.990	182279.	−1429.50	0.983	1038.0
	$(21{+}1)M_\odot$	399.4	0.935	374895.	−5928.50	1.150	502.8	$(12{+}1)M_\odot$	677.4	0.971	537454.	−4630.50	0.761	636.8
	$(18{+}18)M_\odot$	236.9	0.971	23588.	−272.42	1.005	597.7	$(9{+}9)M_\odot$	475.9	0.991	84637.	−625.21	0.917	778.0
	$(18{+}15)M_\odot$	258.8	0.974	28783.	−336.47	0.999	583.7	$(9{+}6)M_\odot$	580.6	0.992	120240.	−772.93	0.897	972.5
	$(18{+}12)M_\odot$	286.2	0.980	35495.	−398.41	0.999	583.5	$(9{+}3)M_\odot$	739.2	0.993	225609.	−1345.20	0.645	862.2
	$(18{+}9)M_\odot$	322.2	0.985	47080.	−528.62	0.994	590.4	$(9{+}1)M_\odot$	883.5	0.963	646639.	−4005.20	0.744	998.9
	$(18{+}6)M_\odot$	363.3	0.987	67729.	−724.86	0.991	696.4	$(6{+}6)M_\odot$	718.5	0.993	167707.	−846.85	0.618	882.4
	$(18{+}3)M_\odot$	420.5	0.977	134932.	−1584.40	1.090	719.7	$(6{+}3)M_\odot$	961.7	0.993	305474.	−1245.00	0.731	1702.1
	$(18{+}1)M_\odot$	462.4	0.957	414195.	−5556.80	1.039	498.0	$(6{+}1)M_\odot$	1265.9	0.952	845361.	−3247.50	0.286	794.4
	$(15{+}15)M_\odot$	284.9	0.983	35272.	−409.03	0.973	566.9	$(3{+}3)M_\odot$	1438.6	0.984	526774.	−1236.00	0.660	2665.3
	$(15{+}12)M_\odot$	318.0	0.984	41849.	−429.80	1.000	630.3	$(3{+}1)M_\odot$	2219.2	0.948	1357892.	−1997.70	0.812	2624.4
	$(15{+}9)M_\odot$	357.6	0.988	54503.	−530.74	0.999	664.9	$(1{+}1)M_\odot$	4278.8	0.946	3170248.	−971.57	1.148	4293.5
EP(3, 3.5, +2)	$(21{+}21)M_\odot$	207.4	0.963	17776.	−213.88	0.906	456.4	$(15{+}6)M_\odot$	418.7	0.990	79266.	−715.61	0.859	608.6
	$(21{+}18)M_\odot$	224.6	0.962	21500.	−274.93	1.000	514.0	$(15{+}3)M_\odot$	489.4	0.987	155367.	−1514.70	0.764	582.1
	$(21{+}15)M_\odot$	242.2	0.973	25876.	−326.29	0.999	515.6	$(15{+}1)M_\odot$	550.1	0.969	465561.	−5102.90	1.016	632.5
	$(21{+}12)M_\odot$	266.0	0.975	30711.	−353.88	1.001	588.2	$(12{+}12)M_\odot$	364.7	0.988	51392.	−454.63	0.925	590.8
	$(21{+}9)M_\odot$	291.7	0.983	40545.	−470.94	0.998	570.7	$(12{+}9)M_\odot$	418.5	0.991	66283.	−535.83	0.900	686.7
	$(21{+}6)M_\odot$	326.0	0.984	59797.	−721.07	0.966	578.2	$(12{+}6)M_\odot$	492.3	0.992	95107.	−715.45	0.909	815.2
	$(21{+}3)M_\odot$	368.2	0.968	119447.	−1604.60	0.841	465.3	$(12{+}3)M_\odot$	594.3	0.990	182223.	−1398.40	0.952	1032.9
	$(21{+}1)M_\odot$	400.6	0.943	376304.	−5970.80	0.854	339.6	$(12{+}1)M_\odot$	677.8	0.970	536824.	−4581.20	1.143	1104.0
	$(18{+}18)M_\odot$	241.9	0.968	25228.	−316.82	0.999	520.1	$(9{+}9)M_\odot$	489.3	0.991	84331.	−581.99	0.931	884.2
	$(18{+}15)M_\odot$	264.3	0.977	29599.	−343.95	0.985	521.5	$(9{+}6)M_\odot$	589.5	0.992	120251.	−736.39	0.790	881.4
	$(18{+}12)M_\odot$	290.4	0.983	35766.	−383.36	1.000	567.6	$(9{+}3)M_\odot$	732.3	0.993	225156.	−1296.10	0.693	936.2
	$(18{+}9)M_\odot$	323.5	0.986	46814.	−492.40	0.915	554.7	$(9{+}1)M_\odot$	883.8	0.962	646930.	−3980.00	0.739	1007.5
	$(18{+}6)M_\odot$	366.5	0.987	68164.	−717.59	1.205	952.9	$(6{+}6)M_\odot$	729.3	0.993	167480.	−799.91	0.605	938.8
	$(18{+}3)M_\odot$	421.1	0.979	134976.	−1565.60	0.836	529.8	$(6{+}3)M_\odot$	984.4	0.993	304768.	−1185.10	0.708	1434.1
	$(18{+}1)M_\odot$	462.6	0.963	415045.	−5571.30	0.832	401.3	$(6{+}1)M_\odot$	1258.8	0.950	846072.	−3223.20	0.748	2076.7
	$(15{+}15)M_\odot$	292.7	0.985	34920.	−375.70	0.968	588.3	$(3{+}3)M_\odot$	1463.3	0.985	525640.	−1161.50	0.550	2366.2
	$(15{+}12)M_\odot$	322.2	0.985	42224.	−417.58	1.000	598.4	$(3{+}1)M_\odot$	2231.3	0.949	1354464.	−1870.70	1.011	2780.0
	$(15{+}9)M_\odot$	364.9	0.988	54819.	−514.04	1.000	650.6	$(1{+}1)M_\odot$	4393.5	0.949	3169592.	−915.61	1.083	4498.8

TABLE VII: Fitting factors for the projection of the target models (in the rows) onto the $(\psi_0, \psi_{3/2}, \alpha, f_{\rm cut})$ Fourier-domain detection template family when S2-H1 noise curve is used. For BBH masses $m_{1,2} = 1, 3, 6, 9, 12, 15, 18, 21 M_\odot$, this table shows the minmax matches between the target models and the Fourier-domain search model, *maximized over the intrinsic parameters* ψ_0, $\psi_{3/2}$, and $f_{\rm cut}$, and over the extrinsic parameter α. For each intersection, the six numbers shown report the *ending frequency* $f_{\rm end}$ (defined in BCV1) of the PN model for the BBH masses quoted, the minmax FF mn, and the search parameters at which the maximum is attained.

PN model	FF (minmax) with $(\psi_0, \psi_{3/2})_{\alpha,\mathrm{cut}}$ template family when LIGO-S2-H2-fit noise curve is used													
		f_{end}	mn	ψ_0	$\psi_{3/2}$	$\alpha f_{\mathrm{cut}}^{2/3}$	f_{cut}		f_{end}	mn	ψ_0	$\psi_{3/2}$	$\alpha f_{\mathrm{cut}}^{2/3}$	f_{cut}
	$(20{+}20)M_\odot$	221.4	0.931	16157.	−274.55	0.953	413.9	$(20{+}5)M_\odot$	341.1	0.978	81407.	−1185.30	1.231	605.0
	$(20{+}15)M_\odot$	252.5	0.939	25800.	−452.35	0.996	403.3	$(10{+}10)M_\odot$	442.7	0.985	75970.	−879.88	1.005	518.3
T(2, 2)	$(15{+}15)M_\odot$	295.1	0.956	36432.	−596.20	1.016	436.5	$(15{+}5)M_\odot$	431.3	0.987	98745.	−1115.80	1.001	529.6
	$(20{+}10)M_\odot$	291.7	0.962	40859.	−669.73	1.006	416.5	$(10{+}5)M_\odot$	583.4	0.990	133486.	−1104.90	0.996	666.8
	$(15{+}10)M_\odot$	352.7	0.975	53323.	−751.56	1.007	492.1	$(5{+}5)M_\odot$	885.5	0.993	229525.	−1195.00	1.070	1204.8
	$(20{+}20)M_\odot$	160.8	0.957	32861.	−404.92	0.957	333.1	$(20{+}5)M_\odot$	282.0	0.972	70211.	−134.67	0.733	375.4
	$(20{+}15)M_\odot$	185.3	0.966	33298.	−229.59	0.996	377.5	$(10{+}10)M_\odot$	324.2	0.973	61792.	131.94	0.437	392.9
T(2, 2.5)	$(15{+}15)M_\odot$	215.7	0.966	36143.	−58.65	0.914	379.5	$(15{+}5)M_\odot$	345.9	0.976	83108.	30.21	0.406	405.3
	$(20{+}10)M_\odot$	219.8	0.967	39683.	−83.64	0.919	363.1	$(10{+}5)M_\odot$	444.5	0.981	117994.	−8.75	0.224	519.1
	$(15{+}10)M_\odot$	260.4	0.968	46121.	42.40	0.715	356.9	$(5{+}5)M_\odot$	644.5	0.987	211075.	−36.16	0.057	713.4
	$(20{+}20)M_\odot$	207.9	0.912	17160.	−306.35	0.994	397.1	$(20{+}5)M_\odot$	276.1	0.973	85627.	−1369.40	1.007	383.4
	$(20{+}15)M_\odot$	234.5	0.939	27470.	−507.03	0.987	371.9	$(10{+}10)M_\odot$	415.8	0.985	79592.	−941.45	0.992	514.0
T(3, 3.5, 0)	$(15{+}15)M_\odot$	277.2	0.954	38628.	−643.02	0.968	412.0	$(15{+}5)M_\odot$	362.3	0.983	104850.	−1298.40	1.001	447.2
	$(20{+}10)M_\odot$	259.2	0.957	44263.	−781.98	1.005	391.1	$(10{+}5)M_\odot$	518.5	0.986	138275.	−1167.60	1.023	618.0
	$(15{+}10)M_\odot$	324.3	0.972	59213.	−913.32	1.230	616.7	$(5{+}5)M_\odot$	831.7	0.990	232229.	−1121.10	0.681	596.0
	$(20{+}20)M_\odot$	207.9	0.916	14653.	−234.34	0.985	441.0	$(20{+}5)M_\odot$	276.1	0.972	85916.	−1409.70	1.011	367.4
	$(20{+}15)M_\odot$	234.5	0.930	26566.	−498.74	1.010	377.1	$(10{+}10)M_\odot$	415.9	0.983	79718.	−978.98	0.996	490.6
T(3, 3.5, −2)	$(15{+}15)M_\odot$	277.2	0.953	37764.	−643.86	0.988	419.7	$(15{+}5)M_\odot$	362.3	0.982	104966.	−1338.60	0.996	439.9
	$(20{+}10)M_\odot$	259.3	0.953	44323.	−812.59	0.984	366.4	$(10{+}5)M_\odot$	518.5	0.987	139121.	−1231.30	0.985	579.7
	$(15{+}10)M_\odot$	324.3	0.971	56626.	−860.22	1.003	453.7	$(5{+}5)M_\odot$	831.7	0.990	235042.	−1233.00	1.161	1198.2
	$(20{+}20)M_\odot$	207.9	0.922	19175.	−360.51	0.983	358.3	$(20{+}5)M_\odot$	276.1	0.972	86306.	−1362.00	1.007	390.0
	$(20{+}15)M_\odot$	234.5	0.943	29474.	−539.32	0.982	390.6	$(10{+}10)M_\odot$	415.8	0.985	79204.	−886.59	0.996	504.2
T(3, 3.5, +2)	$(15{+}15)M_\odot$	277.2	0.957	38769.	−627.96	1.017	445.1	$(15{+}5)M_\odot$	362.3	0.982	105376.	−1276.90	0.993	437.4
	$(20{+}10)M_\odot$	259.2	0.959	45212.	−786.80	1.005	402.4	$(10{+}5)M_\odot$	518.5	0.986	138656.	−1135.50	1.007	607.5
	$(15{+}10)M_\odot$	324.3	0.972	60343.	−922.48	1.206	594.2	$(5{+}5)M_\odot$	831.7	0.991	231044.	−1035.10	0.578	583.1
	$(20{+}20)M_\odot$	142.9	0.874	17913.	−386.65	0.993	318.3	$(20{+}5)M_\odot$	207.8	0.961	93198.	−1751.60	0.998	304.6
	$(20{+}15)M_\odot$	162.5	0.911	29275.	−628.58	0.965	308.2	$(10{+}10)M_\odot$	285.9	0.977	84726.	−1149.20	0.996	412.7
P(2, 2.5)	$(15{+}15)M_\odot$	190.6	0.934	41098.	−804.20	0.996	352.7	$(15{+}5)M_\odot$	267.5	0.976	111700.	−1591.70	0.985	362.8
	$(20{+}10)M_\odot$	185.0	0.935	47291.	−964.78	0.992	325.6	$(10{+}5)M_\odot$	370.0	0.980	142803.	−1330.60	1.012	480.7
	$(15{+}10)M_\odot$	226.3	0.956	61767.	−1074.60	1.002	352.5	$(5{+}5)M_\odot$	571.7	0.986	233876.	−1158.00	0.638	478.1
	$(20{+}20)M_\odot$	216.4	0.933	20869.	−376.34	0.985	370.4	$(20{+}5)M_\odot$	265.0	0.973	87491.	−1386.90	0.997	357.6
	$(20{+}15)M_\odot$	243.6	0.950	29802.	−518.64	1.031	441.7	$(10{+}10)M_\odot$	432.8	0.986	78077.	−801.41	1.012	556.2
P(3, 3.5, 0)	$(15{+}15)M_\odot$	288.5	0.963	38950.	−593.98	0.999	449.4	$(15{+}5)M_\odot$	359.2	0.983	103881.	−1193.00	1.007	450.7
	$(20{+}10)M_\odot$	265.7	0.963	46670.	−781.84	1.004	417.4	$(10{+}5)M_\odot$	531.3	0.987	136455.	−1029.00	1.023	668.4
	$(15{+}10)M_\odot$	336.1	0.975	57428.	−779.19	1.000	462.3	$(5{+}5)M_\odot$	865.6	0.992	229040.	−950.25	0.639	635.5
	$(20{+}20)M_\odot$	216.4	0.921	18173.	−309.89	0.994	412.6	$(20{+}5)M_\odot$	265.0	0.970	87241.	−1399.70	1.019	382.6
	$(20{+}15)M_\odot$	243.6	0.944	29179.	−526.56	0.985	372.8	$(10{+}10)M_\odot$	432.8	0.986	78226.	−844.09	0.975	495.4
P(3, 3.5, −2)	$(15{+}15)M_\odot$	288.5	0.963	39196.	−622.04	1.053	481.2	$(15{+}5)M_\odot$	359.2	0.983	104442.	−1240.10	0.990	445.7
	$(20{+}10)M_\odot$	265.7	0.961	44878.	−761.04	1.002	391.1	$(10{+}5)M_\odot$	531.3	0.987	137164.	−1083.90	1.024	659.3
	$(15{+}10)M_\odot$	336.1	0.975	56544.	−782.81	0.987	460.0	$(5{+}5)M_\odot$	865.6	0.992	230922.	−1032.60	0.627	645.7
	$(20{+}20)M_\odot$	216.4	0.928	20979.	−386.09	1.002	384.2	$(20{+}5)M_\odot$	265.0	0.972	87862.	−1398.70	0.999	357.5
	$(20{+}15)M_\odot$	243.6	0.950	30492.	−538.98	0.996	393.8	$(10{+}10)M_\odot$	432.8	0.986	77778.	−790.55	0.980	502.8
P(3, 3.5, +2)	$(15{+}15)M_\odot$	288.5	0.966	39406.	−601.33	1.000	451.7	$(15{+}5)M_\odot$	359.2	0.982	104437.	−1206.40	1.017	447.4
	$(20{+}10)M_\odot$	265.7	0.964	45099.	−740.98	0.971	376.5	$(10{+}5)M_\odot$	531.3	0.988	135929.	−1007.00	0.983	638.8
	$(15{+}10)M_\odot$	336.1	0.976	56934.	−756.49	0.993	473.8	$(5{+}5)M_\odot$	865.6	0.991	229679.	−956.52	0.674	679.4
	$(20{+}20)M_\odot$	218.1	0.974	14762.	−136.21	1.010	631.3	$(20{+}5)M_\odot$	345.8	0.982	67124.	−775.14	0.870	580.4
	$(20{+}15)M_\odot$	249.1	0.979	21865.	−221.58	0.873	477.8	$(10{+}10)M_\odot$	436.2	0.991	66010.	−516.40	0.909	949.7
EP(2, 2.5)	$(15{+}15)M_\odot$	290.8	0.988	29489.	−279.66	1.004	760.0	$(15{+}5)M_\odot$	433.1	0.988	89968.	−858.62	0.820	688.0
	$(20{+}10)M_\odot$	289.8	0.987	34301.	−377.99	0.911	595.5	$(10{+}5)M_\odot$	579.6	0.989	129159.	−939.64	0.998	1249.7
	$(15{+}10)M_\odot$	348.5	0.988	44703.	−407.71	0.754	599.8	$(5{+}5)M_\odot$	872.4	0.994	231392.	−1137.50	0.616	1084.7
	$(20{+}20)M_\odot$	218.4	0.968	18897.	−226.41	0.991	495.9	$(20{+}5)M_\odot$	351.7	0.987	70906.	−794.39	0.970	627.3
	$(20{+}15)M_\odot$	250.2	0.979	25610.	−294.59	0.951	482.3	$(10{+}10)M_\odot$	434.6	0.991	69091.	−504.36	1.008	882.6
EP(3, 3.5, 0)	$(15{+}15)M_\odot$	289.2	0.985	32816.	−320.26	0.995	604.2	$(15{+}5)M_\odot$	445.3	0.992	92870.	−836.62	0.970	741.1
	$(20{+}10)M_\odot$	294.3	0.986	38077.	−428.78	0.987	567.4	$(10{+}5)M_\odot$	581.6	0.993	129492.	−837.67	0.896	965.8
	$(15{+}10)M_\odot$	350.3	0.990	48968.	−450.69	0.988	707.4	$(5{+}5)M_\odot$	869.0	0.995	227432.	−924.97	0.676	1195.8
	$(20{+}20)M_\odot$	215.6	0.970	18539.	−217.65	0.956	519.9	$(20{+}5)M_\odot$	353.7	0.989	71223.	−816.55	1.208	827.2
	$(20{+}15)M_\odot$	248.3	0.976	24480.	−275.15	0.994	554.5	$(10{+}10)M_\odot$	432.6	0.991	69154.	−531.20	0.944	724.0
EP(3, 3.5, −2)	$(15{+}15)M_\odot$	284.9	0.985	34030.	−372.97	0.999	574.1	$(15{+}5)M_\odot$	439.0	0.992	91882.	−831.39	0.941	767.1
	$(20{+}10)M_\odot$	289.1	0.984	36608.	−406.47	1.007	593.4	$(10{+}5)M_\odot$	580.9	0.993	128992.	−852.83	0.835	868.3
	$(15{+}10)M_\odot$	347.1	0.989	49142.	−476.82	0.999	662.1	$(5{+}5)M_\odot$	864.2	0.995	228556.	−989.62	0.602	1070.8
	$(20{+}20)M_\odot$	220.2	0.968	19543.	−236.32	0.951	500.3	$(20{+}5)M_\odot$	351.8	0.987	71439.	−804.86	1.036	703.9
	$(20{+}15)M_\odot$	250.6	0.978	26809.	−328.38	1.013	532.3	$(10{+}10)M_\odot$	437.4	0.991	69489.	−510.21	0.994	811.0
EP(3, 3.5, +2)	$(15{+}15)M_\odot$	292.7	0.986	34377.	−358.61	1.012	619.3	$(15{+}5)M_\odot$	443.1	0.992	93563.	−851.66	0.907	699.5
	$(20{+}10)M_\odot$	294.8	0.985	37752.	−419.12	0.999	562.2	$(10{+}5)M_\odot$	583.9	0.993	129571.	−832.23	0.802	870.1
	$(15{+}10)M_\odot$	353.5	0.988	50123.	−474.64	0.835	567.5	$(5{+}5)M_\odot$	872.0	0.995	227785.	−924.96	0.831	1554.6

TABLE VIII: Fitting factors for the projection of the target models (in the rows) onto the $(\psi_0, \psi_{3/2}, \alpha, f_{\mathrm{cut}})$ Fourier-domain detection template family when S2-H2 noise curve is used. For BBH masses $m_{1,2} = 5, 10, 15, 20 M_\odot$, this table shows the minmax matches between the target models and the Fourier-domain search model, *maximized over the intrinsic parameters* ψ_0, $\psi_{3/2}$, and f_{cut}, and over the extrinsic parameter α. For each intersection, the six numbers shown report the *ending frequency* f_{end} (defined in BCV1) of the PN model for the BBH masses quoted, the minmax FF mn, and the search parameters at which the maximum is attained.

PN model	FF (minmax) with $(\psi_0, \psi_{3/2})_{\alpha,\mathrm{cut}}$ template family when LIGO-S2-H2-fit noise curve is used													
		f_{end}	mn	ψ_0	$\psi_{3/2}$	$\alpha f_{\mathrm{cut}}^{2/3}$	f_{cut}		f_{end}	mn	ψ_0	$\psi_{3/2}$	$\alpha f_{\mathrm{cut}}^{2/3}$	f_{cut}
T(2, 2)	$(12{+}12)M_\odot$	369.0	0.977	57473.	−822.28	1.253	689.4	$(12{+}1)M_\odot$	633.5	0.995	513878.	−3637.00	1.003	864.0
	$(12{+}9)M_\odot$	420.8	0.984	70908.	−855.14	1.004	523.5	$(9{+}1)M_\odot$	829.6	0.995	627135.	−3371.00	0.651	691.9
	$(12{+}6)M_\odot$	486.2	0.989	100057.	−1026.30	1.001	568.1	$(6{+}3)M_\odot$	972.3	0.994	306121.	−1428.10	0.611	678.4
	$(12{+}3)M_\odot$	568.6	0.992	182873.	−1501.10	0.999	676.1	$(6{+}1)M_\odot$	1200.2	0.993	831692.	−3011.70	0.453	801.3
	$(9{+}9)M_\odot$	491.9	0.988	89733.	−929.26	1.000	576.7	$(3{+}3)M_\odot$	1475.8	0.992	529970.	−1543.10	0.977	2134.0
	$(9{+}6)M_\odot$	587.8	0.990	124087.	−1029.90	0.996	647.2	$(3{+}1)M_\odot$	2156.4	0.976	1364157.	−2436.20	0.870	2755.2
	$(9{+}3)M_\odot$	718.8	0.992	226113.	−1466.50	1.004	883.9	$(1{+}1)M_\odot$	4427.3	0.948	3185476.	−1702.70	1.273	3900.2
	$(6{+}6)M_\odot$	737.9	0.992	171288.	−1111.40	1.000	877.4							
T(2, 2.5)	$(12{+}12)M_\odot$	268.0	0.968	47142.	62.65	0.759	379.9	$(12{+}1)M_\odot$	593.3	0.991	487164.	−1369.80	0.329	611.8
	$(12{+}9)M_\odot$	310.2	0.971	58304.	120.57	0.561	392.6	$(9{+}1)M_\odot$	748.9	0.992	598311.	−1247.40	0.254	760.6
	$(12{+}6)M_\odot$	372.4	0.977	83469.	97.71	0.269	432.3	$(6{+}3)M_\odot$	736.7	0.989	286247.	−179.16	0.049	788.2
	$(12{+}3)M_\odot$	470.1	0.985	165110.	−204.14	0.260	523.6	$(6{+}1)M_\odot$	1043.9	0.995	801566.	−1091.50	0.164	968.6
	$(9{+}9)M_\odot$	360.2	0.976	72227.	182.32	0.262	420.6	$(3{+}3)M_\odot$	1079.3	0.994	507848.	−260.83	0.058	1012.2
	$(9{+}6)M_\odot$	435.9	0.981	107924.	59.42	0.182	500.4	$(3{+}1)M_\odot$	1725.5	0.998	1333384.	−783.19	0.090	1525.4
	$(9{+}3)M_\odot$	574.6	0.987	207384.	−194.78	0.149	632.2	$(1{+}1)M_\odot$	3235.0	0.980	3160256.	−352.95	0.472	4301.8
	$(6{+}6)M_\odot$	537.0	0.985	153270.	24.84	0.067	605.4							
T(3, 3.5, 0)	$(12{+}12)M_\odot$	346.5	0.976	58832.	−830.52	1.002	469.6	$(12{+}1)M_\odot$	467.3	0.987	532298.	−4294.20	0.691	403.6
	$(12{+}9)M_\odot$	390.8	0.981	75783.	−963.02	1.001	454.9	$(9{+}1)M_\odot$	622.5	0.988	641540.	−3748.80	0.555	485.9
	$(12{+}6)M_\odot$	432.1	0.985	104800.	−1116.40	1.000	497.6	$(6{+}3)M_\odot$	864.1	0.989	311079.	−1399.50	1.114	1251.8
	$(12{+}3)M_\odot$	460.2	0.987	190266.	−1688.50	0.998	554.3	$(6{+}1)M_\odot$	930.1	0.979	841377.	−3100.40	0.979	1302.6
	$(9{+}9)M_\odot$	462.0	0.986	93726.	−982.55	1.000	529.7	$(3{+}3)M_\odot$	1386.2	0.991	531458.	−1342.10	0.348	769.5
	$(9{+}6)M_\odot$	540.5	0.987	128921.	−1084.20	1.000	608.6	$(3{+}1)M_\odot$	1811.5	0.967	1364993.	−2148.80	0.900	2393.8
	$(9{+}3)M_\odot$	603.9	0.989	232246.	−1546.10	0.987	742.0	$(1{+}1)M_\odot$	4158.6	0.951	3177038.	−1114.10	1.183	3423.5
	$(6{+}6)M_\odot$	693.1	0.989	174769.	−1082.80	0.998	798.4							
T(3, 3.5, −2)	$(12{+}12)M_\odot$	346.5	0.975	57796.	−827.76	1.020	446.3	$(12{+}1)M_\odot$	467.3	0.987	532710.	−4343.80	0.697	403.8
	$(12{+}9)M_\odot$	390.8	0.980	75901.	−1003.60	0.982	442.4	$(9{+}1)M_\odot$	622.5	0.987	641361.	−3784.50	0.556	478.2
	$(12{+}6)M_\odot$	432.1	0.985	105190.	−1166.30	1.000	488.3	$(6{+}3)M_\odot$	864.1	0.989	311994.	−1469.30	1.126	1224.9
	$(12{+}3)M_\odot$	460.2	0.987	191059.	−1750.70	0.998	549.4	$(6{+}1)M_\odot$	930.1	0.978	842853.	−3181.70	1.008	1337.8
	$(9{+}9)M_\odot$	462.0	0.987	93963.	−1027.30	1.000	536.5	$(3{+}3)M_\odot$	1386.1	0.986	533428.	−1441.60	0.914	1646.6
	$(9{+}6)M_\odot$	540.5	0.988	129474.	−1140.50	0.999	609.7	$(3{+}1)M_\odot$	1811.5	0.964	1368872.	−2282.70	0.816	2275.1
	$(9{+}3)M_\odot$	603.9	0.988	232759.	−1602.90	0.976	696.9	$(1{+}1)M_\odot$	4158.3	0.948	3178171.	−1177.40	1.240	3395.2
	$(6{+}6)M_\odot$	693.1	0.989	175805.	−1155.90	1.003	771.7							
T(3, 3.5, +2)	$(12{+}12)M_\odot$	346.5	0.976	58450.	−788.49	1.002	473.4	$(12{+}1)M_\odot$	467.3	0.987	530978.	−4217.30	0.675	398.8
	$(12{+}9)M_\odot$	390.8	0.982	75721.	−923.07	1.000	459.1	$(9{+}1)M_\odot$	622.4	0.988	640605.	−3681.60	0.549	485.0
	$(12{+}6)M_\odot$	432.1	0.985	104313.	−1062.30	1.000	510.7	$(6{+}3)M_\odot$	864.2	0.989	309650.	−1315.40	1.076	1252.5
	$(12{+}3)M_\odot$	460.2	0.986	190696.	−1661.90	1.002	566.2	$(6{+}1)M_\odot$	930.0	0.979	840060.	−3022.30	0.991	1340.3
	$(9{+}9)M_\odot$	462.0	0.986	93997.	−947.31	1.002	545.1	$(3{+}3)M_\odot$	1386.1	0.988	529948.	−1256.70	0.872	1710.0
	$(9{+}6)M_\odot$	540.6	0.987	128483.	−1027.60	1.003	635.7	$(3{+}1)M_\odot$	1811.6	0.969	1363459.	−2068.20	0.767	2113.0
	$(9{+}3)M_\odot$	603.9	0.988	231522.	−1481.50	0.771	536.2	$(1{+}1)M_\odot$	4158.5	0.953	3175186.	−1034.40	1.289	4087.5
	$(6{+}6)M_\odot$	693.1	0.988	173589.	−1003.70	0.775	574.7							
P(2, 2.5)	$(12{+}12)M_\odot$	238.2	0.964	63604.	−1052.10	1.000	379.8	$(12{+}1)M_\odot$	364.0	0.977	540133.	−4641.20	0.624	311.9
	$(12{+}9)M_\odot$	270.8	0.973	80629.	−1174.10	1.000	374.1	$(9{+}1)M_\odot$	482.7	0.981	646991.	−3945.40	0.509	391.5
	$(12{+}6)M_\odot$	308.3	0.978	110103.	−1329.20	1.000	394.5	$(6{+}3)M_\odot$	616.7	0.988	310659.	−1382.30	0.529	488.2
	$(12{+}3)M_\odot$	346.4	0.978	196198.	−1919.50	0.990	427.5	$(6{+}1)M_\odot$	713.5	0.971	843062.	−3139.00	0.982	1004.1
	$(9{+}9)M_\odot$	317.6	0.980	97552.	−1139.20	1.000	437.2	$(3{+}3)M_\odot$	952.9	0.990	531119.	−1320.90	0.316	663.1
	$(9{+}6)M_\odot$	377.1	0.981	132810.	−1226.60	0.999	485.3	$(3{+}1)M_\odot$	1337.3	0.966	1363352.	−2081.30	0.774	1540.1
	$(9{+}3)M_\odot$	445.8	0.982	233038.	−1582.70	0.691	392.8	$(1{+}1)M_\odot$	2858.7	0.950	3177870.	−1100.70	1.059	3124.0
	$(6{+}6)M_\odot$	476.4	0.983	175879.	−1118.60	0.741	436.6							
P(3, 3.5, 0)	$(12{+}12)M_\odot$	360.6	0.980	58627.	−741.91	1.013	512.7	$(12{+}1)M_\odot$	399.5	0.981	536637.	−4459.10	0.651	346.6
	$(12{+}9)M_\odot$	406.0	0.983	73799.	−813.26	0.999	499.1	$(9{+}1)M_\odot$	545.4	0.984	640400.	−3693.40	0.511	427.6
	$(12{+}6)M_\odot$	442.8	0.985	102868.	−973.26	1.000	536.0	$(6{+}3)M_\odot$	885.5	0.991	308246.	−1241.60	0.534	648.2
	$(12{+}3)M_\odot$	441.6	0.985	189733.	−1607.80	1.001	559.6	$(6{+}1)M_\odot$	850.4	0.984	839006.	−2979.20	0.379	607.1
	$(9{+}9)M_\odot$	480.9	0.987	91978.	−838.80	1.000	567.7	$(3{+}3)M_\odot$	1442.6	0.993	527460.	−1169.40	0.369	858.3
	$(9{+}6)M_\odot$	560.2	0.989	126214.	−916.78	1.001	700.7	$(3{+}1)M_\odot$	1795.8	0.972	1360818.	−1987.10	0.732	1990.5
	$(9{+}3)M_\odot$	598.6	0.989	229541.	−1390.80	0.734	533.5	$(1{+}1)M_\odot$	4327.8	0.954	3174611.	−1012.40	1.269	4127.9
	$(6{+}6)M_\odot$	721.3	0.989	171253.	−898.96	0.725	596.1							
P(3, 3.5, −2)	$(12{+}12)M_\odot$	360.6	0.979	59195.	−792.13	0.996	466.0	$(12{+}1)M_\odot$	399.5	0.981	537121.	−4491.60	0.649	345.3
	$(12{+}9)M_\odot$	406.0	0.983	74256.	−861.42	1.001	500.9	$(9{+}1)M_\odot$	545.4	0.984	641160.	−3738.50	0.517	430.0
	$(12{+}6)M_\odot$	442.8	0.985	103653.	−1030.80	1.000	522.7	$(6{+}3)M_\odot$	885.5	0.992	308714.	−1289.90	0.538	626.7
	$(12{+}3)M_\odot$	441.6	0.986	190683.	−1662.90	0.999	560.1	$(6{+}1)M_\odot$	850.4	0.984	839271.	−3015.00	0.375	601.2
	$(9{+}9)M_\odot$	480.9	0.987	91833.	−867.40	0.994	557.4	$(3{+}3)M_\odot$	1442.6	0.990	529205.	−1253.40	0.951	2297.2
	$(9{+}6)M_\odot$	560.2	0.989	126480.	−959.96	1.001	667.6	$(3{+}1)M_\odot$	1795.8	0.971	1363468.	−2082.50	0.698	2000.0
	$(9{+}3)M_\odot$	598.6	0.988	230239.	−1442.10	0.750	529.4	$(1{+}1)M_\odot$	4327.8	0.952	3176380.	−1084.30	1.338	4420.0
	$(6{+}6)M_\odot$	721.3	0.989	172421.	−969.41	1.116	1023.4							
P(3, 3.5, +2)	$(12{+}12)M_\odot$	360.6	0.981	59575.	−764.70	1.001	489.9	$(12{+}1)M_\odot$	399.5	0.981	536331.	−4440.40	0.641	344.3
	$(12{+}9)M_\odot$	406.0	0.983	74404.	−827.68	1.000	507.7	$(9{+}1)M_\odot$	545.4	0.985	641733.	−3721.50	0.515	432.8
	$(12{+}6)M_\odot$	442.8	0.985	103558.	−988.48	0.997	532.2	$(6{+}3)M_\odot$	885.5	0.991	307458.	−1214.10	1.068	1366.8
	$(12{+}3)M_\odot$	441.6	0.985	190274.	−1616.70	0.999	550.6	$(6{+}1)M_\odot$	850.4	0.985	838631.	−2958.10	0.369	602.0
	$(9{+}9)M_\odot$	480.9	0.986	91287.	−810.50	0.999	562.0	$(3{+}3)M_\odot$	1442.6	0.991	527429.	−1158.30	0.813	1756.7
	$(9{+}6)M_\odot$	560.2	0.988	126174.	−908.94	0.998	679.3	$(3{+}1)M_\odot$	1795.8	0.972	1360940.	−1977.40	0.740	2090.9
	$(9{+}3)M_\odot$	598.6	0.989	228722.	−1358.50	0.690	502.0	$(1{+}1)M_\odot$	4327.8	0.955	3173972.	−986.25	1.266	4040.8
	$(6{+}6)M_\odot$	721.3	0.989	170766.	−878.16	0.705	574.3							
EP(2, 2.5)	$(12{+}12)M_\odot$	363.5	0.990	47576.	−433.26	0.833	666.5	$(12{+}1)M_\odot$	665.0	0.983	548379.	−4989.50	0.796	597.9
	$(12{+}9)M_\odot$	415.2	0.990	64798.	−594.75	0.794	675.8	$(9{+}1)M_\odot$	863.6	0.979	658967.	−4364.30	0.786	879.7
	$(12{+}6)M_\odot$	483.0	0.990	93021.	−775.52	0.769	741.4	$(6{+}3)M_\odot$	965.9	0.995	310989.	−1448.00	0.653	1172.2
	$(12{+}3)M_\odot$	576.3	0.988	184445.	−1592.70	0.702	644.5	$(6{+}1)M_\odot$	1233.3	0.963	855446.	−3521.40	1.679	3600.0
	$(9{+}9)M_\odot$	484.7	0.991	81963.	−632.44	0.756	824.8	$(3{+}3)M_\odot$	1454.1	0.988	535488.	−1480.30	0.750	2218.4
	$(9{+}6)M_\odot$	580.8	0.992	119732.	−844.55	0.729	828.9	$(3{+}1)M_\odot$	2165.6	0.958	1365425.	−2176.60	1.163	2301.0
	$(9{+}3)M_\odot$	721.9	0.993	229617.	−1536.10	0.659	788.8	$(1{+}1)M_\odot$	4362.2	0.947	3179898.	−1178.10	1.233	3817.7
	$(6{+}6)M_\odot$	727.0	0.993	170165.	−993.36	0.635	904.6							
	$(12{+}12)M_\odot$	361.5	0.990	50431.	−431.79	1.000	718.8	$(12{+}1)M_\odot$	680.0	0.987	542393.	−4722.10	0.793	616.9

PN model		$f_{\rm end}$	mn	ψ_0	$\psi_{3/2}$	$\alpha f_{\rm cut}^{2/3}$	$f_{\rm cut}$		$f_{\rm end}$	mn	ψ_0	$\psi_{3/2}$	$\alpha f_{\rm cut}^{2/3}$	$f_{\rm cut}$
	FF (minmax) with $(\psi_0, \psi_{3/2})_{\alpha,\rm cut}$ template family when LIGO-S2-H2-fit noise curve is used													
	$(12{+}9)M_\odot$	419.3	0.991	64998.	-509.77	0.999	785.9	$(9{+}1)M_\odot$	882.5	0.985	652247.	-4095.00	0.752	883.1
	$(12{+}6)M_\odot$	488.8	0.992	93588.	-686.64	1.002	933.6	$(6{+}3)M_\odot$	971.8	0.996	306306.	-1222.90	0.592	1134.3
EP$(3, 3.5, 0)$	$(12{+}3)M_\odot$	598.1	0.992	182153.	-1414.60	0.735	698.6	$(6{+}1)M_\odot$	1264.7	0.975	848451.	-3269.10	0.514	930.1
	$(9{+}9)M_\odot$	488.6	0.992	83294.	-563.88	0.999	987.9	$(3{+}3)M_\odot$	1468.7	0.993	527962.	-1210.30	0.600	1750.7
	$(9{+}6)M_\odot$	584.2	0.993	119174.	-719.35	0.822	953.9	$(3{+}1)M_\odot$	2205.5	0.965	1363519.	-2075.00	1.077	2801.1
	$(9{+}3)M_\odot$	730.5	0.995	225814.	-1322.40	0.694	868.3	$(1{+}1)M_\odot$	4422.6	0.953	3177009.	-1075.30	1.387	5268.6
	$(6{+}6)M_\odot$	724.6	0.994	167578.	-814.23	0.869	1282.8							
	$(12{+}12)M_\odot$	361.2	0.989	50365.	-457.38	0.999	643.0	$(12{+}1)M_\odot$	677.4	0.987	541876.	-4726.00	0.803	622.4
	$(12{+}9)M_\odot$	407.9	0.992	64277.	-516.95	1.014	803.2	$(9{+}1)M_\odot$	883.5	0.985	651769.	-4106.30	1.153	1561.7
	$(12{+}6)M_\odot$	482.3	0.993	93815.	-717.35	0.913	847.9	$(6{+}3)M_\odot$	961.7	0.996	307079.	-1278.20	0.650	1152.0
EP$(3, 3.5, -2)$	$(12{+}3)M_\odot$	586.4	0.991	181335.	-1415.90	0.735	702.9	$(6{+}1)M_\odot$	1265.9	0.975	850051.	-3336.50	0.966	2124.8
	$(9{+}9)M_\odot$	475.9	0.992	83494.	-598.42	0.995	917.6	$(3{+}3)M_\odot$	1438.6	0.993	530196.	-1302.50	0.595	1642.9
	$(9{+}6)M_\odot$	580.6	0.993	119042.	-746.86	0.986	1141.6	$(3{+}1)M_\odot$	2219.2	0.964	1363603.	-2110.70	1.090	2514.6
	$(9{+}3)M_\odot$	739.2	0.993	224872.	-1327.10	0.707	911.1	$(1{+}1)M_\odot$	4278.8	0.950	3177788.	-1121.90	1.358	4641.3
	$(6{+}6)M_\odot$	718.5	0.994	167349.	-842.45	0.758	1097.1							
	$(12{+}12)M_\odot$	364.7	0.989	50631.	-436.36	1.037	708.9	$(12{+}1)M_\odot$	677.8	0.987	543946.	-4756.20	0.774	597.0
	$(12{+}9)M_\odot$	418.5	0.992	64463.	-491.60	1.005	803.5	$(9{+}1)M_\odot$	883.8	0.985	652109.	-4082.00	0.772	905.0
	$(12{+}6)M_\odot$	492.3	0.993	93971.	-690.55	1.002	970.0	$(6{+}3)M_\odot$	984.4	0.996	306690.	-1224.00	0.591	1103.6
EP$(3, 3.5, +2)$	$(12{+}3)M_\odot$	594.3	0.991	182138.	-1407.10	0.720	692.8	$(6{+}1)M_\odot$	1258.8	0.975	847918.	-3244.80	0.492	873.1
	$(9{+}9)M_\odot$	489.3	0.991	83185.	-555.60	0.985	980.5	$(3{+}3)M_\odot$	1463.3	0.993	529247.	-1230.70	0.529	1748.8
	$(9{+}6)M_\odot$	589.5	0.993	118975.	-708.33	0.986	1189.9	$(3{+}1)M_\odot$	2231.3	0.965	1363593.	-2062.40	1.030	2673.8
	$(9{+}3)M_\odot$	732.3	0.994	226032.	-1320.20	0.694	863.7	$(1{+}1)M_\odot$	4393.5	0.953	3176440.	-1050.20	1.277	4566.3
	$(6{+}6)M_\odot$	729.3	0.994	167206.	-797.32	0.806	1217.0							

TABLE IX: Fitting factors for the projection of the target models (in the rows) onto the $(\psi_0, \psi_{3/2}, \alpha, f_{\rm cut})$ Fourier-domain detection template family when S2-H2 noise curve is used. For BBH masses $m_{1,2} = 1, 3, 6, 9, 12 M_\odot$, this table shows the minmax matches between the target models and the Fourier-domain search model, *maximized over the intrinsic parameters* ψ_0, $\psi_{3/2}$, and $f_{\rm cut}$, and over the extrinsic parameter α. For each intersection, the six numbers shown report the *ending frequency* $f_{\rm end}$ (defined in BCV1) of the PN model for the BBH masses quoted, the minmax FF mn, and the search parameters at which the maximum is attained.

PN model		$f_{\rm end}$	mn	ψ_0	$\psi_{3/2}$	$\alpha f_{\rm cut}^{2/3}$	$f_{\rm cut}$		$f_{\rm end}$	mn	ψ_0	$\psi_{3/2}$	$\alpha f_{\rm cut}^{2/3}$	$f_{\rm cut}$
	FF (minmax) with $(\psi_0, \psi_{3/2})_{\alpha,\rm cut}$ template family when LIGO-S2-H2-fit noise curve is used													
	$(21{+}21)M_\odot$	210.8	0.914	13230.	-210.59	1.000	451.1	$(15{+}6)M_\odot$	413.5	0.986	84495.	-1014.40	1.002	491.1
	$(21{+}18)M_\odot$	226.9	0.917	17192.	-282.32	1.000	453.2	$(15{+}3)M_\odot$	469.8	0.990	155871.	-1553.10	0.998	557.1
	$(21{+}15)M_\odot$	245.2	0.935	25136.	-465.28	0.999	372.7	$(15{+}1)M_\odot$	512.2	0.994	439995.	-3839.90	1.003	659.8
	$(21{+}12)M_\odot$	266.2	0.941	31801.	-548.71	1.008	420.9	$(12{+}12)M_\odot$	369.0	0.977	57473.	-822.28	1.253	689.4
	$(21{+}9)M_\odot$	290.2	0.962	44837.	-759.44	0.969	381.0	$(12{+}9)M_\odot$	420.8	0.984	70908.	-855.14	1.004	523.5
	$(21{+}6)M_\odot$	317.5	0.973	64250.	-967.15	0.999	442.4	$(12{+}6)M_\odot$	486.2	0.989	100057.	-1026.30	1.001	568.1
	$(21{+}3)M_\odot$	348.3	0.984	122745.	-1646.00	1.000	435.8	$(12{+}3)M_\odot$	568.6	0.992	182873.	-1501.10	0.999	676.1
	$(21{+}1)M_\odot$	370.4	0.991	347848.	-4164.50	0.999	453.7	$(12{+}1)M_\odot$	633.5	0.995	513878.	-3637.00	1.003	864.0
T$(2, 2)$	$(18{+}18)M_\odot$	246.0	0.928	23480.	-416.48	0.999	403.6	$(9{+}9)M_\odot$	491.9	0.988	89733.	-929.26	1.000	576.7
	$(18{+}15)M_\odot$	268.1	0.951	29823.	-511.39	1.016	438.1	$(9{+}6)M_\odot$	587.8	0.990	124087.	-1029.90	0.996	647.2
	$(18{+}12)M_\odot$	293.9	0.954	37262.	-600.02	0.978	433.6	$(9{+}3)M_\odot$	718.8	0.992	226113.	-1466.50	1.004	883.9
	$(18{+}9)M_\odot$	324.1	0.966	50765.	-778.68	1.001	436.6	$(9{+}1)M_\odot$	829.6	0.995	627135.	-3371.00	0.651	691.9
	$(18{+}6)M_\odot$	359.4	0.979	75346.	-1070.80	1.234	630.6	$(6{+}6)M_\odot$	737.9	0.992	171288.	-1111.40	1.000	877.4
	$(18{+}3)M_\odot$	400.1	0.988	137466.	-1619.90	1.000	487.9	$(6{+}3)M_\odot$	972.3	0.994	306121.	-1428.10	0.611	678.4
	$(18{+}1)M_\odot$	429.9	0.993	387825.	-4024.00	1.001	538.2	$(6{+}1)M_\odot$	1200.2	0.993	831692.	-3011.70	0.453	801.3
	$(15{+}15)M_\odot$	295.1	0.956	36432.	-596.20	1.016	436.5	$(3{+}3)M_\odot$	1475.8	0.992	529970.	-1543.10	0.977	2134.0
	$(15{+}12)M_\odot$	327.5	0.964	46295.	-719.42	1.000	436.4	$(3{+}1)M_\odot$	2156.4	0.976	1364157.	-2436.20	0.870	2755.2
	$(15{+}9)M_\odot$	366.5	0.976	60070.	-845.58	1.000	442.6	$(1{+}1)M_\odot$	4427.3	0.948	3185476.	-1702.70	1.273	3900.2
	$(21{+}21)M_\odot$	153.4	0.957	27782.	-312.55	0.999	322.6	$(15{+}6)M_\odot$	322.4	0.974	70020.	66.23	0.485	392.5
	$(21{+}18)M_\odot$	166.3	0.958	30461.	-299.95	1.000	368.8	$(15{+}3)M_\odot$	397.2	0.982	140449.	-271.89	0.400	444.8
	$(21{+}15)M_\odot$	181.0	0.963	33028.	-242.15	0.989	364.8	$(15{+}1)M_\odot$	485.6	0.990	417133.	-1509.30	0.404	497.6
	$(21{+}12)M_\odot$	200.1	0.966	36469.	-187.94	1.000	378.1	$(12{+}12)M_\odot$	268.0	0.968	47142.	62.65	0.759	379.9
	$(21{+}9)M_\odot$	222.5	0.968	43202.	-145.98	0.994	406.5	$(12{+}9)M_\odot$	310.2	0.971	58304.	120.57	0.561	392.6
	$(21{+}6)M_\odot$	256.4	0.969	57863.	-120.23	0.824	378.9	$(12{+}6)M_\odot$	372.4	0.977	83469.	97.71	0.269	432.3
	$(21{+}3)M_\odot$	307.0	0.976	111095.	-393.48	0.651	365.8	$(12{+}3)M_\odot$	470.1	0.985	165110.	-204.14	0.260	523.6
	$(21{+}1)M_\odot$	358.3	0.984	328756.	-1672.70	0.524	365.1	$(12{+}1)M_\odot$	593.3	0.991	487164.	-1369.80	0.329	611.8
T$(2, 2.5)$	$(18{+}18)M_\odot$	179.0	0.963	32702.	-251.29	0.984	372.1	$(9{+}9)M_\odot$	360.2	0.976	72227.	182.32	0.262	420.6
	$(18{+}15)M_\odot$	196.5	0.965	34511.	-173.67	1.000	366.6	$(9{+}6)M_\odot$	435.9	0.981	107924.	59.42	0.182	500.4
	$(18{+}12)M_\odot$	217.1	0.966	38006.	-86.99	0.999	419.9	$(9{+}3)M_\odot$	574.6	0.987	207384.	-194.78	0.149	632.2
	$(18{+}9)M_\odot$	244.5	0.966	45335.	-29.25	0.837	363.3	$(9{+}1)M_\odot$	748.9	0.992	598311.	-1247.40	0.254	760.6
	$(18{+}6)M_\odot$	286.0	0.968	57226.	141.90	0.600	345.8	$(6{+}6)M_\odot$	537.0	0.985	153270.	24.84	0.067	605.4
	$(18{+}3)M_\odot$	345.2	0.979	122332.	-298.59	0.516	392.3	$(6{+}3)M_\odot$	736.7	0.989	286247.	-179.16	0.049	788.2
	$(18{+}1)M_\odot$	413.0	0.987	366804.	-1600.80	0.469	423.1	$(6{+}1)M_\odot$	1043.9	0.995	801566.	-1091.50	0.164	968.6
	$(15{+}15)M_\odot$	215.7	0.966	36143.	-58.65	0.914	379.5	$(3{+}3)M_\odot$	1079.3	0.994	507848.	-260.83	0.058	1012.2
	$(15{+}12)M_\odot$	240.1	0.967	40898.	3.57	0.921	406.0	$(3{+}1)M_\odot$	1725.5	0.998	1333384.	-783.19	0.090	1525.4
	$(15{+}9)M_\odot$	274.1	0.969	47597.	131.84	0.642	363.5	$(1{+}1)M_\odot$	3235.0	0.980	3160256.	-352.95	0.472	4301.8
	$(21{+}21)M_\odot$	198.0	0.920	15057.	-270.42	0.979	416.7	$(15{+}6)M_\odot$	356.4	0.982	89832.	-1161.60	1.010	461.4
	$(21{+}18)M_\odot$	212.4	0.907	19468.	-358.33	1.000	396.7	$(15{+}3)M_\odot$	370.7	0.985	165075.	-1863.60	1.001	452.8
	$(21{+}15)M_\odot$	226.9	0.930	25965.	-490.98	0.990	348.2	$(15{+}1)M_\odot$	373.9	0.984	463399.	-4816.00	0.999	462.7
	$(21{+}12)M_\odot$	240.7	0.934	33391.	-600.76	0.992	394.6	$(12{+}12)M_\odot$	346.5	0.976	58832.	-830.52	1.002	469.6
	$(21{+}9)M_\odot$	252.5	0.956	46511.	-827.10	1.000	371.9	$(12{+}9)M_\odot$	390.8	0.981	75783.	-963.02	1.001	454.9
	$(21{+}6)M_\odot$	261.3	0.964	70557.	-1222.70	0.999	352.1	$(12{+}6)M_\odot$	432.1	0.985	104800.	-1116.40	1.000	497.6

PN model		FF (minmax) with $(\psi_0, \psi_{3/2})_{\alpha,\mathrm{cut}}$ template family when LIGO-S2-H2-fit noise curve is used												
		$f_{\rm end}$	mn	ψ_0	$\psi_{3/2}$	$\alpha f_{\rm cut}^{2/3}$	$f_{\rm cut}$		$f_{\rm end}$	mn	ψ_0	$\psi_{3/2}$	$\alpha f_{\rm cut}^{2/3}$	$f_{\rm cut}$
	$(21{+}3)M_\odot$	266.2	0.978	132764.	−2112.60	1.000	348.5	$(12{+}3)M_\odot$	460.2	0.987	190266.	−1688.50	0.998	554.3
	$(21{+}1)M_\odot$	267.1	0.982	376569.	−5639.80	1.001	330.3	$(12{+}1)M_\odot$	467.3	0.987	532298.	−4294.20	0.691	403.6
T(3, 3.5, 0)	$(18{+}18)M_\odot$	231.0	0.920	24935.	−462.08	0.999	383.9	$(9{+}9)M_\odot$	462.0	0.986	93726.	−982.55	1.000	529.7
	$(18{+}15)M_\odot$	250.7	0.940	33911.	−652.83	1.097	433.1	$(9{+}6)M_\odot$	540.5	0.987	128921.	−1084.20	1.000	608.6
	$(18{+}12)M_\odot$	270.2	0.956	40228.	−684.93	0.971	373.6	$(9{+}3)M_\odot$	603.9	0.989	232246.	−1546.10	0.987	742.0
	$(18{+}9)M_\odot$	288.0	0.966	55946.	−933.88	1.111	491.8	$(9{+}1)M_\odot$	622.5	0.988	641540.	−3748.80	0.555	485.9
	$(18{+}6)M_\odot$	301.9	0.973	78582.	−1184.80	1.000	412.6	$(6{+}6)M_\odot$	693.1	0.989	174769.	−1082.80	0.998	798.4
	$(18{+}3)M_\odot$	310.0	0.982	146592.	−1995.10	1.000	383.6	$(6{+}3)M_\odot$	864.1	0.989	311079.	−1399.50	1.114	1251.8
	$(18{+}1)M_\odot$	311.6	0.983	413624.	−5242.00	1.000	384.5	$(6{+}1)M_\odot$	930.1	0.979	841377.	−3100.40	0.979	1302.6
	$(15{+}15)M_\odot$	277.2	0.954	38628.	−643.02	0.968	412.0	$(3{+}3)M_\odot$	1386.2	0.991	531458.	−1342.10	0.348	769.5
	$(15{+}12)M_\odot$	305.6	0.965	48673.	−773.66	1.025	406.4	$(3{+}1)M_\odot$	1811.5	0.967	1364993.	−2148.80	0.900	2393.8
	$(15{+}9)M_\odot$	333.2	0.975	64384.	−959.38	1.000	412.6	$(1{+}1)M_\odot$	4158.6	0.951	3177038.	−1114.10	1.183	3423.5
	$(21{+}21)M_\odot$	198.0	0.909	13560.	−235.98	1.003	366.1	$(15{+}6)M_\odot$	356.4	0.983	88883.	−1167.40	1.002	443.3
	$(21{+}18)M_\odot$	212.4	0.921	17818.	−312.17	1.001	457.8	$(15{+}3)M_\odot$	370.7	0.985	164575.	−1883.50	0.999	445.5
	$(21{+}15)M_\odot$	226.9	0.917	24106.	−441.79	1.001	409.1	$(15{+}1)M_\odot$	373.9	0.984	463060.	−4838.10	0.868	378.8
	$(21{+}12)M_\odot$	240.7	0.937	32479.	−587.04	0.941	375.1	$(12{+}12)M_\odot$	346.5	0.975	57796.	−827.76	1.020	446.3
	$(21{+}9)M_\odot$	252.5	0.947	46602.	−856.20	1.006	369.8	$(12{+}9)M_\odot$	390.8	0.980	75901.	−1003.60	0.982	442.4
	$(21{+}6)M_\odot$	261.3	0.961	69456.	−1208.50	1.000	366.3	$(12{+}6)M_\odot$	432.1	0.985	105190.	−1166.30	1.000	488.3
	$(21{+}3)M_\odot$	266.2	0.976	132765.	−2141.30	1.000	343.9	$(12{+}3)M_\odot$	460.2	0.987	191059.	−1750.70	0.998	549.4
	$(21{+}1)M_\odot$	267.1	0.982	376123.	−5652.00	1.000	329.3	$(12{+}1)M_\odot$	467.3	0.987	532710.	−4343.80	0.697	403.8
T(3, 3.5, −2)	$(18{+}18)M_\odot$	231.0	0.929	21739.	−367.17	0.967	433.7	$(9{+}9)M_\odot$	462.0	0.987	93963.	−1027.30	1.000	536.5
	$(18{+}15)M_\odot$	250.7	0.931	29939.	−533.29	1.000	406.6	$(9{+}6)M_\odot$	540.5	0.988	129474.	−1140.50	0.999	609.7
	$(18{+}12)M_\odot$	270.3	0.948	40102.	−710.54	1.000	381.9	$(9{+}3)M_\odot$	603.9	0.988	232759.	−1602.90	0.976	696.9
	$(18{+}9)M_\odot$	288.0	0.965	54318.	−919.09	1.000	384.2	$(9{+}1)M_\odot$	622.5	0.987	641361.	−3784.50	0.556	478.2
	$(18{+}6)M_\odot$	301.9	0.974	78079.	−1196.40	1.002	418.2	$(6{+}6)M_\odot$	693.1	0.989	175805.	−1155.90	1.003	771.7
	$(18{+}3)M_\odot$	310.0	0.982	146850.	−2035.50	1.001	390.8	$(6{+}3)M_\odot$	864.1	0.989	311994.	−1469.30	1.126	1224.9
	$(18{+}1)M_\odot$	311.6	0.984	414234.	−5291.30	1.009	391.1	$(6{+}1)M_\odot$	930.1	0.978	842853.	−3181.70	1.008	1337.8
	$(15{+}15)M_\odot$	277.2	0.953	37764.	−643.86	0.988	419.7	$(3{+}3)M_\odot$	1386.1	0.986	533428.	−1441.60	0.914	1646.6
	$(15{+}12)M_\odot$	305.6	0.960	48170.	−786.14	1.001	412.2	$(3{+}1)M_\odot$	1811.5	0.964	1368872.	−2282.70	0.816	2275.1
	$(15{+}9)M_\odot$	333.2	0.972	62940.	−942.30	1.004	420.8	$(1{+}1)M_\odot$	4158.3	0.948	3178171.	−1177.40	1.240	3395.2
	$(21{+}21)M_\odot$	198.0	0.918	14261.	−230.59	1.042	489.7	$(15{+}6)M_\odot$	356.4	0.983	89280.	−1112.10	1.015	477.0
	$(21{+}18)M_\odot$	212.4	0.925	21945.	−422.53	0.978	357.1	$(15{+}3)M_\odot$	370.7	0.985	164423.	−1807.60	1.000	451.6
	$(21{+}15)M_\odot$	226.9	0.932	25752.	−451.51	0.912	371.6	$(15{+}1)M_\odot$	373.9	0.984	463591.	−4787.00	0.995	457.7
	$(21{+}12)M_\odot$	240.7	0.941	35665.	−658.49	1.000	366.7	$(12{+}12)M_\odot$	346.5	0.976	58450.	−788.49	1.002	473.4
	$(21{+}9)M_\odot$	252.5	0.957	48589.	−867.07	1.269	563.9	$(12{+}9)M_\odot$	390.8	0.982	75721.	−923.07	1.000	459.1
	$(21{+}6)M_\odot$	261.3	0.968	70769.	−1198.10	1.000	367.0	$(12{+}6)M_\odot$	432.1	0.985	104313.	−1062.30	1.000	510.7
	$(21{+}3)M_\odot$	266.2	0.976	135969.	−2194.90	1.160	452.8	$(12{+}3)M_\odot$	460.2	0.986	190696.	−1661.90	1.002	566.2
	$(21{+}1)M_\odot$	267.1	0.981	376809.	−5620.40	1.001	332.4	$(12{+}1)M_\odot$	467.3	0.987	530978.	−4217.30	0.675	398.8
T(3, 3.5, +2)	$(18{+}18)M_\odot$	231.0	0.936	26470.	−491.25	0.988	362.8	$(9{+}9)M_\odot$	462.0	0.986	93997.	−947.31	1.002	545.1
	$(18{+}15)M_\odot$	250.7	0.947	30829.	−520.00	0.972	396.0	$(9{+}6)M_\odot$	540.6	0.987	128483.	−1027.60	1.003	635.7
	$(18{+}12)M_\odot$	270.2	0.956	39893.	−648.29	0.993	428.3	$(9{+}3)M_\odot$	603.9	0.988	231522.	−1481.50	0.771	536.2
	$(18{+}9)M_\odot$	288.0	0.965	54056.	−848.31	1.000	425.2	$(9{+}1)M_\odot$	622.4	0.988	640605.	−3681.60	0.549	485.0
	$(18{+}6)M_\odot$	301.9	0.974	79182.	−1174.30	0.999	403.5	$(6{+}6)M_\odot$	693.1	0.988	173589.	−1003.70	0.775	574.7
	$(18{+}3)M_\odot$	310.0	0.983	146869.	−1971.30	1.000	388.3	$(6{+}3)M_\odot$	864.2	0.989	309650.	−1315.40	1.076	1252.5
	$(18{+}1)M_\odot$	311.6	0.983	413631.	−5210.30	0.999	381.0	$(6{+}1)M_\odot$	930.0	0.979	840060.	−3022.30	0.991	1340.3
	$(15{+}15)M_\odot$	277.2	0.957	38769.	−627.96	1.017	445.1	$(3{+}3)M_\odot$	1386.1	0.988	529948.	−1256.70	0.872	1710.0
	$(15{+}12)M_\odot$	305.6	0.970	50245.	−791.61	1.005	420.7	$(3{+}1)M_\odot$	1811.6	0.969	1363459.	−2068.20	0.767	2113.0
	$(15{+}9)M_\odot$	333.2	0.977	64309.	−919.57	1.008	428.0	$(1{+}1)M_\odot$	4158.5	0.953	3175186.	−1034.40	1.289	4087.5
	$(21{+}21)M_\odot$	136.1	0.875	15608.	−331.69	0.864	320.3	$(15{+}6)M_\odot$	259.2	0.972	95764.	−1429.70	0.995	366.4
	$(21{+}18)M_\odot$	146.4	0.868	20265.	−449.47	0.992	294.4	$(15{+}3)M_\odot$	282.3	0.977	173531.	−2228.30	0.999	363.0
	$(21{+}15)M_\odot$	157.6	0.902	26986.	−588.05	0.983	304.6	$(15{+}1)M_\odot$	292.0	0.971	474889.	−5385.40	0.792	271.5
	$(21{+}12)M_\odot$	169.8	0.908	37187.	−819.99	1.003	300.3	$(12{+}12)M_\odot$	238.2	0.964	63604.	−1052.10	1.000	379.8
	$(21{+}9)M_\odot$	182.6	0.927	49703.	−1024.70	0.991	319.1	$(12{+}9)M_\odot$	270.8	0.973	80629.	−1174.10	1.000	374.1
	$(21{+}6)M_\odot$	195.1	0.945	76416.	−1540.90	0.998	295.9	$(12{+}6)M_\odot$	308.3	0.978	110103.	−1329.20	1.000	394.5
	$(21{+}3)M_\odot$	205.3	0.964	144779.	−2713.30	1.000	288.9	$(12{+}3)M_\odot$	346.4	0.978	196198.	−1919.50	0.990	427.5
	$(21{+}1)M_\odot$	209.0	0.963	405402.	−7111.50	1.001	256.3	$(12{+}1)M_\odot$	364.0	0.977	540133.	−4641.20	0.624	311.9
P(2, 2.5)	$(18{+}18)M_\odot$	158.8	0.889	26066.	−568.75	1.001	309.1	$(9{+}9)M_\odot$	317.6	0.980	97552.	−1139.20	1.000	437.2
	$(18{+}15)M_\odot$	172.9	0.920	35254.	−766.20	0.973	297.4	$(9{+}6)M_\odot$	377.1	0.981	132810.	−1226.60	0.999	485.3
	$(18{+}12)M_\odot$	188.6	0.933	43314.	−863.27	0.948	313.0	$(9{+}3)M_\odot$	445.8	0.982	233038.	−1582.70	0.691	392.8
	$(18{+}9)M_\odot$	205.6	0.946	57468.	−1074.40	1.000	341.3	$(9{+}1)M_\odot$	482.7	0.981	646991.	−3945.40	0.509	391.5
	$(18{+}6)M_\odot$	222.9	0.965	85492.	−1515.10	0.998	320.9	$(6{+}6)M_\odot$	476.4	0.983	175879.	−1118.60	0.741	436.6
	$(18{+}3)M_\odot$	237.8	0.971	157994.	−2515.00	0.999	322.3	$(6{+}3)M_\odot$	616.7	0.988	310659.	−1382.30	0.529	488.2
	$(18{+}1)M_\odot$	243.6	0.966	433954.	−6249.10	1.109	336.9	$(6{+}1)M_\odot$	713.5	0.971	843062.	−3139.00	0.982	1004.1
	$(15{+}15)M_\odot$	190.6	0.934	41098.	−804.20	0.996	352.7	$(3{+}3)M_\odot$	952.9	0.990	531119.	−1320.90	0.316	663.1
	$(15{+}12)M_\odot$	211.1	0.953	53724.	−1019.00	1.006	333.5	$(3{+}1)M_\odot$	1337.3	0.966	1363352.	−2081.30	0.774	1540.1
	$(15{+}9)M_\odot$	234.3	0.966	68813.	−1174.40	0.988	339.9	$(1{+}1)M_\odot$	2858.7	0.950	3177870.	−1100.70	1.059	3124.0
	$(21{+}21)M_\odot$	206.1	0.922	16011.	−261.31	0.999	447.8	$(15{+}6)M_\odot$	359.4	0.983	88286.	−1040.60	1.000	478.7
	$(21{+}18)M_\odot$	221.0	0.935	21738.	−379.12	0.961	399.9	$(15{+}3)M_\odot$	346.3	0.982	165550.	−1835.30	0.999	428.1
	$(21{+}15)M_\odot$	235.6	0.940	27111.	−462.11	1.000	460.2	$(15{+}1)M_\odot$	314.7	0.976	470015.	−5133.30	0.747	289.1
	$(21{+}12)M_\odot$	248.2	0.953	36236.	−639.00	1.000	375.6	$(12{+}12)M_\odot$	360.6	0.980	58627.	−741.91	1.013	512.7
	$(21{+}9)M_\odot$	256.1	0.955	47576.	−799.60	1.005	403.1	$(12{+}9)M_\odot$	406.0	0.983	73799.	−813.26	0.999	499.1
	$(21{+}6)M_\odot$	254.7	0.964	70535.	−1166.40	1.000	373.8	$(12{+}6)M_\odot$	442.8	0.985	102868.	−973.26	1.000	536.0
	$(21{+}3)M_\odot$	239.3	0.973	137442.	−2289.60	1.000	329.4	$(12{+}3)M_\odot$	441.6	0.985	189733.	−1607.80	1.001	559.6
	$(21{+}1)M_\odot$	220.6	0.968	397247.	−6685.70	1.001	273.0	$(12{+}1)M_\odot$	399.5	0.981	536637.	−4459.10	0.651	346.6
P(3, 3.5, 0)	$(18{+}18)M_\odot$	240.4	0.946	27776.	−489.59	0.987	397.8	$(9{+}9)M_\odot$	480.9	0.987	91978.	−838.80	1.000	567.7
	$(18{+}15)M_\odot$	260.7	0.955	32734.	−533.01	0.954	415.5	$(9{+}6)M_\odot$	560.2	0.989	126214.	−916.78	1.001	700.7
	$(18{+}12)M_\odot$	280.1	0.961	41018.	−640.84	1.001	451.1	$(9{+}3)M_\odot$	598.6	0.989	229541.	−1390.80	0.734	533.5
	$(18{+}9)M_\odot$	295.2	0.969	53746.	−794.91	1.000	443.3	$(9{+}1)M_\odot$	545.4	0.984	640400.	−3693.40	0.511	427.6
	$(18{+}6)M_\odot$	299.3	0.977	79800.	−1160.90	0.999	395.1	$(6{+}6)M_\odot$	721.3	0.989	171253.	−898.96	0.725	596.1
	$(18{+}3)M_\odot$	283.5	0.978	149734.	−2083.90	1.001	375.6	$(6{+}3)M_\odot$	885.5	0.991	308246.	−1241.60	0.534	648.2
	$(18{+}1)M_\odot$	259.4	0.970	428582.	−5954.10	1.042	332.2	$(6{+}1)M_\odot$	850.4	0.984	839006.	−2979.20	0.379	607.1

PN model		FF (minmax) with $(\psi_0, \psi_{3/2})_{\alpha,\mathrm{cut}}$ template family when LIGO-S2-H2-fit noise curve is used												
		f_{end}	mn	ψ_0	$\psi_{3/2}$	$\alpha f_{\mathrm{cut}}^{2/3}$	f_{cut}		f_{end}	mn	ψ_0	$\psi_{3/2}$	$\alpha f_{\mathrm{cut}}^{2/3}$	f_{cut}
	(15+15)$M_\odot$	288.5	0.963	38950.	−593.98	0.999	449.4	(3+3)$M_\odot$	1442.6	0.993	527460.	−1169.40	0.369	858.3
	(15+12)$M_\odot$	317.7	0.974	48794.	−698.57	0.988	431.2	(3+1)$M_\odot$	1795.8	0.972	1360818.	−1987.10	0.732	1990.5
	(15+9)$M_\odot$	344.3	0.980	63252.	−839.18	0.985	433.2	(1+1)$M_\odot$	4327.8	0.954	3174611.	−1012.40	1.269	4127.9
	(21+21)$M_\odot$	206.1	0.923	10928.	−124.36	0.951	398.1	(15+6)$M_\odot$	359.4	0.983	89927.	−1116.00	1.001	464.2
	(21+18)$M_\odot$	221.0	0.918	21015.	−380.60	1.001	386.4	(15+3)$M_\odot$	346.3	0.983	166113.	−1877.60	0.999	440.6
	(21+15)$M_\odot$	235.6	0.939	28682.	−541.47	0.970	355.7	(15+1)$M_\odot$	314.7	0.976	470365.	−5161.00	0.759	291.8
	(21+12)$M_\odot$	248.2	0.941	35109.	−622.15	0.999	394.8	(12+12)$M_\odot$	360.6	0.979	59195.	−792.13	0.996	466.0
	(21+9)$M_\odot$	256.1	0.960	48089.	−835.18	1.001	386.2	(12+9)$M_\odot$	406.0	0.983	74256.	−861.42	1.001	500.9
	(21+6)$M_\odot$	254.7	0.968	71125.	−1206.90	0.995	360.4	(12+6)$M_\odot$	442.8	0.985	103653.	−1030.80	1.000	522.7
	(21+3)$M_\odot$	239.3	0.971	137011.	−2290.70	1.002	326.8	(12+3)$M_\odot$	441.6	0.986	190683.	−1662.90	0.999	560.1
	(21+1)$M_\odot$	220.6	0.968	397079.	−6689.90	1.000	272.1	(12+1)$M_\odot$	399.5	0.981	537121.	−4491.60	0.649	345.3
P(3, 3.5, −2)	(18+18)$M_\odot$	240.4	0.931	26083.	−464.08	0.995	383.8	(9+9)$M_\odot$	480.9	0.987	91833.	−867.40	0.994	557.4
	(18+15)$M_\odot$	260.7	0.949	33224.	−584.77	0.994	375.0	(9+6)$M_\odot$	560.2	0.989	126480.	−959.96	1.001	667.6
	(18+12)$M_\odot$	280.1	0.962	41344.	−679.62	1.001	400.7	(9+3)$M_\odot$	598.6	0.988	230239.	−1442.10	0.750	529.4
	(18+9)$M_\odot$	295.2	0.971	53774.	−823.12	1.013	428.7	(9+1)$M_\odot$	545.4	0.984	641160.	−3738.50	0.517	430.0
	(18+6)$M_\odot$	299.3	0.974	79119.	−1163.80	1.000	406.3	(6+6)$M_\odot$	721.3	0.989	172421.	−969.41	1.116	1023.4
	(18+3)$M_\odot$	283.5	0.979	149668.	−2099.10	1.006	361.8	(6+3)$M_\odot$	885.5	0.992	308714.	−1289.90	0.538	626.7
	(18+1)$M_\odot$	259.4	0.970	428819.	−5976.90	1.034	331.8	(6+1)$M_\odot$	850.4	0.984	839271.	−3015.00	0.375	601.2
	(15+15)$M_\odot$	288.5	0.963	39196.	−622.04	1.053	481.2	(3+3)$M_\odot$	1442.6	0.990	529205.	−1253.40	0.951	2297.2
	(15+12)$M_\odot$	317.7	0.969	49656.	−759.88	1.000	416.7	(3+1)$M_\odot$	1795.8	0.971	1363468.	−2082.50	0.698	2000.0
	(15+9)$M_\odot$	344.3	0.976	63136.	−866.84	1.000	435.4	(1+1)$M_\odot$	4327.8	0.952	3176380.	−1084.30	1.338	4420.0
	(21+21)$M_\odot$	206.1	0.927	16591.	−269.70	0.960	428.7	(15+6)$M_\odot$	359.4	0.984	88921.	−1051.00	1.001	476.3
	(21+18)$M_\odot$	221.0	0.935	21418.	−370.94	0.966	371.3	(15+3)$M_\odot$	346.3	0.982	165724.	−1835.10	0.999	429.0
	(21+15)$M_\odot$	235.6	0.943	26235.	−433.10	0.995	436.3	(15+1)$M_\odot$	314.7	0.975	469255.	−5100.80	0.746	288.5
	(21+12)$M_\odot$	248.2	0.949	36264.	−636.59	1.000	376.2	(12+12)$M_\odot$	360.6	0.981	59575.	−764.70	1.001	489.9
	(21+9)$M_\odot$	256.1	0.960	48836.	−836.13	1.178	541.5	(12+9)$M_\odot$	406.0	0.983	74404.	−827.68	1.000	507.7
	(21+6)$M_\odot$	254.7	0.966	70569.	−1161.50	0.999	380.1	(12+6)$M_\odot$	442.8	0.985	103558.	−988.48	0.997	532.2
	(21+3)$M_\odot$	239.3	0.973	137821.	−2299.10	1.000	318.1	(12+3)$M_\odot$	441.6	0.985	190274.	−1616.70	0.999	550.6
	(21+1)$M_\odot$	220.6	0.969	397875.	−6702.40	1.001	273.0	(12+1)$M_\odot$	399.5	0.981	536331.	−4440.40	0.641	344.3
P(3, 3.5, +2)	(18+18)$M_\odot$	240.4	0.945	27116.	−472.43	1.000	381.3	(9+9)$M_\odot$	480.9	0.986	91287.	−810.50	0.999	562.0
	(18+15)$M_\odot$	260.7	0.956	34030.	−574.23	0.975	406.9	(9+6)$M_\odot$	560.2	0.988	126174.	−908.94	0.998	679.3
	(18+12)$M_\odot$	280.1	0.964	41347.	−647.88	1.010	448.7	(9+3)$M_\odot$	598.6	0.989	228722.	−1358.50	0.690	502.0
	(18+9)$M_\odot$	295.2	0.970	54478.	−814.73	1.000	443.8	(9+1)$M_\odot$	545.4	0.985	641733.	−3721.50	0.515	432.8
	(18+6)$M_\odot$	299.3	0.975	79683.	−1152.90	1.004	399.2	(6+6)$M_\odot$	721.3	0.989	170766.	−878.16	0.705	574.3
	(18+3)$M_\odot$	283.5	0.979	149450.	−2069.20	0.988	371.4	(6+3)$M_\odot$	885.5	0.991	307458.	−1214.10	1.068	1366.8
	(18+1)$M_\odot$	259.4	0.970	429390.	−5973.00	1.075	350.8	(6+1)$M_\odot$	850.4	0.985	838631.	−2958.10	0.369	602.0
	(15+15)$M_\odot$	288.5	0.966	39406.	−601.33	1.000	451.7	(3+3)$M_\odot$	1442.6	0.991	527429.	−1158.30	0.813	1756.7
	(15+12)$M_\odot$	317.7	0.973	50261.	−744.40	0.997	420.6	(3+1)$M_\odot$	1795.8	0.972	1360940.	−1977.40	0.740	2090.9
	(15+9)$M_\odot$	344.3	0.978	63008.	−826.25	0.998	444.6	(1+1)$M_\odot$	4327.8	0.955	3173972.	−986.25	1.266	4040.8
	(21+21)$M_\odot$	207.7	0.968	14569.	−162.91	0.778	417.0	(15+6)$M_\odot$	413.1	0.988	75328.	−717.20	0.835	708.9
	(21+18)$M_\odot$	223.7	0.975	15780.	−141.66	0.996	670.6	(15+3)$M_\odot$	479.8	0.984	154655.	−1627.10	0.762	557.4
	(21+15)$M_\odot$	242.1	0.976	21108.	−232.64	1.000	613.2	(15+1)$M_\odot$	540.9	0.980	475579.	−5502.60	0.821	460.8
	(21+12)$M_\odot$	263.7	0.981	26393.	−285.03	1.002	715.4	(12+12)$M_\odot$	363.5	0.990	47576.	−433.26	0.833	666.5
	(21+9)$M_\odot$	289.4	0.986	35971.	−408.76	0.998	645.6	(12+9)$M_\odot$	415.2	0.990	64798.	−594.75	0.794	675.8
	(21+6)$M_\odot$	320.5	0.984	53217.	−620.78	0.802	512.8	(12+6)$M_\odot$	483.0	0.990	93021.	−775.52	0.769	741.4
	(21+3)$M_\odot$	359.7	0.971	111363.	−1495.10	0.826	474.7	(12+3)$M_\odot$	576.3	0.988	184445.	−1592.70	0.702	644.5
	(21+1)$M_\odot$	394.2	0.953	381796.	−6284.90	0.898	321.9	(12+1)$M_\odot$	665.0	0.983	548379.	−4989.50	0.796	597.9
EP(2, 2.5)	(18+18)$M_\odot$	242.3	0.980	19892.	−194.91	0.996	717.4	(9+9)$M_\odot$	484.7	0.991	81963.	−632.44	0.756	824.8
	(18+15)$M_\odot$	264.3	0.980	25435.	−279.77	1.001	623.4	(9+6)$M_\odot$	580.8	0.992	119732.	−844.55	0.729	828.9
	(18+12)$M_\odot$	290.4	0.986	31769.	−337.12	1.000	634.8	(9+3)$M_\odot$	721.9	0.993	229617.	−1536.10	0.659	788.8
	(18+9)$M_\odot$	322.0	0.988	43038.	−457.20	0.897	678.8	(9+1)$M_\odot$	863.6	0.979	658967.	−4364.30	0.786	879.7
	(18+6)$M_\odot$	360.9	0.987	62915.	−675.09	1.221	965.7	(6+6)$M_\odot$	727.0	0.993	170165.	−993.36	0.635	904.6
	(18+3)$M_\odot$	411.1	0.978	131545.	−1600.10	0.799	501.9	(6+3)$M_\odot$	965.9	0.995	310989.	−1448.00	0.653	1172.2
	(18+1)$M_\odot$	456.0	0.970	424222.	−5977.50	0.827	369.9	(6+1)$M_\odot$	1233.3	0.963	855446.	−3521.40	1.679	3600.0
	(15+15)$M_\odot$	290.8	0.988	29489.	−279.66	1.004	760.0	(3+3)$M_\odot$	1454.1	0.988	535488.	−1480.30	0.750	2218.4
	(15+12)$M_\odot$	323.0	0.987	39060.	−405.94	0.884	601.6	(3+1)$M_\odot$	2165.6	0.958	1365425.	−2176.60	1.163	2301.0
	(15+9)$M_\odot$	362.8	0.990	50253.	−474.02	0.999	767.9	(1+1)$M_\odot$	4362.2	0.947	3179898.	−1178.10	1.233	3817.7
	(21+21)$M_\odot$	206.6	0.968	16070.	−170.50	0.968	510.3	(15+6)$M_\odot$	417.4	0.992	77353.	−673.76	0.999	794.4
	(21+18)$M_\odot$	223.5	0.969	20344.	−250.81	0.999	463.8	(15+3)$M_\odot$	488.5	0.988	152875.	−1463.00	0.787	609.2
	(21+15)$M_\odot$	241.7	0.975	22698.	−242.92	0.931	475.1	(15+1)$M_\odot$	549.4	0.983	471226.	−5269.80	0.810	467.6
	(21+12)$M_\odot$	264.9	0.978	29965.	−341.08	1.000	562.4	(12+12)$M_\odot$	361.5	0.990	50431.	−431.79	1.000	718.8
	(21+9)$M_\odot$	291.5	0.985	39632.	−450.16	0.999	604.5	(12+9)$M_\odot$	419.3	0.991	64998.	−509.77	0.999	785.9
	(21+6)$M_\odot$	325.4	0.988	57785.	−671.08	0.985	606.3	(12+6)$M_\odot$	488.8	0.992	93588.	−686.64	1.002	933.6
	(21+3)$M_\odot$	367.7	0.980	113292.	−1449.90	0.877	501.8	(12+3)$M_\odot$	598.1	0.992	182153.	−1414.60	0.735	698.6
	(21+1)$M_\odot$	400.7	0.958	377627.	−6040.30	0.858	330.2	(12+1)$M_\odot$	680.0	0.987	542393.	−4722.10	0.793	616.9
EP(3, 3.5, 0)	(18+18)$M_\odot$	241.9	0.974	24710.	−305.86	1.000	503.6	(9+9)$M_\odot$	488.6	0.992	83294.	−563.88	0.999	987.9
	(18+15)$M_\odot$	264.4	0.980	27761.	−296.01	0.938	482.4	(9+6)$M_\odot$	584.2	0.993	119174.	−719.35	0.822	953.9
	(18+12)$M_\odot$	291.7	0.985	35137.	−370.31	0.932	535.7	(9+3)$M_\odot$	730.5	0.995	225814.	−1322.40	0.694	868.3
	(18+9)$M_\odot$	323.4	0.988	44644.	−438.32	0.995	640.2	(9+1)$M_\odot$	882.5	0.985	652247.	−4095.00	0.752	883.1
	(18+6)$M_\odot$	365.9	0.989	66409.	−680.65	0.947	676.5	(6+6)$M_\odot$	724.6	0.994	167578.	−814.23	0.869	1282.8
	(18+3)$M_\odot$	421.6	0.984	130724.	−1467.30	0.842	552.0	(6+3)$M_\odot$	971.8	0.996	306306.	−1222.90	0.592	1134.3
	(18+1)$M_\odot$	462.6	0.974	417839.	−5670.50	0.832	388.3	(6+1)$M_\odot$	1264.7	0.975	848451.	−3269.10	0.514	930.1
	(15+15)$M_\odot$	289.2	0.985	32816.	−320.26	0.995	604.2	(3+3)$M_\odot$	1468.7	0.993	527962.	−1210.30	0.600	1750.7
	(15+12)$M_\odot$	322.7	0.987	42820.	−438.70	1.000	599.2	(3+1)$M_\odot$	2205.5	0.965	1363519.	−2075.00	1.077	2801.1
	(15+9)$M_\odot$	364.9	0.990	54548.	−509.92	0.999	667.8	(1+1)$M_\odot$	4422.6	0.953	3177009.	−1075.30	1.387	5268.6
	(21+21)$M_\odot$	203.0	0.964	16135.	−193.62	0.962	428.9	(15+6)$M_\odot$	414.7	0.991	77297.	−695.40	0.999	706.5
	(21+18)$M_\odot$	218.7	0.967	18978.	−216.96	0.999	571.6	(15+3)$M_\odot$	487.2	0.988	152429.	−1469.10	0.789	605.3
	(21+15)$M_\odot$	238.8	0.970	23654.	−281.57	0.999	529.3	(15+1)$M_\odot$	549.2	0.983	471021.	−5278.00	0.805	465.6
	(21+12)$M_\odot$	260.9	0.979	29096.	−327.55	0.871	488.8	(12+12)$M_\odot$	361.2	0.989	50365.	−457.38	0.999	643.0
	(21+9)$M_\odot$	290.1	0.981	40548.	−499.67	1.001	569.8	(12+9)$M_\odot$	407.9	0.992	64277.	−516.95	1.014	803.2
	(21+6)$M_\odot$	323.2	0.985	57635.	−687.88	0.997	602.8	(12+6)$M_\odot$	482.3	0.993	93815.	−717.35	0.913	847.9

	FF (minmax) with $(\psi_0, \psi_{3/2})_{\alpha,\mathrm{cut}}$ template family when LIGO-S2-H2-fit noise curve is used													
PN model		f_{end}	mn	ψ_0	$\psi_{3/2}$	$\alpha f_{\mathrm{cut}}^{2/3}$	f_{cut}		f_{end}	mn	ψ_0	$\psi_{3/2}$	$\alpha f_{\mathrm{cut}}^{2/3}$	f_{cut}
	$(21{+}3)M_\odot$	366.7	0.979	113106.	−1458.30	0.890	500.6	$(12{+}3)M_\odot$	586.4	0.991	181335.	−1415.90	0.735	702.9
	$(21{+}1)M_\odot$	399.4	0.954	376846.	−6020.30	1.146	484.4	$(12{+}1)M_\odot$	677.4	0.987	541876.	−4726.00	0.803	622.4
EP(3, 3.5, −2)	$(18{+}18)M_\odot$	236.9	0.974	23558.	−278.02	0.999	602.5	$(9{+}9)M_\odot$	475.9	0.992	83494.	−598.42	0.995	917.6
	$(18{+}15)M_\odot$	258.8	0.976	28892.	−344.49	1.000	579.8	$(9{+}6)M_\odot$	580.6	0.993	119042.	−746.86	0.986	1141.6
	$(18{+}12)M_\odot$	286.2	0.982	35035.	−390.28	1.000	579.1	$(9{+}3)M_\odot$	739.2	0.993	224872.	−1327.10	0.707	911.1
	$(18{+}9)M_\odot$	322.2	0.987	46224.	−506.44	0.999	584.2	$(9{+}1)M_\odot$	883.5	0.985	651769.	−4106.30	1.153	1561.7
	$(18{+}6)M_\odot$	363.3	0.990	65221.	−661.53	0.935	626.6	$(6{+}6)M_\odot$	718.5	0.994	167349.	−842.45	0.758	1097.1
	$(18{+}3)M_\odot$	420.5	0.984	131019.	−1491.40	0.843	539.4	$(6{+}3)M_\odot$	961.7	0.996	307079.	−1278.20	0.650	1152.0
	$(18{+}1)M_\odot$	462.4	0.970	417957.	−5683.80	1.152	583.3	$(6{+}1)M_\odot$	1265.9	0.975	850051.	−3336.50	0.966	2124.8
	$(15{+}15)M_\odot$	284.9	0.985	34030.	−372.97	0.999	574.1	$(3{+}3)M_\odot$	1438.6	0.993	530196.	−1302.50	0.595	1642.9
	$(15{+}12)M_\odot$	318.0	0.986	42000.	−439.05	0.999	640.7	$(3{+}1)M_\odot$	2219.2	0.964	1363603.	−2110.70	1.090	2514.6
	$(15{+}9)M_\odot$	357.6	0.989	54046.	−523.47	1.000	674.4	$(1{+}1)M_\odot$	4278.8	0.950	3177788.	−1121.90	1.358	4641.3
	$(21{+}21)M_\odot$	207.4	0.966	19802.	−284.87	0.937	475.1	$(15{+}6)M_\odot$	418.7	0.991	78386.	−695.11	1.003	789.8
	$(21{+}18)M_\odot$	224.6	0.967	20467.	−249.81	0.999	496.1	$(15{+}3)M_\odot$	489.4	0.988	152662.	−1450.00	0.803	620.8
	$(21{+}15)M_\odot$	242.2	0.976	25484.	−318.23	0.998	501.9	$(15{+}1)M_\odot$	550.1	0.984	471027.	−5257.00	0.811	470.4
	$(21{+}12)M_\odot$	266.0	0.978	30186.	−344.81	0.999	581.5	$(12{+}12)M_\odot$	364.7	0.989	50631.	−436.36	1.037	708.9
	$(21{+}9)M_\odot$	291.7	0.985	39005.	−431.30	1.000	561.2	$(12{+}9)M_\odot$	418.5	0.992	64463.	−491.60	1.005	803.5
	$(21{+}6)M_\odot$	326.0	0.988	57894.	−675.01	1.004	601.2	$(12{+}6)M_\odot$	492.3	0.993	93971.	−690.55	1.002	970.0
	$(21{+}3)M_\odot$	368.2	0.980	113950.	−1464.90	0.868	494.1	$(12{+}3)M_\odot$	594.3	0.991	182138.	−1407.10	0.720	692.8
	$(21{+}1)M_\odot$	400.6	0.960	377964.	−6047.00	0.841	327.5	$(12{+}1)M_\odot$	677.8	0.987	543946.	−4756.20	0.774	597.0
EP(3, 3.5, +2)	$(18{+}18)M_\odot$	241.9	0.972	24831.	−308.86	0.999	504.2	$(9{+}9)M_\odot$	489.3	0.991	83185.	−555.60	0.985	980.5
	$(18{+}15)M_\odot$	264.3	0.980	29187.	−335.82	1.001	520.6	$(9{+}6)M_\odot$	589.5	0.993	118975.	−708.33	0.986	1189.9
	$(18{+}12)M_\odot$	290.4	0.984	36130.	−395.75	0.909	495.6	$(9{+}3)M_\odot$	732.3	0.994	226032.	−1320.20	0.694	863.7
	$(18{+}9)M_\odot$	323.5	0.987	45830.	−468.95	0.864	519.1	$(9{+}1)M_\odot$	883.8	0.985	652109.	−4082.00	0.772	905.0
	$(18{+}6)M_\odot$	366.5	0.990	66258.	−671.53	0.949	695.4	$(6{+}6)M_\odot$	729.3	0.994	167206.	−797.32	0.806	1217.0
	$(18{+}3)M_\odot$	421.1	0.985	131689.	−1490.80	0.847	544.5	$(6{+}3)M_\odot$	984.4	0.996	306690.	−1224.00	0.591	1103.6
	$(18{+}1)M_\odot$	462.6	0.975	417665.	−5660.70	0.835	390.2	$(6{+}1)M_\odot$	1258.8	0.975	847918.	−3244.80	0.492	873.1
	$(15{+}15)M_\odot$	292.7	0.986	34377.	−358.61	1.012	619.3	$(3{+}3)M_\odot$	1463.3	0.993	529247.	−1230.70	0.529	1748.8
	$(15{+}12)M_\odot$	322.2	0.985	42341.	−424.95	0.881	493.7	$(3{+}1)M_\odot$	2231.3	0.965	1363593.	−2062.40	1.030	2673.8
	$(15{+}9)M_\odot$	364.9	0.989	53990.	−494.05	0.998	655.7	$(1{+}1)M_\odot$	4393.5	0.953	3176440.	−1050.20	1.277	4566.3

TABLE X: Fitting factors for the projection of the target models (in the rows) onto the $(\psi_0, \psi_{3/2}, \alpha, f_{\mathrm{cut}})$ Fourier-domain detection template family when S2-H2 noise curve is used. For BBH masses $m_{1,2} = 1, 3, 6, 9, 12, 15, 18, 21 M_\odot$, this table shows the minmax matches between the target models and the Fourier-domain search model, *maximized over the intrinsic parameters* ψ_0, $\psi_{3/2}$, and f_{cut}, and over the extrinsic parameter α. For each intersection, the six numbers shown report the *ending frequency* f_{end} (defined in BCV1) of the PN model for the BBH masses quoted, the minmax FF mn, and the search parameters at which the maximum is attained.

	FF (minmax) with $(\psi_0, \psi_{3/2})_{\alpha,\mathrm{cut}}$ template family when LIGO-S2-L1-fit noise curve is used													
PN model		f_{end}	mn	ψ_0	$\psi_{3/2}$	$\alpha f_{\mathrm{cut}}^{2/3}$	f_{cut}		f_{end}	mn	ψ_0	$\psi_{3/2}$	$\alpha f_{\mathrm{cut}}^{2/3}$	f_{cut}
	$(20{+}20)M_\odot$	221.4	0.953	15771.	−269.98	0.993	382.0	$(20{+}5)M_\odot$	341.1	0.986	81939.	−1200.10	1.013	398.7
	$(20{+}15)M_\odot$	252.5	0.955	24285.	−423.80	0.997	356.7	$(10{+}10)M_\odot$	442.7	0.990	78838.	−957.11	1.013	467.0
T(2, 2)	$(15{+}15)M_\odot$	295.1	0.969	36350.	−613.70	0.999	373.3	$(15{+}5)M_\odot$	431.3	0.991	101616.	−1188.80	0.997	482.9
	$(20{+}10)M_\odot$	291.7	0.974	41562.	−704.63	1.000	358.2	$(10{+}5)M_\odot$	583.4	0.992	133214.	−1088.70	1.267	936.3
	$(15{+}10)M_\odot$	352.7	0.985	55827.	−830.73	1.006	421.6	$(5{+}5)M_\odot$	885.5	0.996	229757.	−1197.90	0.873	1174.0
	$(20{+}20)M_\odot$	160.8	0.781	40846.	−671.67	2.345	193.6	$(20{+}5)M_\odot$	282.0	0.975	70102.	−126.67	0.790	403.4
	$(20{+}15)M_\odot$	185.3	0.975	38371.	−369.69	0.931	305.3	$(10{+}10)M_\odot$	324.2	0.979	57095.	260.07	0.391	372.0
T(2, 2.5)	$(15{+}15)M_\odot$	215.7	0.974	39408.	−140.98	0.957	366.5	$(15{+}5)M_\odot$	345.9	0.982	80123.	111.56	0.204	381.7
	$(20{+}10)M_\odot$	219.8	0.973	44096.	−200.92	0.866	324.5	$(10{+}5)M_\odot$	444.5	0.986	113960.	83.58	0.397	1301.5
	$(15{+}10)M_\odot$	260.4	0.973	48037.	1.04	0.789	377.2	$(5{+}5)M_\odot$	644.5	0.994	211786.	−66.21	0.084	1710.2
	$(20{+}20)M_\odot$	207.9	0.933	15484.	−265.49	1.005	366.5	$(20{+}5)M_\odot$	276.1	0.981	89327.	−1485.30	1.005	341.0
	$(20{+}15)M_\odot$	234.5	0.954	27526.	−523.36	1.002	332.4	$(10{+}10)M_\odot$	415.8	0.990	81256.	−979.38	1.027	464.8
T(3, 3.5, 0)	$(15{+}15)M_\odot$	277.2	0.969	36766.	−607.20	0.986	368.9	$(15{+}5)M_\odot$	362.3	0.987	109596.	−1423.00	1.017	406.1
	$(20{+}10)M_\odot$	259.2	0.969	45459.	−828.74	1.001	336.7	$(10{+}5)M_\odot$	518.5	0.989	139423.	−1188.00	1.007	600.8
	$(15{+}10)M_\odot$	324.3	0.981	58534.	−900.55	1.014	406.2	$(5{+}5)M_\odot$	831.7	0.995	232873.	−1123.80	0.965	1297.5
	$(20{+}20)M_\odot$	207.9	0.943	11575.	−156.07	0.986	399.9	$(20{+}5)M_\odot$	276.1	0.979	91086.	−1576.00	0.996	326.2
	$(20{+}15)M_\odot$	234.5	0.946	24947.	−466.58	1.022	342.1	$(10{+}10)M_\odot$	415.9	0.989	83541.	−1077.40	0.997	427.9
T(3, 3.5, −2)	$(15{+}15)M_\odot$	277.2	0.968	35646.	−605.96	1.005	377.0	$(15{+}5)M_\odot$	362.3	0.987	108422.	−1430.90	0.999	398.0
	$(20{+}10)M_\odot$	259.3	0.965	44384.	−830.73	1.002	329.4	$(10{+}5)M_\odot$	518.5	0.990	138972.	−1217.30	0.982	559.6
	$(15{+}10)M_\odot$	324.3	0.981	58021.	−907.86	0.994	382.4	$(5{+}5)M_\odot$	831.7	0.995	234142.	−1204.20	0.997	1197.8
	$(20{+}20)M_\odot$	207.9	0.938	18057.	−336.02	1.001	327.4	$(20{+}5)M_\odot$	276.1	0.981	88601.	−1432.30	1.016	356.8
	$(20{+}15)M_\odot$	234.5	0.959	26433.	−469.19	0.991	347.1	$(10{+}10)M_\odot$	415.8	0.990	81245.	−939.74	1.005	451.9
T(3, 3.5, +2)	$(15{+}15)M_\odot$	277.2	0.971	42135.	−749.38	1.255	532.7	$(15{+}5)M_\odot$	362.3	0.986	106532.	−1294.70	0.982	369.7
	$(20{+}10)M_\odot$	259.2	0.971	45490.	−807.02	1.022	358.2	$(10{+}5)M_\odot$	518.5	0.989	138581.	−1122.00	0.986	577.6
	$(15{+}10)M_\odot$	324.3	0.982	59970.	−907.56	0.990	390.4	$(5{+}5)M_\odot$	831.7	0.995	232686.	−1067.60	0.868	1130.5
	$(20{+}20)M_\odot$	142.9	0.893	14474.	−279.85	1.001	314.8	$(20{+}5)M_\odot$	207.8	0.967	97160.	−1892.10	0.988	275.5
	$(20{+}15)M_\odot$	162.5	0.927	27346.	−582.94	0.997	294.8	$(10{+}10)M_\odot$	285.9	0.985	88353.	−1250.50	1.014	375.9
P(2, 2.5)	$(15{+}15)M_\odot$	190.6	0.949	40209.	−788.82	0.986	321.1	$(15{+}5)M_\odot$	267.5	0.982	116178.	−1714.10	0.995	332.0
	$(20{+}10)M_\odot$	185.0	0.947	46331.	−944.51	0.963	290.3	$(10{+}5)M_\odot$	370.0	0.984	144665.	−1365.90	1.025	478.9
	$(15{+}10)M_\odot$	226.3	0.966	64211.	−1163.20	1.008	330.1	$(5{+}5)M_\odot$	571.7	0.992	235284.	−1187.50	0.672	492.8
	$(20{+}20)M_\odot$	216.4	0.948	19971.	−370.14	0.989	330.4	$(20{+}5)M_\odot$	265.0	0.980	91773.	−1524.60	0.998	321.6
	$(20{+}15)M_\odot$	243.6	0.965	28263.	−485.98	0.985	355.2	$(10{+}10)M_\odot$	432.8	0.990	80119.	−845.69	1.001	493.1
P(3, 3.5, 0)	$(15{+}15)M_\odot$	288.5	0.976	39754.	−634.12	0.974	378.9	$(15{+}5)M_\odot$	359.2	0.987	106635.	−1261.60	0.991	417.0
	$(20{+}10)M_\odot$	265.7	0.974	47292.	−824.53	1.105	421.5	$(10{+}5)M_\odot$	531.3	0.990	136499.	−1017.60	1.289	971.2
	$(15{+}10)M_\odot$	336.1	0.984	59201.	−839.34	1.002	402.5	$(5{+}5)M_\odot$	865.6	0.996	229267.	−944.82	1.038	1734.8

PN model		FF (minmax) with $(\psi_0, \psi_{3/2})_{\alpha,\mathrm{cut}}$ template family when LIGO-S2-L1-fit noise curve is used												
		f_{end}	mn	ψ_0	$\psi_{3/2}$	$\alpha f_{\mathrm{cut}}^{2/3}$	f_{cut}		f_{end}	mn	ψ_0	$\psi_{3/2}$	$\alpha f_{\mathrm{cut}}^{2/3}$	f_{cut}
P$(3, 3.5, -2)$	$(20{+}20)M_\odot$	216.4	0.941	16513.	−273.57	0.993	369.3	$(20{+}5)M_\odot$	265.0	0.978	90496.	−1504.50	1.000	337.6
	$(20{+}15)M_\odot$	243.6	0.958	28196.	−513.97	0.980	323.9	$(10{+}10)M_\odot$	432.8	0.989	80809.	−905.41	1.007	473.0
	$(15{+}15)M_\odot$	288.5	0.975	44644.	−799.99	1.251	528.8	$(15{+}5)M_\odot$	359.2	0.987	106954.	−1299.40	1.012	426.9
	$(20{+}10)M_\odot$	265.7	0.971	45695.	−797.61	1.015	349.9	$(10{+}5)M_\odot$	531.3	0.990	137332.	−1075.80	1.154	779.5
	$(15{+}10)M_\odot$	336.1	0.984	61958.	−952.61	1.250	571.1	$(5{+}5)M_\odot$	865.6	0.996	230854.	−1022.90	0.811	1159.4
P$(3, 3.5, +2)$	$(20{+}20)M_\odot$	216.4	0.944	19042.	−339.16	1.014	347.2	$(20{+}5)M_\odot$	265.0	0.979	91918.	−1525.70	0.993	321.1
	$(20{+}15)M_\odot$	243.6	0.963	29468.	−520.27	0.969	327.7	$(10{+}10)M_\odot$	432.8	0.989	80591.	−853.70	0.992	478.3
	$(15{+}15)M_\odot$	288.5	0.977	40310.	−640.06	0.951	358.5	$(15{+}5)M_\odot$	359.2	0.986	103762.	−1171.80	0.998	407.3
	$(20{+}10)M_\odot$	265.7	0.973	48006.	−851.25	1.092	398.7	$(10{+}5)M_\odot$	531.3	0.990	136654.	−1014.50	1.043	709.5
	$(15{+}10)M_\odot$	336.1	0.985	58668.	−810.90	1.011	419.9	$(5{+}5)M_\odot$	865.6	0.996	229184.	−933.48	0.882	1443.1
EP$(2, 2.5)$	$(20{+}20)M_\odot$	218.1	0.985	15137.	−153.88	0.988	513.1	$(20{+}5)M_\odot$	345.8	0.993	66377.	−770.18	1.194	849.0
	$(20{+}15)M_\odot$	249.1	0.987	26627.	−365.96	0.842	407.0	$(10{+}10)M_\odot$	436.2	0.994	66342.	−531.14	1.083	1274.8
	$(15{+}15)M_\odot$	290.8	0.994	30826.	−324.84	0.877	555.1	$(15{+}5)M_\odot$	433.1	0.993	89979.	−870.14	0.864	740.8
	$(20{+}10)M_\odot$	289.8	0.991	33660.	−361.76	0.842	441.7	$(10{+}5)M_\odot$	579.6	0.993	129599.	−962.58	1.067	1582.4
	$(15{+}10)M_\odot$	348.5	0.994	44653.	−412.70	0.936	710.7	$(5{+}5)M_\odot$	872.4	0.997	234021.	−1203.70	0.658	1244.8
EP$(3, 3.5, 0)$	$(20{+}20)M_\odot$	218.4	0.975	19498.	−251.00	0.869	349.2	$(20{+}5)M_\odot$	351.7	0.994	70733.	−801.03	1.117	691.0
	$(20{+}15)M_\odot$	250.2	0.987	28629.	−390.52	0.975	433.7	$(10{+}10)M_\odot$	434.6	0.992	68186.	−482.70	0.784	629.3
	$(15{+}15)M_\odot$	289.2	0.991	35822.	−404.80	0.898	454.6	$(15{+}5)M_\odot$	445.3	0.993	91911.	−813.09	0.998	785.1
	$(20{+}10)M_\odot$	294.3	0.991	40055.	−489.91	0.903	437.3	$(10{+}5)M_\odot$	581.6	0.994	128457.	−812.57	1.085	1537.0
	$(15{+}10)M_\odot$	350.3	0.993	49832.	−475.67	1.388	1037.8	$(5{+}5)M_\odot$	869.0	0.997	229038.	−965.14	0.664	1409.1
EP$(3, 3.5, -2)$	$(20{+}20)M_\odot$	215.6	0.982	18753.	−233.01	0.990	467.0	$(20{+}5)M_\odot$	353.7	0.993	71123.	−818.47	0.952	531.3
	$(20{+}15)M_\odot$	248.3	0.986	25376.	−308.36	0.977	452.2	$(10{+}10)M_\odot$	432.6	0.992	69072.	−530.93	1.155	1032.3
	$(15{+}15)M_\odot$	284.9	0.990	35472.	−418.78	0.908	431.4	$(15{+}5)M_\odot$	439.0	0.994	91892.	−835.00	0.885	657.3
	$(20{+}10)M_\odot$	289.1	0.990	38425.	−463.37	0.915	438.9	$(10{+}5)M_\odot$	580.9	0.994	128099.	−838.44	0.960	1365.9
	$(15{+}10)M_\odot$	347.1	0.992	50018.	−498.84	0.932	546.8	$(5{+}5)M_\odot$	864.2	0.997	228906.	−1003.00	0.746	1642.5
EP$(3, 3.5, +2)$	$(20{+}20)M_\odot$	220.2	0.978	19289.	−241.40	0.880	380.2	$(20{+}5)M_\odot$	351.8	0.994	71490.	−814.77	0.951	555.3
	$(20{+}15)M_\odot$	250.6	0.986	24820.	−276.87	0.983	415.7	$(10{+}10)M_\odot$	437.4	0.992	69638.	−513.12	0.991	845.6
	$(15{+}15)M_\odot$	292.7	0.992	35841.	−397.69	0.945	477.3	$(15{+}5)M_\odot$	443.1	0.994	91853.	−810.33	1.073	889.9
	$(20{+}10)M_\odot$	294.8	0.990	39676.	−479.41	0.918	428.8	$(10{+}5)M_\odot$	583.9	0.994	128130.	−802.66	1.030	1670.2
	$(15{+}10)M_\odot$	353.5	0.992	50155.	−470.57	0.930	590.5	$(5{+}5)M_\odot$	872.0	0.997	228499.	−944.36	0.643	1449.2

TABLE XI: Fitting factors for the projection of the target models (in the rows) onto the $(\psi_0, \psi_{3/2}, \alpha, f_{\mathrm{cut}})$ Fourier-domain detection template family when S2-L1 noise curve is used. For BBH masses $m_{1,2} = 5, 10, 15, 20 M_\odot$, this table shows the minmax matches between the target models and the Fourier-domain search model, *maximized over the intrinsic parameters* ψ_0, $\psi_{3/2}$, and f_{cut}, and over the extrinsic parameter α. For each intersection, the six numbers shown report the *ending frequency* f_{end} (defined in BCV1) of the PN model for the BBH masses quoted, the minmax FF mn, and the search parameters at which the maximum is attained.

PN model		FF (minmax) with $(\psi_0, \psi_{3/2})_{\alpha,\mathrm{cut}}$ template family when LIGO-S2-L1-fit noise curve is used												
		f_{end}	mn	ψ_0	$\psi_{3/2}$	$\alpha f_{\mathrm{cut}}^{2/3}$	f_{cut}		f_{end}	mn	ψ_0	$\psi_{3/2}$	$\alpha f_{\mathrm{cut}}^{2/3}$	f_{cut}
T$(2, 2)$	$(12{+}12)M_\odot$	369.0	0.986	57171.	−815.57	0.996	424.0	$(12{+}1)M_\odot$	633.5	0.997	513975.	−3638.60	0.975	921.1
	$(12{+}9)M_\odot$	420.8	0.990	72578.	−900.26	0.994	444.1	$(9{+}1)M_\odot$	829.6	0.998	627622.	−3378.70	0.901	1322.0
	$(12{+}6)M_\odot$	486.2	0.991	102022.	−1069.40	1.001	525.7	$(6{+}3)M_\odot$	972.3	0.997	306590.	−1435.30	0.487	635.7
	$(12{+}3)M_\odot$	568.6	0.993	182825.	−1494.00	1.008	709.0	$(6{+}1)M_\odot$	1200.2	0.998	832821.	−3028.30	0.405	791.4
	$(9{+}9)M_\odot$	491.9	0.992	90564.	−941.32	1.001	517.2	$(3{+}3)M_\odot$	1475.8	0.998	530442.	−1542.70	0.660	2122.9
	$(9{+}6)M_\odot$	587.8	0.992	124323.	−1027.90	0.997	657.1	$(3{+}1)M_\odot$	2156.4	0.994	1362013.	−2360.60	0.614	3131.4
	$(9{+}3)M_\odot$	718.8	0.995	225871.	−1455.20	1.018	1030.1	$(1{+}1)M_\odot$	4427.3	0.987	3181667.	−1583.10	0.587	4781.5
	$(6{+}6)M_\odot$	737.9	0.994	170472.	−1084.00	0.974	929.2							
T$(2, 2.5)$	$(12{+}12)M_\odot$	268.0	0.973	46643.	92.08	0.665	345.4	$(12{+}1)M_\odot$	593.3	0.996	486144.	−1354.90	0.469	1112.4
	$(12{+}9)M_\odot$	310.2	0.977	53696.	253.11	0.433	363.7	$(9{+}1)M_\odot$	748.9	0.997	599077.	−1276.80	0.377	1587.2
	$(12{+}6)M_\odot$	372.4	0.983	80201.	177.79	0.186	420.9	$(6{+}3)M_\odot$	736.7	0.996	287889.	−230.39	0.000	700.0
	$(12{+}3)M_\odot$	470.1	0.990	164036.	−187.61	0.551	1352.1	$(6{+}1)M_\odot$	1043.9	0.999	802876.	−1129.40	0.154	865.6
	$(9{+}9)M_\odot$	360.2	0.982	70731.	220.09	0.112	405.6	$(3{+}3)M_\odot$	1079.3	0.998	510281.	−324.30	0.289	1479.7
	$(9{+}6)M_\odot$	435.9	0.987	105479.	112.62	0.026	482.9	$(3{+}1)M_\odot$	1725.5	0.999	1334067.	−793.73	0.193	3317.7
	$(9{+}3)M_\odot$	574.6	0.993	206146.	−176.88	0.012	607.5	$(1{+}1)M_\odot$	3235.0	0.995	3157071.	−257.10	0.234	3882.0
	$(6{+}6)M_\odot$	537.0	0.992	152905.	22.09	0.003	586.2							
T$(3, 3.5, 0)$	$(12{+}12)M_\odot$	346.5	0.985	61028.	−900.00	1.000	402.3	$(12{+}1)M_\odot$	467.3	0.993	535296.	−4364.10	0.652	396.3
	$(12{+}9)M_\odot$	390.8	0.987	78578.	−1038.20	0.999	404.2	$(9{+}1)M_\odot$	622.5	0.995	645885.	−3846.10	0.525	486.3
	$(12{+}6)M_\odot$	432.1	0.988	107283.	−1173.90	0.999	473.8	$(6{+}3)M_\odot$	864.1	0.996	310769.	−1379.50	0.852	1244.7
	$(12{+}3)M_\odot$	460.2	0.990	191530.	−1711.20	0.983	549.2	$(6{+}1)M_\odot$	930.1	0.994	843057.	−3117.80	0.353	613.4
	$(9{+}9)M_\odot$	462.0	0.990	95334.	−1014.50	1.000	479.2	$(3{+}3)M_\odot$	1386.2	0.997	531335.	−1322.70	0.513	1668.3
	$(9{+}6)M_\odot$	540.5	0.990	129732.	−1092.70	1.000	602.1	$(3{+}1)M_\odot$	1811.5	0.992	1361183.	−2032.20	0.495	2040.3
	$(9{+}3)M_\odot$	603.9	0.994	232209.	−1532.50	0.659	486.2	$(1{+}1)M_\odot$	4158.6	0.989	3174639.	−1026.30	0.467	4492.0
	$(6{+}6)M_\odot$	693.1	0.993	175087.	−1081.30	1.130	1097.1							
T$(3, 3.5, -2)$	$(12{+}12)M_\odot$	346.5	0.983	65604.	−1074.60	1.198	503.7	$(12{+}1)M_\odot$	467.3	0.993	536235.	−4428.80	0.663	398.4
	$(12{+}9)M_\odot$	390.8	0.986	79257.	−1098.30	0.999	396.5	$(9{+}1)M_\odot$	622.5	0.995	646979.	−3916.40	0.532	484.9
	$(12{+}6)M_\odot$	432.1	0.989	106586.	−1193.70	1.002	460.7	$(6{+}3)M_\odot$	864.1	0.996	312471.	−1469.20	0.884	1211.9
	$(12{+}3)M_\odot$	460.2	0.990	191825.	−1758.70	1.001	553.8	$(6{+}1)M_\odot$	930.1	0.994	843659.	−3178.10	0.360	600.1
	$(9{+}9)M_\odot$	462.0	0.991	96136.	−1075.20	0.999	477.2	$(3{+}3)M_\odot$	1386.1	0.996	532769.	−1407.40	0.604	1774.3
	$(9{+}6)M_\odot$	540.5	0.991	130247.	−1148.20	0.995	595.7	$(3{+}1)M_\odot$	1811.5	0.991	1363002.	−2117.90	0.604	2493.0
	$(9{+}3)M_\odot$	603.9	0.993	232788.	−1590.90	0.676	474.2	$(1{+}1)M_\odot$	4158.3	0.988	3177212.	−1122.00	0.398	3990.7
	$(6{+}6)M_\odot$	693.1	0.993	175637.	−1140.10	0.692	510.3							
	$(12{+}12)M_\odot$	346.5	0.985	62131.	−900.83	1.001	412.3	$(12{+}1)M_\odot$	467.3	0.993	534452.	−4301.70	0.642	393.3
	$(12{+}9)M_\odot$	390.8	0.987	78782.	−1003.40	1.000	412.7	$(9{+}1)M_\odot$	622.4	0.994	646429.	−3816.30	0.519	491.1
	$(12{+}6)M_\odot$	432.1	0.988	106354.	−1106.30	1.001	486.6	$(6{+}3)M_\odot$	864.2	0.996	309270.	−1294.40	1.015	1783.5

PN model		$f_{\rm end}$	mn	ψ_0	$\psi_{3/2}$	$\alpha f_{\rm cut}^{2/3}$	$f_{\rm cut}$		$f_{\rm end}$	mn	ψ_0	$\psi_{3/2}$	$\alpha f_{\rm cut}^{2/3}$	$f_{\rm cut}$
	FF (minmax) with $(\psi_0, \psi_{3/2})_{\alpha,{\rm cut}}$ template family when LIGO-S2-L1-fit noise curve is used													
$\mathrm{T}(3, 3.5, +2)$	$(12{+}3)M_\odot$	460.2	0.990	190922.	−1654.10	1.001	569.9	$(6{+}1)M_\odot$	930.0	0.994	840777.	−3017.10	0.347	609.0
	$(9{+}9)M_\odot$	462.0	0.990	96305.	−995.98	0.998	505.0	$(3{+}3)M_\odot$	1386.1	0.997	529735.	−1237.10	0.574	1693.6
	$(9{+}6)M_\odot$	540.6	0.990	128662.	−1018.70	1.006	638.3	$(3{+}1)M_\odot$	1811.6	0.993	1359536.	−1949.10	0.514	2319.6
	$(9{+}3)M_\odot$	603.9	0.993	230797.	−1449.90	0.617	461.4	$(1{+}1)M_\odot$	4158.5	0.989	3172726.	−945.70	0.436	4308.0
	$(6{+}6)M_\odot$	693.1	0.992	173879.	−1001.80	0.634	504.7							
$\mathrm{P}(2, 2.5)$	$(12{+}12)M_\odot$	238.2	0.974	65573.	−1118.60	0.973	323.8	$(12{+}1)M_\odot$	364.0	0.987	545419.	−4785.20	0.636	312.5
	$(12{+}9)M_\odot$	270.8	0.981	84929.	−1301.60	1.005	340.1	$(9{+}1)M_\odot$	482.7	0.991	651703.	−4055.70	0.503	390.6
	$(12{+}6)M_\odot$	308.3	0.983	114256.	−1435.00	1.001	375.5	$(6{+}3)M_\odot$	616.7	0.995	311812.	−1401.10	0.449	475.0
	$(12{+}3)M_\odot$	346.4	0.983	199554.	−1998.00	1.001	433.8	$(6{+}1)M_\odot$	713.5	0.992	845801.	−3181.90	0.349	522.5
	$(9{+}9)M_\odot$	317.6	0.986	101447.	−1237.00	1.000	390.2	$(3{+}3)M_\odot$	952.9	0.997	531517.	−1309.90	0.335	646.7
	$(9{+}6)M_\odot$	377.1	0.985	134856.	−1265.10	1.001	471.9	$(3{+}1)M_\odot$	1337.3	0.992	1359374.	−1956.60	0.161	590.6
	$(9{+}3)M_\odot$	445.8	0.989	233888.	−1593.10	0.638	376.7	$(1{+}1)M_\odot$	2858.7	0.989	3174012.	−979.95	0.434	3916.8
	$(6{+}6)M_\odot$	476.4	0.988	178298.	−1172.10	0.675	421.9							
$\mathrm{P}(3, 3.5, 0)$	$(12{+}12)M_\odot$	360.6	0.988	60967.	−808.63	1.001	430.8	$(12{+}1)M_\odot$	399.5	0.989	542346.	−4604.90	0.640	343.5
	$(12{+}9)M_\odot$	406.0	0.988	76532.	−882.11	1.001	452.7	$(9{+}1)M_\odot$	545.4	0.993	648328.	−3889.30	0.500	438.6
	$(12{+}6)M_\odot$	442.8	0.988	103759.	−985.00	1.002	516.9	$(6{+}3)M_\odot$	885.5	0.996	307439.	−1212.40	0.771	1344.3
	$(12{+}3)M_\odot$	441.6	0.989	191120.	−1632.60	0.992	560.9	$(6{+}1)M_\odot$	850.4	0.994	841210.	−3011.30	0.338	593.0
	$(9{+}9)M_\odot$	480.9	0.990	93027.	−852.64	1.008	555.0	$(3{+}3)M_\odot$	1442.6	0.998	526955.	−1143.70	0.320	865.0
	$(9{+}6)M_\odot$	560.2	0.991	126064.	−901.42	0.994	715.2	$(3{+}1)M_\odot$	1795.8	0.994	1357962.	−1893.10	0.143	657.1
	$(9{+}3)M_\odot$	598.6	0.994	229258.	−1373.00	0.600	476.3	$(1{+}1)M_\odot$	4327.8	0.990	3172165.	−924.18	0.454	4605.1
	$(6{+}6)M_\odot$	721.3	0.993	171153.	−890.20	0.984	1078.8							
$\mathrm{P}(3, 3.5, -2)$	$(12{+}12)M_\odot$	360.6	0.987	60423.	−828.48	0.995	399.3	$(12{+}1)M_\odot$	399.5	0.989	539071.	−4532.70	0.630	338.8
	$(12{+}9)M_\odot$	406.0	0.989	77134.	−937.73	0.999	438.9	$(9{+}1)M_\odot$	545.4	0.993	642457.	−3760.80	0.495	425.2
	$(12{+}6)M_\odot$	442.8	0.988	104630.	−1044.50	1.002	496.1	$(6{+}3)M_\odot$	885.5	0.996	307914.	−1261.30	0.846	1432.2
	$(12{+}3)M_\odot$	441.6	0.989	190468.	−1641.90	0.997	555.5	$(6{+}1)M_\odot$	850.4	0.994	840560.	−3026.60	0.352	581.2
	$(9{+}9)M_\odot$	480.9	0.990	93186.	−893.01	1.002	538.3	$(3{+}3)M_\odot$	1442.6	0.997	528954.	−1233.00	0.440	1546.9
	$(9{+}6)M_\odot$	560.2	0.991	126393.	−946.37	0.998	676.2	$(3{+}1)M_\odot$	1795.8	0.993	1359399.	−1961.20	0.502	2356.2
	$(9{+}3)M_\odot$	598.6	0.993	231075.	−1455.20	0.962	813.8	$(1{+}1)M_\odot$	4327.8	0.989	3173289.	−980.87	0.532	4893.2
	$(6{+}6)M_\odot$	721.3	0.993	170776.	−916.09	0.571	497.6							
$\mathrm{P}(3, 3.5, +2)$	$(12{+}12)M_\odot$	360.6	0.988	62105.	−835.17	1.001	422.3	$(12{+}1)M_\odot$	399.5	0.990	539325.	−4511.10	0.625	338.6
	$(12{+}9)M_\odot$	406.0	0.989	77101.	−895.51	1.000	449.3	$(9{+}1)M_\odot$	545.4	0.992	650210.	−3925.40	0.511	442.6
	$(12{+}6)M_\odot$	442.8	0.988	104566.	−1002.30	1.000	512.8	$(6{+}3)M_\odot$	885.5	0.997	306898.	−1190.10	0.876	1663.3
	$(12{+}3)M_\odot$	441.6	0.988	190658.	−1612.30	0.954	517.0	$(6{+}1)M_\odot$	850.4	0.994	840716.	−2989.10	0.335	588.2
	$(9{+}9)M_\odot$	480.9	0.989	93137.	−849.50	1.001	558.1	$(3{+}3)M_\odot$	1442.6	0.997	526817.	−1130.40	0.458	1349.6
	$(9{+}6)M_\odot$	560.2	0.990	126048.	−893.97	0.944	644.2	$(3{+}1)M_\odot$	1795.8	0.994	1357061.	−1859.80	0.151	656.6
	$(9{+}3)M_\odot$	598.6	0.993	228945.	−1355.80	0.587	471.2	$(1{+}1)M_\odot$	4327.8	0.990	3171538.	−898.14	0.477	4703.8
	$(6{+}6)M_\odot$	721.3	0.993	171364.	−887.84	0.920	970.5							
$\mathrm{EP}(2, 2.5)$	$(12{+}12)M_\odot$	363.5	0.994	47695.	−439.54	1.131	950.3	$(12{+}1)M_\odot$	665.0	0.993	554241.	−5133.70	0.778	552.1
	$(12{+}9)M_\odot$	415.2	0.994	63077.	−554.16	0.910	752.8	$(9{+}1)M_\odot$	863.6	0.991	663250.	−4445.80	1.011	1224.9
	$(12{+}6)M_\odot$	483.0	0.993	91911.	−758.66	0.710	697.9	$(6{+}3)M_\odot$	965.9	0.997	313558.	−1504.70	0.728	1538.7
	$(12{+}3)M_\odot$	576.3	0.993	185313.	−1629.20	0.646	570.6	$(6{+}1)M_\odot$	1233.3	0.987	853820.	−3448.10	0.917	1647.6
	$(9{+}9)M_\odot$	484.7	0.994	80762.	−608.88	1.095	1450.9	$(3{+}3)M_\odot$	1454.1	0.995	534864.	−1445.50	0.634	1862.3
	$(9{+}6)M_\odot$	580.8	0.994	119438.	−848.30	0.679	865.7	$(3{+}1)M_\odot$	2165.6	0.990	1363941.	−2112.30	0.586	2221.5
	$(9{+}3)M_\odot$	721.9	0.996	231465.	−1589.20	0.609	690.0	$(1{+}1)M_\odot$	4362.2	0.988	3176028.	−1057.30	0.508	4717.3
	$(6{+}6)M_\odot$	727.0	0.996	171880.	−1044.40	0.509	714.6							
$\mathrm{EP}(3, 3.5, 0)$	$(12{+}12)M_\odot$	361.5	0.992	51544.	−458.45	0.994	668.9	$(12{+}1)M_\odot$	680.0	0.994	546828.	−4829.80	0.964	782.7
	$(12{+}9)M_\odot$	419.3	0.992	65430.	−518.04	1.001	813.2	$(9{+}1)M_\odot$	882.5	0.993	655246.	−4148.60	0.985	1292.0
	$(12{+}6)M_\odot$	488.8	0.993	93138.	−679.18	1.107	1246.7	$(6{+}3)M_\odot$	971.8	0.998	308322.	−1270.10	0.485	1015.7
	$(12{+}3)M_\odot$	598.1	0.995	181969.	−1419.60	0.887	962.5	$(6{+}1)M_\odot$	1264.7	0.991	846841.	−3202.80	0.953	2102.1
	$(9{+}9)M_\odot$	488.6	0.993	82301.	−540.26	1.072	1264.4	$(3{+}3)M_\odot$	1468.7	0.997	529447.	−1232.60	0.525	1772.3
	$(9{+}6)M_\odot$	584.2	0.994	117604.	−687.13	0.953	1612.4	$(3{+}1)M_\odot$	2205.5	0.993	1359671.	−1957.50	0.630	2980.3
	$(9{+}3)M_\odot$	730.5	0.996	226927.	−1355.70	0.564	737.0	$(1{+}1)M_\odot$	4422.6	0.989	3172329.	−936.90	0.563	5398.2
	$(6{+}6)M_\odot$	724.6	0.995	167844.	−826.26	0.657	1219.5							
$\mathrm{EP}(3, 3.5, -2)$	$(12{+}12)M_\odot$	361.2	0.991	51539.	−485.94	0.999	621.0	$(12{+}1)M_\odot$	677.4	0.994	546967.	−4851.30	1.110	962.3
	$(12{+}9)M_\odot$	407.9	0.993	64956.	−531.32	0.962	714.2	$(9{+}1)M_\odot$	883.5	0.993	655554.	−4180.20	0.989	1290.3
	$(12{+}6)M_\odot$	482.3	0.994	91775.	−670.48	0.960	963.1	$(6{+}3)M_\odot$	961.7	0.998	308298.	−1305.30	0.620	1320.4
	$(12{+}3)M_\odot$	586.4	0.994	181591.	−1435.40	0.653	624.6	$(6{+}1)M_\odot$	1265.9	0.991	847417.	−3246.20	0.938	2007.8
	$(9{+}9)M_\odot$	475.9	0.992	82567.	−576.02	0.744	657.2	$(3{+}3)M_\odot$	1438.6	0.997	530802.	−1302.70	0.494	1722.0
	$(9{+}6)M_\odot$	580.6	0.994	118314.	−735.31	0.952	1367.3	$(3{+}1)M_\odot$	2219.2	0.992	1360927.	−2019.90	0.577	2479.1
	$(9{+}3)M_\odot$	739.2	0.996	227403.	−1398.70	0.549	698.8	$(1{+}1)M_\odot$	4278.8	0.988	3174026.	−1002.90	0.499	4412.4
	$(6{+}6)M_\odot$	718.5	0.995	168278.	−873.13	0.480	762.7							
$\mathrm{EP}(3, 3.5, +2)$	$(12{+}12)M_\odot$	364.7	0.991	51740.	−462.88	1.000	642.8	$(12{+}1)M_\odot$	677.8	0.994	547116.	−4828.70	1.071	921.3
	$(12{+}9)M_\odot$	418.5	0.993	65089.	−504.37	0.938	730.5	$(9{+}1)M_\odot$	883.8	0.993	655132.	−4136.10	0.779	912.0
	$(12{+}6)M_\odot$	492.3	0.994	92675.	−662.06	0.814	794.7	$(6{+}3)M_\odot$	984.4	0.998	307904.	−1250.50	0.469	946.9
	$(12{+}3)M_\odot$	594.3	0.994	181864.	−1410.50	0.665	636.7	$(6{+}1)M_\odot$	1258.8	0.991	846430.	−3180.70	0.404	640.7
	$(9{+}9)M_\odot$	489.3	0.992	82197.	−532.02	0.957	1107.8	$(3{+}3)M_\odot$	1463.3	0.997	528669.	−1203.60	0.441	1676.5
	$(9{+}6)M_\odot$	589.5	0.994	118265.	−696.98	0.911	1380.5	$(3{+}1)M_\odot$	2231.3	0.992	1359708.	−1944.30	0.608	2908.8
	$(9{+}3)M_\odot$	732.3	0.996	227936.	−1373.10	0.546	693.9	$(1{+}1)M_\odot$	4393.5	0.989	3172509.	−928.47	0.514	5010.7
	$(6{+}6)M_\odot$	729.3	0.996	167445.	−809.41	0.462	788.7							

TABLE XII: Fitting factors for the projection of the target models (in the rows) onto the $(\psi_0, \psi_{3/2}, \alpha, f_{\rm cut})$ Fourier-domain detection template family when S2-L1 noise curve is used. For BBH masses $m_{1,2} = 1, 3, 6, 9, 12 M_\odot$, this table shows the minmax matches between the target models and the Fourier-domain search model, *maximized over the intrinsic parameters* ψ_0, $\psi_{3/2}$, and $f_{\rm cut}$, and over the extrinsic parameter α. For each intersection, the six numbers shown report the *ending frequency* $f_{\rm end}$ (defined in BCV1) of the PN model for the BBH masses quoted, the minmax FF mn, and the search parameters at which the maximum is attained.

PN model	FF (minmax) with $(\psi_0, \psi_{3/2})_{\alpha,\mathrm{cut}}$ template family when LIGO-S2-L1-fit noise curve is used													
		$f_{\rm end}$	mn	ψ_0	$\psi_{3/2}$	$\alpha f_{\rm cut}^{2/3}$	$f_{\rm cut}$		$f_{\rm end}$	mn	ψ_0	$\psi_{3/2}$	$\alpha f_{\rm cut}^{2/3}$	$f_{\rm cut}$
	$(21{+}21)M_\odot$	210.8	0.938	11398.	−165.57	1.000	407.1	$(15{+}6)M_\odot$	413.5	0.990	86667.	−1068.20	0.999	437.8
	$(21{+}18)M_\odot$	226.9	0.939	15554.	−245.36	0.999	407.5	$(15{+}3)M_\odot$	469.8	0.992	156179.	−1553.50	1.002	549.9
	$(21{+}15)M_\odot$	245.2	0.948	23924.	−443.20	0.991	321.3	$(15{+}1)M_\odot$	512.2	0.995	439269.	−3821.30	1.151	848.9
	$(21{+}12)M_\odot$	266.2	0.956	30673.	−531.04	0.998	370.8	$(12{+}12)M_\odot$	369.0	0.986	57171.	−815.57	0.996	424.0
	$(21{+}9)M_\odot$	290.2	0.973	45622.	−801.12	0.995	343.0	$(12{+}9)M_\odot$	420.8	0.990	72578.	−900.26	0.994	444.1
	$(21{+}6)M_\odot$	317.5	0.983	69667.	−1140.90	1.212	517.1	$(12{+}6)M_\odot$	486.2	0.991	102022.	−1069.40	1.001	525.7
	$(21{+}3)M_\odot$	348.3	0.989	125488.	−1724.50	0.999	391.7	$(12{+}3)M_\odot$	568.6	0.993	182825.	−1494.00	1.008	709.0
	$(21{+}1)M_\odot$	370.4	0.992	347125.	−4141.10	1.000	450.3	$(12{+}1)M_\odot$	633.5	0.997	513975.	−3638.60	0.975	921.1
T(2, 2)	$(18{+}18)M_\odot$	246.0	0.944	22174.	−390.87	0.994	357.5	$(9{+}9)M_\odot$	491.9	0.992	90564.	−941.32	1.001	517.2
	$(18{+}15)M_\odot$	268.1	0.965	28703.	−492.65	1.003	367.9	$(9{+}6)M_\odot$	587.8	0.992	124323.	−1027.90	0.997	657.1
	$(18{+}12)M_\odot$	293.9	0.969	36826.	−600.27	1.002	396.4	$(9{+}3)M_\odot$	718.8	0.995	225871.	−1455.20	1.018	1030.1
	$(18{+}9)M_\odot$	324.1	0.977	52408.	−839.22	0.999	384.0	$(9{+}1)M_\odot$	829.6	0.998	627622.	−3378.70	0.901	1322.0
	$(18{+}6)M_\odot$	359.4	0.986	76608.	−1104.10	1.001	406.6	$(6{+}6)M_\odot$	737.9	0.994	170472.	−1084.00	0.974	929.2
	$(18{+}3)M_\odot$	400.1	0.991	138181.	−1629.80	1.000	448.3	$(6{+}3)M_\odot$	972.3	0.997	306590.	−1435.30	0.487	635.7
	$(18{+}1)M_\odot$	429.9	0.994	386255.	−3979.00	1.004	546.1	$(6{+}1)M_\odot$	1200.2	0.998	832821.	−3028.30	0.405	791.4
	$(15{+}15)M_\odot$	295.1	0.969	36350.	−613.70	0.999	373.3	$(3{+}3)M_\odot$	1475.8	0.998	530442.	−1542.70	0.660	2122.9
	$(15{+}12)M_\odot$	327.5	0.975	46598.	−739.91	1.001	383.6	$(3{+}1)M_\odot$	2156.4	0.994	1362013.	−2360.60	0.614	3131.4
	$(15{+}9)M_\odot$	366.5	0.984	62640.	−925.87	1.000	386.5	$(1{+}1)M_\odot$	4427.3	0.987	3181667.	−1583.10	0.587	4781.5
	$(21{+}21)M_\odot$	153.4	0.771	34454.	−545.96	2.361	185.6	$(15{+}6)M_\odot$	322.4	0.979	67472.	140.22	0.286	366.5
	$(21{+}18)M_\odot$	166.3	0.790	39271.	−570.43	2.310	194.6	$(15{+}3)M_\odot$	397.2	0.987	140027.	−264.08	0.283	435.5
	$(21{+}15)M_\odot$	181.0	0.974	36724.	−343.06	0.999	329.0	$(15{+}1)M_\odot$	485.6	0.994	415735.	−1479.60	0.339	488.4
	$(21{+}12)M_\odot$	200.1	0.975	40813.	−301.91	0.998	349.4	$(12{+}12)M_\odot$	268.0	0.973	46643.	92.08	0.665	345.4
	$(21{+}9)M_\odot$	222.5	0.974	47959.	−266.53	0.955	376.0	$(12{+}9)M_\odot$	310.2	0.977	53696.	253.11	0.433	363.7
	$(21{+}6)M_\odot$	256.4	0.973	59350.	−147.33	0.826	369.0	$(12{+}6)M_\odot$	372.4	0.983	80201.	177.79	0.186	420.9
	$(21{+}3)M_\odot$	307.0	0.980	110424.	−364.91	0.555	346.5	$(12{+}3)M_\odot$	470.1	0.990	164036.	−187.61	0.551	1352.1
	$(21{+}1)M_\odot$	358.3	0.989	327883.	−1652.30	0.479	360.9	$(12{+}1)M_\odot$	593.3	0.996	486144.	−1354.90	0.469	1112.4
T(2, 2.5)	$(18{+}18)M_\odot$	179.0	0.808	44989.	−602.70	2.234	201.7	$(9{+}9)M_\odot$	360.2	0.982	70731.	220.09	0.112	405.6
	$(18{+}15)M_\odot$	196.5	0.974	40320.	−334.15	0.994	340.0	$(9{+}6)M_\odot$	435.9	0.987	105479.	112.62	0.026	482.9
	$(18{+}12)M_\odot$	217.1	0.973	42704.	−209.97	0.996	395.7	$(9{+}3)M_\odot$	574.6	0.993	206146.	−176.88	0.012	607.5
	$(18{+}9)M_\odot$	244.5	0.971	46539.	−47.33	0.782	333.5	$(9{+}1)M_\odot$	748.9	0.997	599077.	−1276.80	0.377	1587.2
	$(18{+}6)M_\odot$	286.0	0.974	54584.	221.89	0.465	319.1	$(6{+}6)M_\odot$	537.0	0.992	152905.	22.09	0.003	586.2
	$(18{+}3)M_\odot$	345.2	0.984	121645.	−280.66	0.414	378.9	$(6{+}3)M_\odot$	736.7	0.996	287889.	−230.39	0.000	700.0
	$(18{+}1)M_\odot$	413.0	0.992	364457.	−1542.20	0.400	414.9	$(6{+}1)M_\odot$	1043.9	0.999	802876.	−1129.40	0.154	865.6
	$(15{+}15)M_\odot$	215.7	0.974	39408.	−140.98	0.957	366.5	$(3{+}3)M_\odot$	1079.3	0.998	510281.	−324.30	0.289	1479.7
	$(15{+}12)M_\odot$	240.1	0.972	43659.	−58.64	0.899	386.3	$(3{+}1)M_\odot$	1725.5	0.999	1334067.	−793.73	0.193	3317.7
	$(15{+}9)M_\odot$	274.1	0.973	49239.	91.56	0.774	398.9	$(1{+}1)M_\odot$	3235.0	0.995	3157071.	−257.10	0.234	3882.0
	$(21{+}21)M_\odot$	198.0	0.944	13190.	−218.28	0.996	377.1	$(15{+}6)M_\odot$	356.4	0.988	92664.	−1238.60	1.020	413.5
	$(21{+}18)M_\odot$	212.4	0.927	16304.	−273.05	1.000	364.5	$(15{+}3)M_\odot$	370.7	0.988	166540.	−1891.70	0.999	438.9
	$(21{+}15)M_\odot$	226.9	0.943	25137.	−485.66	1.001	312.3	$(15{+}1)M_\odot$	373.9	0.989	466274.	−4884.70	1.000	469.8
	$(21{+}12)M_\odot$	240.7	0.951	31683.	−566.40	1.000	364.8	$(12{+}12)M_\odot$	346.5	0.985	61028.	−900.00	1.000	402.3
	$(21{+}9)M_\odot$	252.5	0.966	54060.	−1090.30	1.184	415.8	$(12{+}9)M_\odot$	390.8	0.987	78578.	−1038.20	0.999	404.2
	$(21{+}6)M_\odot$	261.3	0.972	72743.	−1302.10	1.000	320.2	$(12{+}6)M_\odot$	432.1	0.988	107283.	−1173.90	0.999	473.8
	$(21{+}3)M_\odot$	266.2	0.983	138005.	−2273.90	0.985	310.3	$(12{+}3)M_\odot$	460.2	0.990	191530.	−1711.20	0.983	549.2
	$(21{+}1)M_\odot$	267.1	0.985	380493.	−5746.90	1.000	314.9	$(12{+}1)M_\odot$	467.3	0.993	535296.	−4364.10	0.652	396.3
T(3, 3.5, 0)	$(18{+}18)M_\odot$	231.0	0.937	23202.	−423.12	1.001	351.5	$(9{+}9)M_\odot$	462.0	0.990	95334.	−1014.50	1.000	479.2
	$(18{+}15)M_\odot$	250.7	0.954	31931.	−601.20	1.000	327.8	$(9{+}6)M_\odot$	540.5	0.990	129732.	−1092.70	1.000	602.1
	$(18{+}12)M_\odot$	270.2	0.968	42587.	−776.24	0.992	337.9	$(9{+}3)M_\odot$	603.9	0.994	232209.	−1532.50	0.659	486.2
	$(18{+}9)M_\odot$	288.0	0.977	55327.	−924.09	0.998	360.9	$(9{+}1)M_\odot$	622.5	0.995	645885.	−3846.10	0.525	486.3
	$(18{+}6)M_\odot$	301.9	0.982	81161.	−1267.80	0.999	370.0	$(6{+}6)M_\odot$	693.1	0.993	175087.	−1081.30	1.130	1097.1
	$(18{+}3)M_\odot$	310.0	0.986	149747.	−2077.70	0.999	358.6	$(6{+}3)M_\odot$	864.1	0.996	310769.	−1379.50	0.852	1244.7
	$(18{+}1)M_\odot$	311.6	0.987	416063.	−5299.90	0.998	372.4	$(6{+}1)M_\odot$	930.1	0.994	843057.	−3117.80	0.353	613.4
	$(15{+}15)M_\odot$	277.2	0.969	36766.	−607.20	0.986	368.9	$(3{+}3)M_\odot$	1386.2	0.997	531335.	−1322.70	0.513	1668.3
	$(15{+}12)M_\odot$	305.6	0.975	51508.	−877.49	1.008	351.0	$(3{+}1)M_\odot$	1811.5	0.992	1361183.	−2032.20	0.495	2040.3
	$(15{+}9)M_\odot$	333.2	0.983	66974.	−1039.90	0.999	358.6	$(1{+}1)M_\odot$	4158.6	0.989	3174639.	−1026.30	0.467	4492.0
	$(21{+}21)M_\odot$	198.0	0.927	12006.	−199.24	0.980	317.9	$(15{+}6)M_\odot$	356.4	0.988	90905.	−1219.50	0.996	388.2
	$(21{+}18)M_\odot$	212.4	0.945	15271.	−246.52	0.969	391.0	$(15{+}3)M_\odot$	370.7	0.988	166454.	−1925.20	1.001	431.8
	$(21{+}15)M_\odot$	226.9	0.938	20874.	−359.10	0.998	371.7	$(15{+}1)M_\odot$	373.9	0.989	465149.	−4887.10	1.012	469.5
	$(21{+}12)M_\odot$	240.7	0.956	31974.	−588.63	0.977	355.5	$(12{+}12)M_\odot$	346.5	0.983	65604.	−1074.60	1.198	503.7
	$(21{+}9)M_\odot$	252.5	0.959	46439.	−865.85	1.006	333.5	$(12{+}9)M_\odot$	390.8	0.986	79257.	−1098.30	0.999	396.5
	$(21{+}6)M_\odot$	261.3	0.971	70316.	−1247.10	0.996	335.0	$(12{+}6)M_\odot$	432.1	0.989	106586.	−1193.70	1.002	460.7
	$(21{+}3)M_\odot$	266.2	0.982	136808.	−2267.50	0.999	316.6	$(12{+}3)M_\odot$	460.2	0.990	191825.	−1758.70	1.001	553.8
	$(21{+}1)M_\odot$	267.1	0.985	379399.	−5741.20	1.000	316.6	$(12{+}1)M_\odot$	467.3	0.993	536235.	−4428.80	0.663	398.4
T(3, 3.5, −2)	$(18{+}18)M_\odot$	231.0	0.951	19991.	−331.27	0.965	384.3	$(9{+}9)M_\odot$	462.0	0.991	96136.	−1075.20	0.999	477.2
	$(18{+}15)M_\odot$	250.7	0.949	28266.	−500.12	1.002	368.1	$(9{+}6)M_\odot$	540.5	0.991	130247.	−1148.20	0.995	595.7
	$(18{+}12)M_\odot$	270.3	0.960	40205.	−731.15	1.000	341.1	$(9{+}3)M_\odot$	603.9	0.993	232788.	−1590.90	0.676	474.2
	$(18{+}9)M_\odot$	288.0	0.974	56012.	−986.89	0.995	333.0	$(9{+}1)M_\odot$	622.5	0.995	646979.	−3916.40	0.532	484.9
	$(18{+}6)M_\odot$	301.9	0.983	80608.	−1274.50	1.021	378.4	$(6{+}6)M_\odot$	693.1	0.993	175637.	−1140.10	0.692	510.3
	$(18{+}3)M_\odot$	310.0	0.986	149765.	−2112.80	1.000	360.6	$(6{+}3)M_\odot$	864.1	0.996	312471.	−1469.20	0.884	1211.9
	$(18{+}1)M_\odot$	311.6	0.988	416629.	−5348.20	0.998	375.0	$(6{+}1)M_\odot$	930.1	0.994	843659.	−3178.10	0.360	600.1
	$(15{+}15)M_\odot$	277.2	0.968	35646.	−605.96	1.005	377.0	$(3{+}3)M_\odot$	1386.1	0.996	532769.	−1407.40	0.604	1774.3
	$(15{+}12)M_\odot$	305.6	0.971	49500.	−840.24	1.000	365.5	$(3{+}1)M_\odot$	1811.5	0.991	1363002.	−2117.90	0.604	2493.0
	$(15{+}9)M_\odot$	333.2	0.981	65852.	−1037.60	0.999	368.8	$(1{+}1)M_\odot$	4158.3	0.988	3177212.	−1122.00	0.398	3990.7
	$(21{+}21)M_\odot$	198.0	0.944	12622.	−189.45	0.950	382.9	$(15{+}6)M_\odot$	356.4	0.989	93089.	−1212.10	0.991	404.5
	$(21{+}18)M_\odot$	212.4	0.939	20749.	−401.36	0.994	320.8	$(15{+}3)M_\odot$	370.7	0.988	166390.	−1850.30	1.001	441.0
	$(21{+}15)M_\odot$	226.9	0.954	25185.	−453.59	0.994	374.4	$(15{+}1)M_\odot$	373.9	0.989	465571.	−4828.80	1.010	474.5
	$(21{+}12)M_\odot$	240.7	0.954	35335.	−665.69	1.001	328.0	$(12{+}12)M_\odot$	346.5	0.985	62131.	−900.83	1.001	412.3
	$(21{+}9)M_\odot$	252.5	0.968	46978.	−821.11	0.980	347.7	$(12{+}9)M_\odot$	390.8	0.987	78782.	−1003.40	1.000	412.7
	$(21{+}6)M_\odot$	261.3	0.977	72394.	−1260.00	1.006	326.5	$(12{+}6)M_\odot$	432.1	0.988	106354.	−1106.30	1.001	486.6
	$(21{+}3)M_\odot$	266.2	0.983	136446.	−2196.50	1.001	329.4	$(12{+}3)M_\odot$	460.2	0.990	190922.	−1654.10	1.001	569.9
	$(21{+}1)M_\odot$	267.1	0.985	380962.	−5735.90	1.000	316.6	$(12{+}1)M_\odot$	467.3	0.993	534452.	−4301.70	0.642	393.3
T(3, 3.5, +2)	$(18{+}18)M_\odot$	231.0	0.949	24972.	−453.58	0.978	308.6	$(9{+}9)M_\odot$	462.0	0.990	96305.	−995.98	0.998	505.0

FF (minmax) with $(\psi_0, \psi_{3/2})_{\alpha,\mathrm{cut}}$ template family when LIGO-S2-L1-fit noise curve is used

PN model		f_{end}	mn	ψ_0	$\psi_{3/2}$	$\alpha f_{\mathrm{cut}}^{2/3}$	f_{cut}		f_{end}	mn	ψ_0	$\psi_{3/2}$	$\alpha f_{\mathrm{cut}}^{2/3}$	f_{cut}
	$(18{+}15)M_\odot$	250.7	0.961	34772.	-659.54	1.129	436.5	$(9{+}6)M_\odot$	540.6	0.990	128662.	-1018.70	1.006	638.3
	$(18{+}12)M_\odot$	270.2	0.970	41388.	-708.11	1.011	383.0	$(9{+}3)M_\odot$	603.9	0.993	230797.	-1449.90	0.617	461.4
	$(18{+}9)M_\odot$	288.0	0.977	58565.	-1002.30	1.253	525.8	$(9{+}1)M_\odot$	622.4	0.994	646429.	-3816.30	0.519	491.1
	$(18{+}6)M_\odot$	301.9	0.982	83698.	-1313.90	1.000	363.3	$(6{+}6)M_\odot$	693.1	0.992	173879.	-1001.80	0.634	504.7
	$(18{+}3)M_\odot$	310.0	0.986	149866.	-2046.60	1.001	363.9	$(6{+}3)M_\odot$	864.2	0.996	309270.	-1294.40	1.015	1783.5
	$(18{+}1)M_\odot$	311.6	0.987	417275.	-5305.10	1.000	375.3	$(6{+}1)M_\odot$	930.0	0.994	840777.	-3017.10	0.347	609.0
	$(15{+}15)M_\odot$	277.2	0.971	42135.	-749.38	1.255	532.7	$(3{+}3)M_\odot$	1386.1	0.997	529735.	-1237.10	0.574	1693.6
	$(15{+}12)M_\odot$	305.6	0.979	52980.	-879.19	1.013	367.6	$(3{+}1)M_\odot$	1811.6	0.993	1359536.	-1949.10	0.514	2319.6
	$(15{+}9)M_\odot$	333.2	0.982	64385.	-898.81	0.976	342.3	$(1{+}1)M_\odot$	4158.5	0.989	3172726.	-945.70	0.436	4308.0
	$(21{+}21)M_\odot$	136.1	0.905	13672.	-279.38	0.815	294.1	$(15{+}6)M_\odot$	259.2	0.980	100630.	-1576.00	1.000	336.6
	$(21{+}18)M_\odot$	146.4	0.879	17053.	-352.67	0.998	296.5	$(15{+}3)M_\odot$	282.3	0.982	177991.	-2341.70	1.000	343.6
	$(21{+}15)M_\odot$	157.6	0.905	26817.	-594.85	0.908	251.8	$(15{+}1)M_\odot$	292.0	0.980	484339.	-5669.20	0.782	274.3
	$(21{+}12)M_\odot$	169.8	0.917	33539.	-715.57	1.006	290.0	$(12{+}12)M_\odot$	238.2	0.974	65573.	-1118.60	0.973	323.8
	$(21{+}9)M_\odot$	182.6	0.939	48067.	-985.03	0.966	295.3	$(12{+}9)M_\odot$	270.8	0.981	84929.	-1301.60	1.005	340.1
	$(21{+}6)M_\odot$	195.1	0.952	77069.	-1573.60	1.000	286.9	$(12{+}6)M_\odot$	308.3	0.983	114256.	-1435.00	1.001	375.5
	$(21{+}3)M_\odot$	205.3	0.970	150651.	-2908.20	0.995	273.2	$(12{+}3)M_\odot$	346.4	0.983	199554.	-1998.00	1.001	433.8
	$(21{+}1)M_\odot$	209.0	0.970	420040.	-7593.20	1.000	252.6	$(12{+}1)M_\odot$	364.0	0.987	545419.	-4785.20	0.636	312.5
P(2, 2.5)	$(18{+}18)M_\odot$	158.8	0.899	32058.	-800.88	1.196	378.6	$(9{+}9)M_\odot$	317.6	0.986	101447.	-1237.00	1.000	390.2
	$(18{+}15)M_\odot$	172.9	0.929	32990.	-708.10	1.002	279.1	$(9{+}6)M_\odot$	377.1	0.985	134856.	-1265.10	1.001	471.9
	$(18{+}12)M_\odot$	188.6	0.947	43011.	-868.01	1.010	313.5	$(9{+}3)M_\odot$	445.8	0.989	233888.	-1593.10	0.638	376.7
	$(18{+}9)M_\odot$	205.6	0.957	57584.	-1092.70	0.993	315.4	$(9{+}1)M_\odot$	482.7	0.991	651703.	-4055.70	0.503	390.6
	$(18{+}6)M_\odot$	222.9	0.972	90136.	-1669.80	1.000	291.7	$(6{+}6)M_\odot$	476.4	0.988	178298.	-1172.10	0.675	421.9
	$(18{+}3)M_\odot$	237.8	0.978	164506.	-2711.60	1.001	301.2	$(6{+}3)M_\odot$	616.7	0.995	311812.	-1401.10	0.449	475.0
	$(18{+}1)M_\odot$	243.6	0.974	448658.	-6713.60	1.000	289.3	$(6{+}1)M_\odot$	713.5	0.992	845801.	-3181.90	0.349	522.5
	$(15{+}15)M_\odot$	190.6	0.949	40209.	-788.82	0.986	321.1	$(3{+}3)M_\odot$	952.9	0.997	531517.	-1309.90	0.335	646.7
	$(15{+}12)M_\odot$	211.1	0.960	54459.	-1051.20	0.971	280.8	$(3{+}1)M_\odot$	1337.3	0.992	1359374.	-1956.60	0.161	590.6
	$(15{+}9)M_\odot$	234.3	0.974	71865.	-1277.20	1.005	310.5	$(1{+}1)M_\odot$	2858.7	0.989	3174012.	-979.95	0.434	3916.8
	$(21{+}21)M_\odot$	206.1	0.945	13987.	-212.02	1.000	400.3	$(15{+}6)M_\odot$	359.4	0.989	92512.	-1153.30	0.995	418.3
	$(21{+}18)M_\odot$	221.0	0.952	20579.	-349.56	0.979	356.4	$(15{+}3)M_\odot$	346.3	0.986	168177.	-1895.80	1.001	419.3
	$(21{+}15)M_\odot$	235.6	0.958	26861.	-466.80	1.018	411.2	$(15{+}1)M_\odot$	314.7	0.983	474300.	-5254.10	0.782	291.7
	$(21{+}12)M_\odot$	248.2	0.963	38031.	-712.73	1.008	332.5	$(12{+}12)M_\odot$	360.6	0.988	60967.	-808.63	1.001	430.8
	$(21{+}9)M_\odot$	256.1	0.968	51740.	-948.57	1.238	493.4	$(12{+}9)M_\odot$	406.0	0.988	76532.	-882.11	1.001	452.7
	$(21{+}6)M_\odot$	254.7	0.974	72886.	-1248.80	1.003	342.7	$(12{+}6)M_\odot$	442.8	0.988	103759.	-985.00	1.002	516.9
	$(21{+}3)M_\odot$	239.3	0.979	142947.	-2459.50	0.980	291.3	$(12{+}3)M_\odot$	441.6	0.989	191120.	-1632.60	0.992	560.9
	$(21{+}1)M_\odot$	220.6	0.975	408913.	-7056.30	0.994	263.1	$(12{+}1)M_\odot$	399.5	0.989	542346.	-4604.90	0.640	343.5
P(3, 3.5, 0)	$(18{+}18)M_\odot$	240.4	0.960	27377.	-493.90	1.008	354.8	$(9{+}9)M_\odot$	480.9	0.990	93027.	-852.64	1.008	555.0
	$(18{+}15)M_\odot$	260.7	0.969	36398.	-662.63	1.266	541.5	$(9{+}6)M_\odot$	560.2	0.991	126064.	-901.42	0.994	715.2
	$(18{+}12)M_\odot$	280.1	0.974	40727.	-645.56	0.986	382.8	$(9{+}3)M_\odot$	598.6	0.994	229258.	-1373.00	0.600	476.3
	$(18{+}9)M_\odot$	295.2	0.980	56022.	-872.51	1.001	391.7	$(9{+}1)M_\odot$	545.4	0.993	648328.	-3889.30	0.500	438.6
	$(18{+}6)M_\odot$	299.3	0.983	83727.	-1276.70	1.000	351.9	$(6{+}6)M_\odot$	721.3	0.993	171153.	-890.20	0.984	1078.8
	$(18{+}3)M_\odot$	283.5	0.984	154789.	-2226.30	1.001	343.5	$(6{+}3)M_\odot$	885.5	0.996	307439.	-1212.40	0.771	1344.3
	$(18{+}1)M_\odot$	259.4	0.977	437971.	-6229.60	0.994	304.7	$(6{+}1)M_\odot$	850.4	0.994	841210.	-3011.30	0.338	593.0
	$(15{+}15)M_\odot$	288.5	0.976	39754.	-634.12	0.974	378.9	$(3{+}3)M_\odot$	1442.6	0.998	526955.	-1143.70	0.320	865.0
	$(15{+}12)M_\odot$	317.7	0.981	55238.	-902.66	1.190	496.2	$(3{+}1)M_\odot$	1795.8	0.994	1357962.	-1893.10	0.143	657.1
	$(15{+}9)M_\odot$	344.3	0.986	66755.	-938.62	1.003	389.6	$(1{+}1)M_\odot$	4327.8	0.990	3172165.	-924.18	0.454	4605.1
	$(21{+}21)M_\odot$	206.1	0.949	13920.	-226.47	1.006	379.4	$(15{+}6)M_\odot$	359.4	0.988	91877.	-1160.20	1.000	406.1
	$(21{+}18)M_\odot$	221.0	0.934	19791.	-356.09	0.978	333.1	$(15{+}3)M_\odot$	346.3	0.987	168425.	-1927.60	1.000	420.4
	$(21{+}15)M_\odot$	235.6	0.952	26176.	-480.32	1.001	322.7	$(15{+}1)M_\odot$	314.7	0.983	474632.	-5276.60	0.773	289.5
	$(21{+}12)M_\odot$	248.2	0.955	33646.	-592.75	1.003	357.9	$(12{+}12)M_\odot$	360.6	0.987	60423.	-828.48	0.995	399.3
	$(21{+}9)M_\odot$	256.1	0.971	48551.	-865.24	0.995	333.7	$(12{+}9)M_\odot$	406.0	0.989	77134.	-937.73	0.999	438.9
	$(21{+}6)M_\odot$	254.7	0.976	73527.	-1299.00	1.037	341.8	$(12{+}6)M_\odot$	442.8	0.988	104630.	-1044.50	1.002	496.1
	$(21{+}3)M_\odot$	239.3	0.978	141848.	-2444.70	0.997	303.7	$(12{+}3)M_\odot$	441.6	0.989	190468.	-1641.90	0.997	555.5
	$(21{+}1)M_\odot$	220.6	0.974	408313.	-7047.50	0.999	265.3	$(12{+}1)M_\odot$	399.5	0.989	539071.	-4532.70	0.630	338.8
P(3, 3.5, −2)	$(18{+}18)M_\odot$	240.4	0.946	23879.	-412.30	1.000	349.0	$(9{+}9)M_\odot$	480.9	0.990	93186.	-893.01	1.002	538.3
	$(18{+}15)M_\odot$	260.7	0.961	32010.	-563.45	1.002	331.4	$(9{+}6)M_\odot$	560.2	0.991	126393.	-946.37	0.998	676.2
	$(18{+}12)M_\odot$	280.1	0.972	44828.	-795.91	0.989	342.3	$(9{+}3)M_\odot$	598.6	0.993	231075.	-1455.20	0.962	813.8
	$(18{+}9)M_\odot$	295.2	0.980	56192.	-900.76	1.001	364.9	$(9{+}1)M_\odot$	545.4	0.993	642457.	-3760.80	0.495	425.2
	$(18{+}6)M_\odot$	299.3	0.982	82427.	-1266.00	1.000	363.5	$(6{+}6)M_\odot$	721.3	0.993	170776.	-916.09	0.571	497.6
	$(18{+}3)M_\odot$	283.5	0.984	153474.	-2200.10	1.000	335.9	$(6{+}3)M_\odot$	885.5	0.996	307914.	-1261.30	0.846	1432.2
	$(18{+}1)M_\odot$	259.4	0.978	437471.	-6229.40	1.011	313.9	$(6{+}1)M_\odot$	850.4	0.994	840560.	-3026.60	0.352	581.2
	$(15{+}15)M_\odot$	288.5	0.975	44644.	-799.99	1.251	528.8	$(3{+}3)M_\odot$	1442.6	0.997	528954.	-1233.00	0.440	1546.9
	$(15{+}12)M_\odot$	317.7	0.978	51617.	-827.39	1.000	363.6	$(3{+}1)M_\odot$	1795.8	0.993	1359399.	-1961.20	0.502	2356.2
	$(15{+}9)M_\odot$	344.3	0.984	66815.	-977.82	1.000	382.3	$(1{+}1)M_\odot$	4327.8	0.989	3173289.	-980.87	0.532	4893.2
	$(21{+}21)M_\odot$	206.1	0.943	13184.	-175.32	0.850	328.6	$(15{+}6)M_\odot$	359.4	0.989	91548.	-1113.50	0.975	403.8
	$(21{+}18)M_\odot$	221.0	0.949	22247.	-408.59	0.948	315.0	$(15{+}3)M_\odot$	346.3	0.985	168892.	-1911.00	1.001	418.3
	$(21{+}15)M_\odot$	235.6	0.960	24689.	-401.27	1.005	386.2	$(15{+}1)M_\odot$	314.7	0.983	474831.	-5259.70	0.779	290.9
	$(21{+}12)M_\odot$	248.2	0.960	36835.	-670.99	0.994	329.7	$(12{+}12)M_\odot$	360.6	0.988	62105.	-835.17	1.001	422.3
	$(21{+}9)M_\odot$	256.1	0.971	49110.	-850.88	1.034	392.9	$(12{+}9)M_\odot$	406.0	0.989	77101.	-895.51	1.000	449.3
	$(21{+}6)M_\odot$	254.7	0.976	73018.	-1245.40	0.996	345.2	$(12{+}6)M_\odot$	442.8	0.988	104566.	-1002.30	1.000	512.8
	$(21{+}3)M_\odot$	239.3	0.979	143566.	-2477.30	1.009	297.1	$(12{+}3)M_\odot$	441.6	0.988	190658.	-1612.30	0.954	517.0
	$(21{+}1)M_\odot$	220.6	0.975	408328.	-7029.00	1.001	263.1	$(12{+}1)M_\odot$	399.5	0.990	539325.	-4511.10	0.625	338.6
P(3, 3.5, +2)	$(18{+}18)M_\odot$	240.4	0.957	28568.	-535.30	0.996	330.1	$(9{+}9)M_\odot$	480.9	0.989	93137.	-849.50	1.001	558.1
	$(18{+}15)M_\odot$	260.7	0.967	37992.	-712.56	1.174	462.3	$(9{+}6)M_\odot$	560.2	0.990	126048.	-893.97	0.944	644.2
	$(18{+}12)M_\odot$	280.1	0.975	42468.	-690.28	0.960	357.5	$(9{+}3)M_\odot$	598.6	0.993	228945.	-1355.80	0.587	471.2
	$(18{+}9)M_\odot$	295.2	0.981	56553.	-884.66	1.000	387.7	$(9{+}1)M_\odot$	545.4	0.992	650210.	-3925.40	0.511	442.6
	$(18{+}6)M_\odot$	299.3	0.983	83390.	-1263.80	1.000	355.1	$(6{+}6)M_\odot$	721.3	0.993	171364.	-887.84	0.920	970.5
	$(18{+}3)M_\odot$	283.5	0.985	154345.	-2201.00	1.001	342.1	$(6{+}3)M_\odot$	885.5	0.997	306898.	-1190.10	0.876	1663.3
	$(18{+}1)M_\odot$	259.4	0.977	437525.	-6210.10	1.000	308.4	$(6{+}1)M_\odot$	850.4	0.994	840716.	-2989.10	0.335	588.2
	$(15{+}15)M_\odot$	288.5	0.977	40310.	-640.06	0.951	358.5	$(3{+}3)M_\odot$	1442.6	0.997	526817.	-1130.40	0.458	1349.6
	$(15{+}12)M_\odot$	317.7	0.981	52401.	-811.39	0.997	361.6	$(3{+}1)M_\odot$	1795.8	0.994	1357061.	-1859.80	0.151	656.6
	$(15{+}9)M_\odot$	344.3	0.985	67550.	-959.06	1.001	391.5	$(1{+}1)M_\odot$	4327.8	0.990	3171538.	-898.14	0.477	4703.8

PN model		$f_{\rm end}$	mn	ψ_0	$\psi_{3/2}$	$\alpha f_{\rm cut}^{2/3}$	$f_{\rm cut}$		$f_{\rm end}$	mn	ψ_0	$\psi_{3/2}$	$\alpha f_{\rm cut}^{2/3}$	$f_{\rm cut}$
	FF (minmax) with $(\psi_0, \psi_{3/2})_{\alpha,{\rm cut}}$ template family when LIGO-S2-L1-fit noise curve is used													
	$(21{+}21)M_\odot$	207.7	0.983	13189.	−116.07	0.930	406.3	$(15{+}6)M_\odot$	413.1	0.995	74841.	−712.57	0.804	645.5
	$(21{+}18)M_\odot$	223.7	0.986	15681.	−146.45	1.000	573.3	$(15{+}3)M_\odot$	479.8	0.991	151996.	−1571.70	1.196	1080.8
	$(21{+}15)M_\odot$	242.1	0.985	20578.	−229.82	1.001	515.1	$(15{+}1)M_\odot$	540.9	0.988	480442.	−5641.90	1.134	671.7
	$(21{+}12)M_\odot$	263.7	0.989	25769.	−280.62	0.870	486.8	$(12{+}12)M_\odot$	363.5	0.994	47695.	−439.54	1.131	950.3
	$(21{+}9)M_\odot$	289.4	0.992	37330.	−445.94	0.943	500.0	$(12{+}9)M_\odot$	415.2	0.994	63077.	−554.16	0.910	752.8
	$(21{+}6)M_\odot$	320.5	0.993	53019.	−623.88	0.897	509.3	$(12{+}6)M_\odot$	483.0	0.993	91911.	−758.66	0.710	697.9
	$(21{+}3)M_\odot$	359.7	0.988	104967.	−1344.20	1.291	918.6	$(12{+}3)M_\odot$	576.3	0.993	185313.	−1629.20	0.646	570.6
	$(21{+}1)M_\odot$	394.2	0.966	378935.	−6220.70	0.864	316.7	$(12{+}1)M_\odot$	665.0	0.993	554241.	−5133.70	0.778	552.1
EP(2, 2.5)	$(18{+}18)M_\odot$	242.3	0.989	19143.	−182.12	0.966	570.0	$(9{+}9)M_\odot$	484.7	0.994	80762.	−608.88	1.095	1450.9
	$(18{+}15)M_\odot$	264.3	0.988	26161.	−311.13	0.998	520.2	$(9{+}6)M_\odot$	580.8	0.994	119438.	−848.30	0.679	865.7
	$(18{+}12)M_\odot$	290.4	0.991	33382.	−386.89	0.985	531.5	$(9{+}3)M_\odot$	721.9	0.996	231465.	−1589.20	0.609	690.0
	$(18{+}9)M_\odot$	322.0	0.993	42839.	−456.72	0.996	672.3	$(9{+}1)M_\odot$	863.6	0.991	663250.	−4445.80	1.011	1224.9
	$(18{+}6)M_\odot$	360.9	0.994	64052.	−717.04	1.074	699.8	$(6{+}6)M_\odot$	727.0	0.996	171880.	−1044.40	0.509	714.6
	$(18{+}3)M_\odot$	411.1	0.990	125696.	−1459.60	1.398	1181.8	$(6{+}3)M_\odot$	965.9	0.997	313558.	−1504.70	0.728	1538.7
	$(18{+}1)M_\odot$	456.0	0.978	422921.	−5949.40	1.023	454.6	$(6{+}1)M_\odot$	1233.3	0.987	853820.	−3448.10	0.917	1647.6
	$(15{+}15)M_\odot$	290.8	0.994	30826.	−324.84	0.877	555.1	$(3{+}3)M_\odot$	1454.1	0.995	534864.	−1445.50	0.634	1862.3
	$(15{+}12)M_\odot$	323.0	0.992	39182.	−410.73	1.004	604.3	$(3{+}1)M_\odot$	2165.6	0.990	1363941.	−2112.30	0.586	2221.5
	$(15{+}9)M_\odot$	362.8	0.993	51071.	−498.31	1.290	1049.0	$(1{+}1)M_\odot$	4362.2	0.988	3176028.	−1057.30	0.508	4717.3
	$(21{+}21)M_\odot$	206.6	0.979	16582.	−197.41	0.875	386.7	$(15{+}6)M_\odot$	417.4	0.994	77360.	−675.66	0.918	684.8
	$(21{+}18)M_\odot$	223.5	0.978	20902.	−279.24	1.000	399.6	$(15{+}3)M_\odot$	488.5	0.993	151187.	−1430.10	1.070	973.3
	$(21{+}15)M_\odot$	241.7	0.983	26264.	−334.22	0.893	378.9	$(15{+}1)M_\odot$	549.4	0.990	473488.	−5334.40	1.141	713.4
	$(21{+}12)M_\odot$	264.9	0.986	31307.	−388.28	1.002	479.9	$(12{+}12)M_\odot$	361.5	0.992	51544.	−458.45	0.994	668.9
	$(21{+}9)M_\odot$	291.5	0.991	40144.	−467.37	0.939	470.2	$(12{+}9)M_\odot$	419.3	0.992	65430.	−518.04	1.001	813.2
	$(21{+}6)M_\odot$	325.4	0.992	58391.	−691.03	0.976	518.6	$(12{+}6)M_\odot$	488.8	0.993	93138.	−679.18	1.107	1246.7
	$(21{+}3)M_\odot$	367.7	0.992	108849.	−1344.50	1.105	705.7	$(12{+}3)M_\odot$	598.1	0.995	181969.	−1419.60	0.887	962.5
	$(21{+}1)M_\odot$	400.7	0.970	373284.	−5928.50	0.830	326.6	$(12{+}1)M_\odot$	680.0	0.994	546828.	−4829.80	0.964	782.7
EP(3, 3.5, 0)	$(18{+}18)M_\odot$	241.9	0.982	26341.	−362.32	0.963	399.9	$(9{+}9)M_\odot$	488.6	0.993	82301.	−540.26	1.072	1264.4
	$(18{+}15)M_\odot$	264.4	0.988	30466.	−375.84	0.999	454.1	$(9{+}6)M_\odot$	584.2	0.994	117604.	−687.13	0.953	1612.4
	$(18{+}12)M_\odot$	291.7	0.991	36499.	−409.49	1.017	525.2	$(9{+}3)M_\odot$	730.5	0.996	226927.	−1355.70	0.564	737.0
	$(18{+}9)M_\odot$	323.4	0.993	46908.	−499.92	1.000	576.3	$(9{+}1)M_\odot$	882.5	0.993	655246.	−4148.60	0.985	1292.0
	$(18{+}6)M_\odot$	365.9	0.994	66313.	−682.30	0.979	595.9	$(6{+}6)M_\odot$	724.6	0.995	167844.	−826.26	0.657	1219.5
	$(18{+}3)M_\odot$	421.6	0.993	129281.	−1439.70	1.070	762.3	$(6{+}3)M_\odot$	971.8	0.998	308322.	−1270.10	0.485	1015.7
	$(18{+}1)M_\odot$	462.6	0.984	419790.	−5744.00	0.813	370.9	$(6{+}1)M_\odot$	1264.7	0.991	846841.	−3202.80	0.953	2102.1
	$(15{+}15)M_\odot$	289.2	0.991	35822.	−404.80	0.898	454.6	$(3{+}3)M_\odot$	1468.7	0.997	529447.	−1232.60	0.525	1772.3
	$(15{+}12)M_\odot$	322.7	0.991	43831.	−464.31	1.012	547.8	$(3{+}1)M_\odot$	2205.5	0.993	1359671.	−1957.50	0.630	2980.3
	$(15{+}9)M_\odot$	364.9	0.992	55081.	−520.19	1.066	702.9	$(1{+}1)M_\odot$	4422.6	0.989	3172329.	−936.90	0.563	5398.2
	$(21{+}21)M_\odot$	203.0	0.976	17309.	−236.90	0.997	384.8	$(15{+}6)M_\odot$	414.7	0.993	77221.	−695.27	1.028	757.4
	$(21{+}18)M_\odot$	218.7	0.979	19473.	−235.82	0.920	428.7	$(15{+}3)M_\odot$	487.2	0.993	150606.	−1433.70	0.762	586.0
	$(21{+}15)M_\odot$	238.8	0.977	24075.	−304.62	0.879	365.3	$(15{+}1)M_\odot$	549.2	0.991	473168.	−5340.20	0.858	455.3
	$(21{+}12)M_\odot$	260.9	0.985	30356.	−368.24	0.834	386.7	$(12{+}12)M_\odot$	361.2	0.991	51539.	−485.94	0.999	621.0
	$(21{+}9)M_\odot$	290.1	0.989	41026.	−520.57	1.000	478.5	$(12{+}9)M_\odot$	407.9	0.993	64956.	−531.32	0.962	714.2
	$(21{+}6)M_\odot$	323.2	0.992	58372.	−719.11	0.999	518.7	$(12{+}6)M_\odot$	482.3	0.994	91775.	−670.48	0.960	963.1
	$(21{+}3)M_\odot$	366.7	0.992	111278.	−1426.50	1.107	661.5	$(12{+}3)M_\odot$	586.4	0.994	181591.	−1435.40	0.653	624.6
	$(21{+}1)M_\odot$	399.4	0.972	374567.	−5975.30	0.857	326.3	$(12{+}1)M_\odot$	677.4	0.994	546967.	−4851.30	1.110	962.3
EP(3, 3.5, −2)	$(18{+}18)M_\odot$	236.9	0.984	24078.	−290.81	0.933	445.8	$(9{+}9)M_\odot$	475.9	0.992	82567.	−576.02	0.744	657.2
	$(18{+}15)M_\odot$	258.8	0.986	29584.	−373.05	0.997	486.8	$(9{+}6)M_\odot$	580.6	0.994	118314.	−735.31	0.952	1367.3
	$(18{+}12)M_\odot$	286.2	0.989	36207.	−429.87	1.004	494.3	$(9{+}3)M_\odot$	739.2	0.996	227403.	−1398.70	0.549	698.8
	$(18{+}9)M_\odot$	322.2	0.991	47141.	−531.33	0.988	508.6	$(9{+}1)M_\odot$	883.5	0.993	655554.	−4180.20	0.989	1290.3
	$(18{+}6)M_\odot$	363.3	0.993	65301.	−667.38	1.005	634.0	$(6{+}6)M_\odot$	718.5	0.995	168278.	−873.13	0.480	762.7
	$(18{+}3)M_\odot$	420.5	0.993	127369.	−1406.20	0.829	546.7	$(6{+}3)M_\odot$	961.7	0.998	308298.	−1305.30	0.620	1320.4
	$(18{+}1)M_\odot$	462.4	0.981	418082.	−5702.50	1.145	572.1	$(6{+}1)M_\odot$	1265.9	0.991	847417.	−3246.20	0.938	2007.8
	$(15{+}15)M_\odot$	284.9	0.990	35472.	−418.78	0.908	431.4	$(3{+}3)M_\odot$	1438.6	0.997	530802.	−1302.70	0.494	1722.0
	$(15{+}12)M_\odot$	318.0	0.991	43550.	−485.31	0.943	491.8	$(3{+}1)M_\odot$	2219.2	0.992	1360927.	−2019.90	0.577	2479.1
	$(15{+}9)M_\odot$	357.6	0.993	55149.	−552.06	1.003	587.3	$(1{+}1)M_\odot$	4278.8	0.988	3174026.	−1002.90	0.499	4412.4
	$(21{+}21)M_\odot$	207.4	0.979	15925.	−177.19	0.910	385.0	$(15{+}6)M_\odot$	418.7	0.993	77404.	−671.84	1.011	796.1
	$(21{+}18)M_\odot$	224.6	0.977	19963.	−246.71	0.978	408.3	$(15{+}3)M_\odot$	489.4	0.993	150730.	−1413.30	0.752	593.1
	$(21{+}15)M_\odot$	242.2	0.984	25081.	−306.02	0.957	392.1	$(15{+}1)M_\odot$	550.1	0.990	474406.	−5352.80	1.144	712.3
	$(21{+}12)M_\odot$	266.0	0.987	31450.	−389.80	1.002	495.1	$(12{+}12)M_\odot$	364.7	0.991	51740.	−462.88	1.000	642.8
	$(21{+}9)M_\odot$	291.7	0.990	40622.	−481.69	1.050	529.3	$(12{+}9)M_\odot$	418.5	0.993	65089.	−504.37	0.938	730.5
	$(21{+}6)M_\odot$	326.0	0.992	59147.	−712.31	0.980	508.9	$(12{+}6)M_\odot$	492.3	0.994	92675.	−662.06	0.814	794.7
	$(21{+}3)M_\odot$	368.2	0.992	111277.	−1403.20	0.865	488.8	$(12{+}3)M_\odot$	594.3	0.994	181864.	−1410.50	0.665	636.7
	$(21{+}1)M_\odot$	400.6	0.972	374223.	−5951.20	0.826	325.8	$(12{+}1)M_\odot$	677.8	0.994	547116.	−4828.70	1.071	921.3
EP(3, 3.5, +2)	$(18{+}18)M_\odot$	241.9	0.981	25955.	−351.34	0.998	429.3	$(9{+}9)M_\odot$	489.3	0.992	82197.	−532.02	0.957	1107.8
	$(18{+}15)M_\odot$	264.3	0.987	31473.	−406.91	0.975	427.3	$(9{+}6)M_\odot$	589.5	0.994	118265.	−696.98	0.911	1380.5
	$(18{+}12)M_\odot$	290.4	0.990	37395.	−433.52	0.989	478.2	$(9{+}3)M_\odot$	732.3	0.996	227936.	−1373.10	0.546	693.9
	$(18{+}9)M_\odot$	323.5	0.991	47115.	−499.94	0.922	493.9	$(9{+}1)M_\odot$	883.8	0.993	655132.	−4136.10	0.779	912.0
	$(18{+}6)M_\odot$	366.5	0.994	65582.	−656.60	0.895	531.3	$(6{+}6)M_\odot$	729.3	0.996	167445.	−809.41	0.462	788.7
	$(18{+}3)M_\odot$	421.1	0.993	129604.	−1445.00	1.263	981.6	$(6{+}3)M_\odot$	984.4	0.998	307904.	−1250.50	0.469	946.9
	$(18{+}1)M_\odot$	462.6	0.982	419055.	−5714.00	1.146	572.4	$(6{+}1)M_\odot$	1258.8	0.991	846430.	−3180.70	0.404	640.7
	$(15{+}15)M_\odot$	292.7	0.992	35841.	−397.69	0.945	477.3	$(3{+}3)M_\odot$	1463.3	0.997	528669.	−1203.60	0.441	1676.5
	$(15{+}12)M_\odot$	322.2	0.991	44139.	−472.70	1.009	535.7	$(3{+}1)M_\odot$	2231.3	0.992	1359708.	−1944.30	0.608	2908.8
	$(15{+}9)M_\odot$	364.9	0.992	55196.	−523.89	0.963	573.9	$(1{+}1)M_\odot$	4393.5	0.989	3172509.	−928.47	0.514	5010.7

PN model		FF (minmax) with $(\psi_0, \psi_{3/2})_{\alpha,\mathrm{cut}}$ template family when LIGO-S2-L1-fit noise curve is used												
		f_{end}	mn	ψ_0	$\psi_{3/2}$	$\alpha f_{\mathrm{cut}}^{2/3}$	f_{cut}		f_{end}	mn	ψ_0	$\psi_{3/2}$	$\alpha f_{\mathrm{cut}}^{2/3}$	f_{cut}

TABLE XIII: Fitting factors for the projection of the target models (in the rows) onto the $(\psi_0, \psi_{3/2}, \alpha, f_{\mathrm{cut}})$ Fourier-domain detection template family when S2-L1 noise curve is used. For BBH masses $m_{1,2} = 1, 3, 6, 9, 12, 15, 18, 21 M_\odot$, this table shows the minmax matches between the target models and the Fourier-domain search model, *maximized over the intrinsic parameters* ψ_0, $\psi_{3/2}$, and f_{cut}, and over the extrinsic parameter α. For each intersection, the six numbers shown report the *ending frequency* f_{end} (defined in BCV1) of the PN model for the BBH masses quoted, the minmax FF mn, and the search parameters at which the maximum is attained.

[1] A. Buonanno, Y. Chen, and M. Vallisneri, Phys. Rev. D **67**, 024016 (2003).

[2] L. Blanchet, T. Damour, B. R. Iyer, C. M. Will and A. G. Wiseman, *Phys. Rev. Lett.* **74**, 3515 (1995); L. Blanchet, *Phys. Rev. D* **54**, 1417 (1996); L. Blanchet, *Class. Quantum Grav.* **15**, 113 (1998); L. Blanchet, G. Faye, B. R. Iyer, B. Joguet, *Phys. Rev. D* **65**, 061501 (2002); T. Damour, P. Jaranowski and G. Schäfer, *Phys. Lett. B* **513**, 147 (2001).

[3] T. Damour, B. R. Iyer and B. S. Sathyaprakash, Phys. Rev. D **57**, 885 (1998).

[4] A. Buonanno and T. Damour, *Phys. Rev. D* **59**, 084006 (1999); A. Buonanno and T. Damour, *Phys. Rev. D* **62**, 064015 (2000).

[5] T. Damour, P. Jaranowski and G. Schäfer, *Phys. Rev. D* **62**, 084011 (2000).

[6] T. Damour, B. R. Iyer and B. S. Sathyaprakash, *Phys. Rev. D* **63**, 044023 (2001).

[7] Here we mean the absolute value of the Fourier transform of the numerical time-domain waveform, cut at the ending frequency (instantaneous orbital frequency at the ending time) of the time-domain evolution.